Old Dominion University
ODU Digital Commons

OEAS Theses and Dissertations | Ocean, Earth & Atmospheric Sciences

Spring 2016

The Marine Cyanate Cycle

Brittany Widner
Old Dominion University, bwidn001@odu.edu

Follow this and additional works at: https://digitalcommons.odu.edu/oeas_etds

 Part of the Analytical Chemistry Commons, Biogeochemistry Commons, and the Oceanography Commons

Recommended Citation
Widner, Brittany. "The Marine Cyanate Cycle" (2016). Doctor of Philosophy (PhD), dissertation, Ocean/Earth/Atmos Sciences, Old Dominion University, DOI: 10.25777/bdhy-2t83
https://digitalcommons.odu.edu/oeas_etds/1

This Dissertation is brought to you for free and open access by the Ocean, Earth & Atmospheric Sciences at ODU Digital Commons. It has been accepted for inclusion in OEAS Theses and Dissertations by an authorized administrator of ODU Digital Commons. For more information, please contact digitalcommons@odu.edu.

THE MARINE CYANATE CYCLE

by

Brittany Widner
B.S. May 2008, The University of Akron
M.S. August 2011, Old Dominion University

A Dissertation Submitted to the Faculty of
Old Dominion University in Partial Fulfillment of the
Requirements for the Degree of

DOCTOR OF PHILOSOPHY

OCEANOGRAPHY

OLD DOMINION UNIVERSITY
May 2016

Approved by:

Margaret R. Mulholland (Co-Director)

Kenneth Mopper (Co-Director)

Anton F. Post (Member)

Lesley H. Greene (Member)

ABSTRACT

THE MARINE CYANATE CYCLE

Brittany Widner
Old Dominion University, 2016
Co-Directors: Dr. Margaret R. Mulholland
Dr. Kenneth Mopper

Cyanate (OCN^-) is a reduced nitrogen compound with the potential to serve as a nitrogen and carbon source for marine microbes. Evidence from genomes and culture studies indicated that several marine cyanobacterial groups, including representatives of the globally important genera *Synechococcus* and *Prochlorococcus*, might be capable of cyanate assimilation. However, prior to this study, the distribution, bioavailability, and production pathways of cyanate were unknown in natural systems due to the absence of a sensitive cyanate assay; and the ability of organisms to assimilate cyanate on relevant timescales was unknown because we lacked a suitable tracer for measuring uptake. I developed a cyanate assay to measure cyanate concentrations in estuarine and seawater samples, and then measured distribution at sites in the coastal western temperate North Atlantic (NA) and eastern tropical South Pacific (ETSP) including the Oxygen Deficient Zone. Cyanate concentrations ranged from below the limit of detection (0.4 nM) to 65 nM in natural samples examined to date. Cyanate was produced photochemically and in senescent diatom cultures, but cyanate was not detectable in wet and dry offshore atmospheric deposition. Using a custom-synthesized $^{13}C^{15}N$-labeled cyanate compound, I also measured rates of cyanate uptake by natural microbial communities in the NA and ETSP. Cyanate N uptake ranged from undetectable (< 0.02) to 13 nmol l^{-1} h^{-1} and was significantly higher than cyanate C uptake on all cruises. Cyanate N uptake was up to 10% of total measured N uptake at an offshore oligotrophic station in the NA but contributed a smaller fraction of total measured N uptake (< 2%) at coastal stations in the NA and ETSP. The results of this dissertation indicate that: 1) cyanate concentrations are measureable in the marine environment and cyanate has a biological-like distribution in marine systems; 2) cyanate is taken up in surface waters, probably by phytoplankton; 3) cyanate is produced photochemically in sunlit waters and from degradation of organic matter throughout the water column or through

direct release by phytoplankton; and 4) cyanate is consumed in the mesopelagic region probably by either conversion to ammonium and then to nitrate or by cyanate-supported anaerobic ammonium oxidation (cyanammox) in oxygen deficient waters.

Copyright, 2016, by Brittany Widner, All Rights Reserved.

ACKNOWLEDGMENTS

My utmost gratitude goes to Margie Mulholland for her excellent feedback over the years, her exuberant optimism, her unfailing intellectual and financial support of all my ideas, and for many inspiring scientific discussions. I thank Ken Mopper for sharing his analytical expertise. I thank Anton Post for providing context and enthusiasm for this work and Lesley Greene for helpful criticisms over the years. Everyone in the Mulholland and Mopper lab groups has contributed to the success of this dissertation. I would especially like to thank Peter Bernhardt for his assistance on cruises, his deft navigation of countless logistical hurdles, running uptake samples, and for a million other things in the laboratory and at sea. I thank K.C. Filippino for advice about chemical analysis of seawater, especially nutrient methods, culture maintenance when I was at sea, and intellectual support. I thank Luni Sun for help with photochemical experiments. Ivy Ozmon, Leo Procise, and Ryan Morse introduced me to the lab and helped me get my bearings as a new student, and Ian Sammler provided assistance with cultures. Molly Mikan and Dreux Chappell provided cultures for this work, Alexander Bochdansky guided many of the statistical analyses, and Stefanie Mack provided valuable advice with matlab and photo-editing software. I thank the Department of Ocean, Earth and Atmospheric Sciences at Old Dominion University for support via the Jacques S. Zaneveld scholarship and for support of presentations of this work at international meetings through the Dorothy Brown Smith travel scholarship.

For cruises in the North Atlantic, I acknowledge Antonio Mannino and Michael Novak at NASA and Jerry Prezioso, Tamara Holzwarth-Davis with NOAA's Ecosystem Monitoring (EcoMon) Project for assistance in the field and with data processing. Kim Hyde at NOAA provided valuable assistance processing the ocean color and temperature data. I thank Christian Kernisan, Lynn Price, and C.J. Staryk for help with uptake experiments and nutrient sampling and Peter Sedwick, Bettina Sohst, and Christine Sookhdeo for providing atmospheric deposition samples. I thank the captains and crews of the *R/V Slover*, *R/V Bigelow*, *R/V Sharp*, and *R/V Delaware II* for help with sample and data collection. I thank NSF and NASA for support of this research.

For the cruise in the South Pacific, I enthusiastically thank Bess Ward and Al Devol for inviting me on the cruise and supporting my science objectives while at sea. I thank Bonnie Chang for assistance with ammonium sample collection and analysis. Bonnie also assisted in sampling when the time needed for my myriad projects exceeded the time I had available to complete them. I thank Calvin Mordy for the nutrient data and Emilio Garcia-Robledo and Niels Peter Revsbech for measuring O_2 concentrations in the incubation bags. I would like to acknowledge NSF for funding this work and the captain and crew of the *R/V Nathaniel B. Palmer*.

TABLE OF CONTENTS

Page

Page

LIST OF TABLES

Table Page

LIST OF FIGURES

Figure Page

Figure Page

CHAPTER I

INTRODUCTION

Nitrogen (N) is a vital macronutrient for all living organisms that limits phytoplankton growth in much of the world's oceans. N speciation controls phytoplankton community composition and primary production in N-limited regions and drives global marine carbon flux on glacial/interglacial timescales (McElroy 1983). Dissolved inorganic nitrogen (DIN), nitrate (NO_3^-), nitrite (NO_2^-), and ammonium (NH_4^+), and labile dissolved organic N (DON) are available as N sources to marine microbes (Mulholland and Lomas 2008). DON can comprise a substantial fraction of N uptake with urea alone accounting for > 50% of N uptake in some systems (Mulholland and Lomas 2008; Sipler and Bronk 2015). Urea and cyanate can be utilized in place of NH_4^+ by some aerobic ammonia oxidizers (Alonso-Sáez et al. 2012; Koops and Pommerening-Röser 2001; Palatinszky et al. 2015; Qin et al. 2014). Despite its significance in biogeochemical cycles, the DON pool remains poorly characterized (Sipler and Bronk 2015), and we lack sensitive methods for measuring many components of the DON pool.

Cyanate (OCN^-) is a simple organic N compound that may be available as a source of N and C for microbes. The genes for uptake and assimilation of cyanate (OCN^-), cyanate hydratase (see Appendix A for enzyme structure) and a cyanate transporter, have been identified in strains of the ubiquitous marine cyanobacteria, *Prochlorococcus* and *Synechococcus*, which, together account for two thirds of marine and one third of global primary productivity (Bryant 2003; Field et al. 1998). Microorganisms, including *Prochlorococcus* MED4, *Synechococcus* WH8102, and the harmful marine dinoflagellate, *Prorocentrum donghaiense*, have been grown on culture media supplied with OCN^- as the sole N source (Berube et al. 2015; Dorr and Knowles 1989; Harano et al. 1997; Hu et al. 2012; Kamennaya et al. 2008; Miller and Espie 1994; Taussig 1960; Wood et al. 1998).

Possible sources of cyanate to natural waters include abiotic decomposition of urea (Dirnhuber and Schutz 1948) produced autochthonously and supplied via urban and agricultural runoff (Glibert et al. 2006), and industrial water discharges (Lin et al. 2008). OCN^- may also be released to marine systems by rapid decomposition of carbamoyl phosphate (Allen and Jones 1964, see Appendix B for proposed intracellular pathway and Appendix C for abiotic pathway)

and other metabolic intermediates, direct release by intact cells, as a result of cell death, cell lysis, and sloppy feeding (Sorokin et al. 2001).

Despite the evidence for a "cyanate cycle", prior to this work, research was hampered by the lack of methods for measuring cyanate concentrations in the environment, its uptake by microorganisms, and its production in aquatic systems. I developed a nanomolar cyanate assay for estuarine and sea water employing derivatization to a fluorescent product and high performance liquid chromatography (Chapter II) and employed this method and stable isotope ($^{15}N^{13}C$) techniques to address three questions: 1) What is the distribution of cyanate in marine systems? 2) What are the sources of cyanate to marine systems? 3) Is cyanate bioavailable?

The distribution of a dissolved constituent reflects the balance of production and consumption of that constituent, and the distributions of most dissolved N species are controlled biologically by assimilatory processes, such as N uptake for growth, and dissimilatory processes, such as nitrification and denitrification (Gruber 2008). In N-limited regions, biologically available N cycling intermediates, such as NH_4^+ and NO_2^-, are generally present at nanomolar or sub-nanomolar concentrations throughout most of the water column. Higher concentrations of NH_4^+ and NO_2^- are often present near the base of the euphotic zone where production and consumption are spatially uncoupled (Gruber 2008). The NO_3^- distribution is also controlled biologically, but, while the NO_3^- distribution is similar to those of NH_4^+ and NO_2^- in surface waters, NO_3^- concentrations are uniformly high below the euphotic zone. Biologically unavailable DON compounds can also accumulate in the deep ocean where they are present in micromolar concentrations. The vertical distribution of cyanate, therefore, should reveal clues as to its bioavailability and production. In this dissertation, I describe the distribution of cyanate and discuss its implications for biological and geochemical nitrogen cycling in diverse environments. I also provide direct measurements of several likely sources of cyanate to marine systems. Because of the genomic and culture evidence for cyanate uptake by cyanobacteria, I assessed cyanate bioavailability using measurements of cyanate uptake primarily in the euphotic zone.

In Chapter III I present the initial measurements of the cyanate distribution in the western temperate coastal North Atlantic (NA) and measurements of cyanate production in laboratory and field studies. A transect of cyanate concentrations was measured across the Gulf of Maine which encompasses geographical diversity in advection, nutrient supply, sediment exchange, and

microbial community composition. Cyanate production was measured from photochemistry, wet and dry atmospheric deposition, and organic matter degradation. To evaluate biological release of cyanate from organic matter, cyanate production was measured in diatom and cyanobacterial cultures in experiments designed to mimic phytoplankton growth in the euphotic zone and the degradation of sinking phytoplankton in the dark ocean.

In Chapter IV I present cyanate distribution and uptake data from the NA which has a broad continental shelf, abundant riverine input, and a seasonally variable water column (Townsend et al. 2006). The cyanate distribution was measured at stations on the continental shelf, in the basin of the Gulf of Maine, and on the continental shelf slope. I compared cyanate concentrations between these regions and between onshore and offshore locations. I examined relationships between cyanate concentrations and phytoplankton biomass, the primary nitrite maximum, and the nitracline. Seasonal, regional, and vertical variability in cyanate N and C uptake were described using measurements of uptake from four cruises (May/June 2010, November 2010, May/June 2011, and August 2012) across the study region.

The eastern tropical South Pacific (ETSP) is a region with a narrow continental shelf, high primary productivity, low seasonal variability, and coastal and equatorial upwelling (Pennington et al. 2006). The oxygen deficient zone (ODZ) located below this highly productive region contributes significantly to the marine loss of fixed N (Codispoti 2007; Codispoti et al. 2001). In Chapter V, the vertical distribution of cyanate was measured along two transects. The first was located 200 nm off the coastline and parallel to the coastline, and the second was a longitudinal transect along 17 °S. The cyanate distribution was compared to those of NH_4^+, NO_2^-, and NO_3^- as well as chlorophyll *a* and dissolved oxygen concentrations and temperature and salinity. To determine whether cyanate was an important N source in this region, I compared cyanate, urea, and NH_4^+ uptake kinetics. I also calculated the fraction of measured N uptake attributed to cyanate. Cyanate N and C uptake rates were measured over a diurnal cycle in surface water, and cyanate, urea, and NH_4^+ uptake rates were measured in the ODZ where rates of N uptake have not been previously measured. ODZ uptake rates were compared to rates of anammox supported by cyanate, urea, and NH_4^+.

In Chapter VI, I synthesize the cyanate distributions, production rates, and uptake rates described in Chapters II - V with recent discoveries made by other researchers regarding cyanate bioavailability to describe the marine cyanate cycle.

CHAPTER II

CHROMATOGRAPHIC DETERMINATION OF NANOMOLAR CYANATE CONCENTRATIONS IN ESTUARINE AND MARINE WATERS BY PRECOLUMN FLUORESCENCE DERIVATIZATION

PREFACE

The content of this Chapter is reprinted with permission from Widner, B., Mulholland, M.R., and Mopper, K. 2013. Chromatographic determination of nanomolar cyanate concentrations in estuarine and sea waters by precolumn fluorescence derivatization. Anal. Chem. 85(14): 6661-6666. Copyright 2013. American Chemical Society. See Appendix D for the copyright permission, and the manuscript can be found online at http://pubs.acs.org/doi/abs/10.1021/ac400351c.

INTRODUCTION

In the marine environment, N is often the nutrient that limits primary productivity by phytoplankton. However, because dissolved N is stable in a variety of chemical forms and oxidation states in aquatic environments, the N cycle is complex and involves feedbacks between various dissolved N pools and the microbes, including phytoplankton and bacteria, that mediate their production, consumption, and transformation. Phytoplankton and bacteria take up both organic N and inorganic N compounds (Mulholland and Lomas 2008) and the genetic capability for uptake and assimilation of this diverse N pool has recently been confirmed within individual microbes and microbial communities (Hewson and Fuhrman 2008; Scanlan and Post 2008). Based on recent genomic and physiological evidence, it has been hypothesized that cyanate (OCN^-), a reduced N compound, contributes to the N and C requirements of marine microbial communities (Kamennaya and Post 2011; Palenik et al. 2003; Rocap et al. 2003).

Genes encoding a cyanate-specific transporter as well as an enzyme catalyzing intracellular cyanate decomposition, cyanase, have been identified in strains of the globally important marine cyanobacterial groups, *Prochlorococcus* and *Synechococcus* (Palenik et al.

2003). Because these two genera are thought to account for up to two-thirds of oceanic primary production and one-third of global primary production (Bryant 2003), cyanate could be a quantitatively significant component of the marine N cycle that has not yet been examined. Genes related to cyanate metabolism have also been identified in other marine microorganisms (Berg et al. 2008; Kamennaya and Post 2011). In addition, *Synechococcus* WH8102 (Kamennaya and Post 2011), *Prochlorococcus* MED4 (Kamennaya and Post 2011), the dinoflagellate *Prorocentrum donghaiense* (Hu et al. 2012), and some heterotrophic bacteria (Dorr and Knowles 1989; Guilloton and Karst 1987; Wood et al. 1998) have been cultured in media containing cyanate as the sole N source, attesting to the bioavailability of this compound. Potential sources of cyanate to natural waters include discharges from gold mining, combustion, and protein manufacturing (Lin et al. 2008), *in situ* release of cyanate by the microbial community as a by-product of cellular metabolism (Sorokin et al. 2001), cyanate release through cell lysis or "sloppy feeding" by grazers, spontaneous decomposition of the metabolic intermediate carbamoyl phosphate (Allen and Jones 1964, Appendices B and C) and other organic cellular metabolites, herbicide runoff (Koshiishi et al. 1997), and urea runoff from urban and agricultural settings (Glibert et al. 2006) followed by spontaneous aqueous decomposition to cyanate (Dirnhuber and Schutz 1948).

Despite the growing evidence that cyanate is bioavailable to aquatic microorganisms and there are many potential sources of cyanate to aquatic systems, it is unclear whether cyanate contributes to the N demands of microorganisms in nature because there are no measurements of cyanate in aquatic systems. The distributions of nutrient elements provide clues as to their chemical and biological reactivity in natural systems, and quantifying cyanate distributions is a necessary first step toward understanding the cycling of this compound in natural aquatic systems. In many estuarine and seawater samples, dissolved inorganic N concentrations range from at or below the limit of analytical detection (1-2 nM for most dissolved N compounds) to 35 μM (McCarthy and Bronk 2008). In offshore marine surface waters, where phytoplankton are often N limited, tight coupling of production and consumption of reduced inorganic N leads to ambient concentrations that are often at or near the limit of analytical detection, even though reduced inorganic N contributes the bulk of the N fueling primary productivity (Gruber 2008). Cyanate concentrations are likely to be similarly low in surface waters in N-depleted oceanic

regions, therefore quantification of cyanate in surface waters requires a detection limit in the low nanomolar range.

While methods for quantitative cyanate determination have been developed for medical and industrial use, these methods generally have detection limits (low micromolar range) higher than those appropriate for natural waters. Methods for measuring cyanate concentrations in aqueous solutions include both colorimetric and chromatographic techniques and many employ derivatization steps. A qualitative test for measuring the presence of cyanate in aqueous saline solutions (Marier and Rose 1964) was developed using a copper cyanate-pyridine complex (Werner 1923), but this method was not quantitative. Ion chromatographic (IC) methods have also been developed for cyanate determination (Black and Schulz 1999; Lin et al. 2004; Nonomura and Hobo 1989), but these are largely inappropriate for seawater samples because the chloride ion and other anions produce large interfering peaks and because the ~2 μM detection limit is not low enough for natural waters. Cyanate was measured in blood by derivatization with 2-nitro-5-thiobenzoic acid followed by high performance liquid chromatography (HPLC) (Eiger and Black 1985); however, like the IC methods, the 1 μM detection limit of this method is likely not low enough for most natural aquatic samples. Cyanate concentrations in freshwater bioremediation tanks were measured after converting OCN^- to NH_4^+ using the cyanase enzyme, and then measuring NH_4^+ colorimetrically (Luque-Almagro et al. 2003), but this method also has a relatively high detection limit (0.5 μM) and would need to account for NH_4^+ already present in natural waters. A colorimetric method for quantitative cyanate determination in aqueous solution based on the derivatization of cyanate to 2,4-quinazolinedione (benzoylene urea) from 2-aminobenzoic acid (anthranilic acid) (Guilloton and Karst 1985; Lange and Sheibley 1963) was employed to measure cyanate in gold mine drainage samples (Zvinowanda et al. 2008) and was adapted by Lundquist et al. (1993) to quantify cyanate in blood plasma using HPLC and fluorescence detection to an 8 nM detection limit. We have significantly modified this method to measure cyanate concentrations at the low nanomolar level in natural aqueous samples. Here we report not only the method itself but also the first measurements of cyanate concentrations in estuarine and marine waters.

METHODS

Derivatization Procedure

Cyanate was measured in saline and brackish natural water samples by reacting it with 2-aminobenzoic acid in aqueous solution to form the 2,4-quinazolinedione derivative followed by HPLC with fluorescence detection to quantify 2,4-quinazolinedione against a standard curve as described below. A 30 mM aqueous solution of 2-aminobenzoic acid was prepared from a solid stock (Sigma-Aldrich, ≥ 99.5% purity) by heating at 80 ºC until fully dissolved. After cooling to room temperature, the solution was stored for up to three days. As recommended by Guilloton and Karst (1985), the 2-aminobenozoic acid solution was prepared in an amber glass bottle and stored in an opaque bottle. 2,4-Quinazolinedione was purchased from Acros organics (98%). Potassium cyanate (KOCN, Sigma-Aldrich, 96%) was stored in a desiccator to slow decomposition of OCN^- to NH_4^+ and CO_2 (Amell 1956). Primary KOCN standards were prepared in deionized water (DI) and were stored at 4 ºC for up to one month. Working standards were prepared fresh in artificial seawater of the same salinity as the samples. Standard curves were prepared by derivatizing standards and samples simultaneously using the same reagents for each set of samples.

Samples were derivatized as follows. A 1 mL, filtered (0.2 µm) sample or standard solution was combined with 0.4 mL 30 mM 2-aminobenzoic acid in a combusted 4 mL amber borosilicate glass vial (Fisher Scientific) with a polyproplene "top hat" cap (Sigma-Aldrich, PTFE/silicone septum). The vials were placed in a 35 °C water bath for 30 minutes. Immediately upon removal from the water bath, 1.4 mL 12N HCl (reagent grade) was added to each sample (6N HCl final concentration). Samples were then run immediately on an HPLC equipped with a refrigerated autosampler (4 ºC).

HPLC Conditions

A modular Shimadzu HPLC was used to measure cyanate concentrations in derivatized aqueous samples. The pumps were model LC-10ATvp, the degasser was a DGU-14A, the autosampler was a SIL-10advp, the fluorescence detector was a RF-10AXL, and the system controller was a SCL-10Avp. Shimadzu CLASS-VP VP1 software was employed for peak enumeration and integration. Mobile phase components were HPLC grade methanol (99.9%;

Fisher Scientific), HPLC grade trifluoroacetic acid (TFA) (97%, Fisher Scientific), and Nanopure deionized water from a Barnstead system. The mobile phase was 60:40 5% TFA/100% MeOH and the flow rate was 100 µL/min.

We used a poly(styrene-divinylbenzene) column with broad pH stability (Hamilton, PRP-1, 2.1x150 mm, 5 µm). Cyanate (as 2,4-quinazolinedione) was quantified using a fluorescence detector set at excitation and emission wavelengths of 312 nm and 370 nm, respectively. Sample injection volume was 100 µL and the run time was 20 minutes.

The PRP-1 column is stable for at least two years (~120 L mobile phase), however certain HPLC components, specifically the autosampler, were easily damaged by the concentrated HCl (6 N) in the samples. To minimize instrument damage and disruption of analyses, we recommend use of acid-tolerant components, pre-injection neutralization, or frequent autosampler preventative maintenance and consumable replacement.

Separation was first achieved using an isocratic mobile phase of 86:14 5% TFA/acetonitrile (ACN) and a flow rate of 110 µL/min. We later determined that use of methanol (MeOH) as the organic solvent was more cost effective than ACN. Subsequently, the method was altered so that the mobile phase was 60:40 5% TFA/100% MeOH and the flow rate was 100 µL/min. Although lower column backpressure and shorter retention times were observed using ACN as the organic modifier, both sets of conditions yielded similar precision and accuracy. We recommend use of MeOH, however the results presented here from the Chesapeake Bay Mouth were analyzed using ACN.

Statistical Calculations and Recovery

Concentrations calculated from both peak area and peak height were very accurate, but at low cyanate concentrations (<2 nM, lower S/N) peak height yielded better precision. Therefore, we used peak height to calculate cyanate concentrations using a standard curve prepared from stock KOCN. R^2 values for standard curves were 0.9999 or better for all analyses. The limit of detection (LOD) was calculated as three times the standard deviation of seven blanks.

The derivatization yield was determined by calculation of absolute recovery using the peak height of a derivatized 50 nM KOCN standard divided by the peak height of 50 nM 2,4-quinazolinedione in the reagent matrix. Analytical recovery was calculated to assess the efficiency of the derivatization procedure in a sample matrix. A natural sample was spiked with 50 nM KOCN, and the cyanate concentration of this spiked sample was divided by the sum of a

50 nM standard plus the sample cyanate concentration. Absolute recovery and analytical recovery were calculated each time samples were analyzed.

Determination of Reagent, Standard, and Sample Stability

To measure reagent stability, a 30 mM aqueous 2-aminobenzoic acid solution was stored for one month. At time points of 3, 10, and 30 days, the absolute recovery was determined using the stored reagent to derivatize a freshly prepared 50 nM KOCN standard.

To determine optimal storage conditions for samples destined for cyanate analysis, a 50 nM KOCN spike was added to a water sample collected from the Elizabeth River on February 4, 2012 when salinity was 20. Salinity measurements in natural waters are unitless values which roughly correspond to the parts per thousand (ppt) salinity measured in artificial seawater (Harrison et al. 1980). Aliquots of the spiked sample (1 mL) were transferred to twelve 8 mL borosilicate tubes and then divided into four groups of three. One group each was frozen at two different temperatures, -20 ºC and -80 ºC. Another group was frozen at -20 ºC after the addition of a preservative (10 mg/L final concentration of $HgCl_2$). The last group of samples was immediately derivatized prior to storage at -20 ºC. At the same time that natural samples were prepared and stored, standard curves were prepared, divided into four groups, and stored in the same way as spiked natural water samples. After 14 and 270 days, the concentration of cyanate in the natural water sample was measured and calculated using both a standard curve prepared and stored on the same date and under the same conditions as the sample. These were compared to standard curves that had been prepared fresh, the day samples were analyzed. The cyanate concentrations calculated from the freshly prepared standard curve was used for all statistical analyses except in the case of the samples derivatized at the time of sample collection where a stored standard curve was used.

The stability of primary stock KOCN standards (100 mM) stored at 4 ºC was evaluated after 30 days by calculating the change in absolute recovery. Seawater differs from freshwater in ionic strength, buffering capacity, and pH; therefore the stability of the primary standard was tested in freshwater (0 ppt) and artificial seawater (20 and 35 ppt).

Natural Samples: Collection and Processing

Samples were collected from twelve stations along a north-south transect across the Chesapeake Bay Mouth (CBM) on November 7, 2011 aboard the *Research Vessel (R/V) Fay*

Slover. This 25 km transect crosses a highly variable estuarine region influenced by three channels through which estuarine and oceanic waters exchange. At each station, Niskin bottles were used to collect water samples from two depths: the first approximately 2 meters below the surface and the second at the depth of maximum chlorophyll fluorescence (460 nm excitation, 685 nm emission) which generally corresponds to the depth where phytoplankton concentrations are highest. Water was filtered directly from the Niskin bottle through a 0.2 µm Supor Pall capsule filter using a peristaltic pump and constant positive pressure (5 mm Hg), and the filtrate was collected in sterile 50 mL polypropylene centrifuge tubes. Duplicate 1 mL sample aliquots were transferred from the polypropylene tubes into 8 mL acid-washed and combusted borosilicate tubes with polycarbonate screw caps. Samples were stored in a -20 ºC freezer aboard the ship and derivatized immediately upon return to the laboratory (within four hours of collection).

In addition to the estuarine CBM samples, cyanate concentrations were analyzed at a station on the North American mid-Atlantic continental shelf from samples collected on August 10, 2012, during a cruise aboard the *R/V Henry B. Bigelow*. This station was located approximately 65 km offshore in relatively shallow waters (55 m) that are strongly influenced by coastal currents and riverine inputs (Townsend et al. 2004). As for the CBM cruise, water samples were collected approximately 2 meters below the surface and at the fluorescence maximum using Niskin bottles. Samples were filtered through a 0.2 µm Supor polycarbonate filter by gravity directly from the Niskin bottle, and the filtrate was collected in sterile 15 mL polypropylene centrifuge tubes. Triplicate 1 mL aliquots were transferred to 4 mL pre-combusted amber borosilicate glass vials, and samples were immediately stored at -20 ºC and derivatized within 48 hours of collection onboard the ship. Derivatized samples were then stored at -20 ºC until analysis.

RESULTS AND DISCUSSION

Derivatization Optimization and Parameters

There are two reactions in the formation of 2,4-quinazolinedione from cyanate and 2-aminobenzoic acid. In the first reaction, 2-aminobenzoic acid and cyanate react to form 2-

ureidobenzoic acid (Step I, Figure 1). Second, strong acid converts 2-ureidobenzoic acid to 2,4-quinazolinedione (Step II, Figure 1).

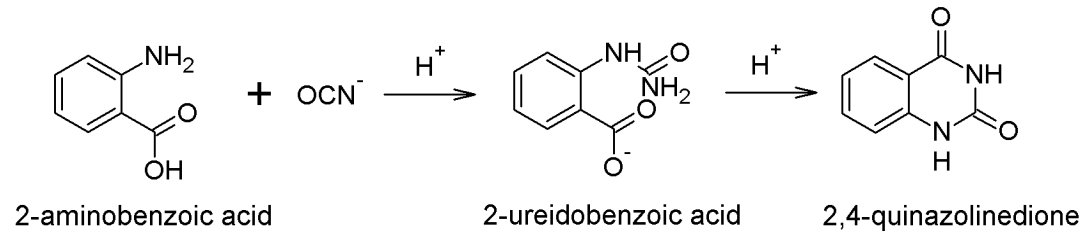

Figure 1. Derivatization reaction modified from Guilloton and Karst (1985).

The derivatization was optimized to reduce the reagent blank and maximize recovery of 2,4-quinazolinedione. All optimizations were performed using a Sargasso Sea sample (location in Table 1) to account for matrix effects. In Step I, recovery was consistent at or above 8.5 mM 2-aminobenzoic acid (Figure 2 left). The optimal reaction temperature was 35 °C, and the optimal reaction time was 30 minutes (Figure 2 right). We examined the pH of Step I and found consistent recovery between pH 3.5 and 5 (data not shown). The pH of 2-aminobenzoic acid (30 mM) was 3.7, and when this was added to a sample (pH 8.4) the resulting pH was 4.5. The pH of typical marine and estuarine samples ranges from 7.5 to 8.4 (ref), so it is unnecessary to buffer the Step I reaction.

Table 1. Matrix effects as determined by analytical recovery and the method of standard additions.

Sample	Latitude (ºN)	Longitude (ºW)	Depth (m)	Salinity	Analytical Recovery (%)[1]	[OCN^-] (nM) [2]	[OCN^-] (nM) [3]
Sargasso Sea	40.5	70.2	140	35	106	2.64 (0.12)	2.88 (0.08)
Virginia Beach	36.8	75.0	1	29	101	13.6 (0.94)	13.5 (0.86)
Chesapeake Bay	36.9	76.3	1	20	94.4	35.2 (0.51)	38.7 (0.90)

[1] Analytical recovery calculated from DI standard curve.
[2] [OCN^-] calculated from DI standard curve
[3] [OCN^-] calculated by method of standard additions.

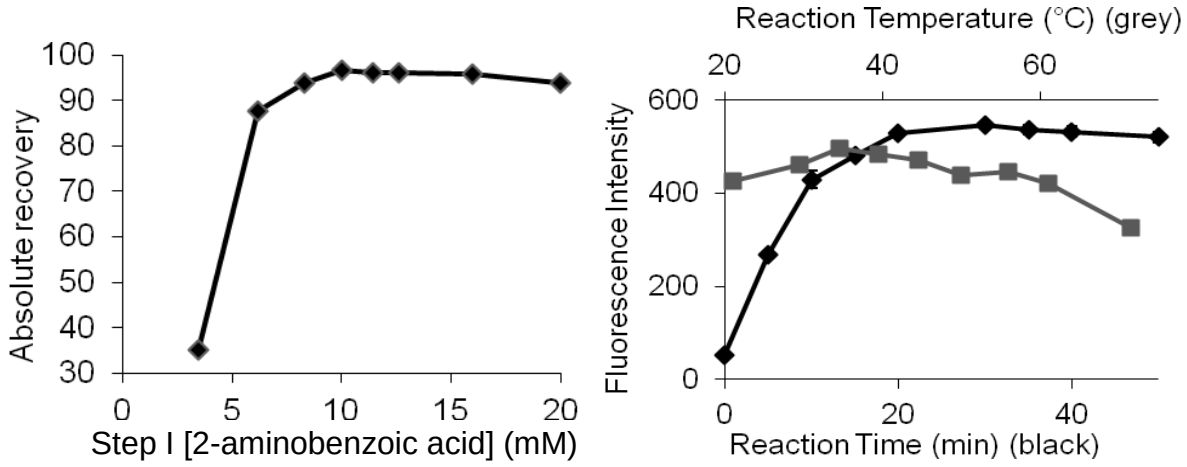

Figure 2. Derivatization Step I optimization. Change in recovery in relation to final concentration of 2-aminobenzoic acid (left) and change in fluorescence intensity due to Step I reaction temperature (grey squares) and time (black diamonds) (right). Optimizations were determined using a 1 µM KOCN spike in a sample from the Sargasso Sea and analyzed on a spectrofluorophotometer (emission 312 nm, excitation 370 nm). Recovery was verified in an unmanipulated sample after optimization. In both panels, error bars represent ± 1 standard deviation (*n*=3).

Step II was also optimized. Recovery decreased below 6 N HCl (final concentration) and was consistent above 6N. The Step II reaction proceeded rapidly and with full recovery at room temperature (data not shown). This result differs from previously published methods (Guilloton and Karst 1985; Lundquist et al. 1993) where the reaction temperature was 100 °C. Additionally, Lundquist et al. (1993) halted both reaction steps by immersion of samples in an ice bath, but we consistently obtained ≥ 98% recovery without cooling samples.

To lower the LOD, decrease the blank signal, and eliminate interfering and contaminating compounds, 2-aminobenzoic acid was recrystallized twice in hot water. The blank peak height was reduced approximately two-fold by this process, but the LOD decreased only marginally (~ 9%) to 0.4 nM (SD of seven blanks, 1.24%). Despite this limited improvement, 2-aminobenzoic acid recrystallization is recommended to minimize variability between reagent batches. However, over the one month period, the retention time shifted by as much as one minute and the standard curve slope varied by 10%, highlighting the need to run standard curves with each group of samples. Within a 24 hour period, the retention times and the slopes were essentially constant.

Potential matrix effects were investigated by comparing the cyanate concentration calculated from an external standard curve prepared in deionized water (DI) and a standard curve prepared using the method of standard additions in three different matrices: open ocean water from the Sargasso Sea in the North Atlantic, a coastal sample collected from the Virginia Beach, VA, fishing pier located in coastal waters near the mouth of the Chesapeake Bay, and an estuarine sample from the Chesapeake Bay. These three locations differ in salinity (Table 1) and dissolved organic matter (DOM) concentration and composition, with the estuarine sample being strongly influenced by terrestrial DOM (Minor et al. 2006). The analytical recoveries were between 94 and 106%, and the cyanate concentration calculated from the DI curve did not deviate more than 10% from the concentration calculated using the method of standard additions (Table 1). Given this negligible matrix effect, we recommend that external standards be prepared in deionized water for estuarine and marine samples. When sampling a very different matrix from those examined here we recommend a matrix comparison between the method of standard additions and a DI standard curve.

Reagent, Standard, and Sample Stability

When 2-aminobenzoic acid solutions (40 mM) older than three days were used to derivatize freshly prepared 50 nM KOCN, absolute recoveries of standard additions were inconsistent; on some occasions absolute recovery decreased, while on others it was as high as 280%. We therefore recommend the solution be stored no longer than three days.

After 270 days, the mean concentrations of cyanate in stored samples ranged from 84.8% to 131% of those in the original fresh sample (Table 2). The relative standard deviations (RSD) of the samples did not increase when stored at -80 °C or when derivatized before storage at -20 °C (RSD < 1.0%, Table 2); however the RSD increased 50-fold and 7-fold during storage at -20 °C with and without $HgCl_2$ preservation, respectively (Table 2). These large standard deviations would be problematic for samples in which cyanate concentrations are near the LOD of 0.4 nM. For unmanipulated samples stored at -20 ^{o}C, the cyanate concentrations increased 31% during storage (Table 2). In addition, the standards stored at -20 °C with and without $HgCl_2$ preservation produced poor standard curves compared to those from the other treatments and the freshly prepared standard curve (see R^2 values, Table 2). For these reasons long-term storage at -20 °C with or without the addition of a preservative is not recommended.

The high variability of the -20 ^{o}C samples stored with and without $HgCl_2$ precluded comparison of all treatment mean cyanate concentrations to the cyanate concentration measured at the time of sample collection using ANOVA (Brown-Forsythe test, $F = 3.73$, $p = 0.04$). Therefore, we compared the mean cyanate concentrations of the treatments which did not violate ANOVA assumptions (storage at -80 °C and immediate derivatization followed by storage at -20 °C) to the mean cyanate concentration before storage and found a significant difference (ANOVA, $F = 280.73$, $p << 0.05$). The concentration of cyanate in samples stored at -80 °C was not statistically different from the concentration measured in fresh samples (Dunnett's test, $p = 0.96$), but the concentration of cyanate in samples derivatized at the time of sample collection and stored at -20 °C was 15% lower than the concentration measured in fresh samples (Dunnett's test, $p << 0.05$). There was no significant difference in cyanate concentration and no change in RSD when treatment means were compared after 14 days of storage (data not shown). We therefore recommend that for sample storage lasting longer than two weeks, samples be stored at -80 ºC immediately following collection until derivatization and analysis. If storage at -80 ºC is

not possible, samples should be derivatized immediately and stored at -20 ºC, and if storage will be less than two weeks, any of the methods tested produce consistent results.

KOCN primary stocks (100 mM) were stable up to one month at 4 ºC, and no differences in stability were observed between salinities. We recommend that fresh KOCN stock be prepared after one month in storage.

Table 2. Determination of sample stability under different storage conditions. Results are from samples stored for 270 days.

	Stored standard curve			Fresh standard curve[2]	
Treatment[1]	[OCN^-] (nM)[3]	standard deviation (nM)[3]	standard curve R^{2} [2]	[OCN^-] (nM)[3]	standard deviation (nM)[3]
time zero	n/a	n/a	n/a	70.5	0.64
-20	65.9	4.82	0.9827	92.5	5.55
-80	69.2	0.14	0.9996	70.6	0.09
-20p	55.1	31.8	0.9369	68.3	26.8
-20d	59.8	0.62	0.9991	62.0	0.63

[1] Elizabeth River samples (20 ppt) spiked with KOCN (50 nM) stored under conditions: time zero- concentration measured immediately after sample collection, -20 were stored at -20ºC, -80 were stored at -80 ºC, -20p were stored at -20 ºC after preservation with $HgCl_2$, and -20d were derivatized immediately after sample collection and stored at -20 ºC.

[2] R^2 of freshly prepared standard curve was 0.9997. $R^2$of the time zero standard curve was 0.9999.

[3] OCN^- concentrations and standard deviations were calculated from three replicates for all treatments.

HPLC and Detection Optimization

Fluorescence emission and excitation wavelengths were selected to maximize 2,4-quinazolinedione fluorescence and minimize 2-aminobenzoic acid fluorescence. At the excitation wavelength of 312 nm, the wavelength of maximum emission by 2,4-quinazolinedione is 370 nm, while the wavelength of maximum emission by 2-aminobenzoic acid is 418 nm (Figure 3).

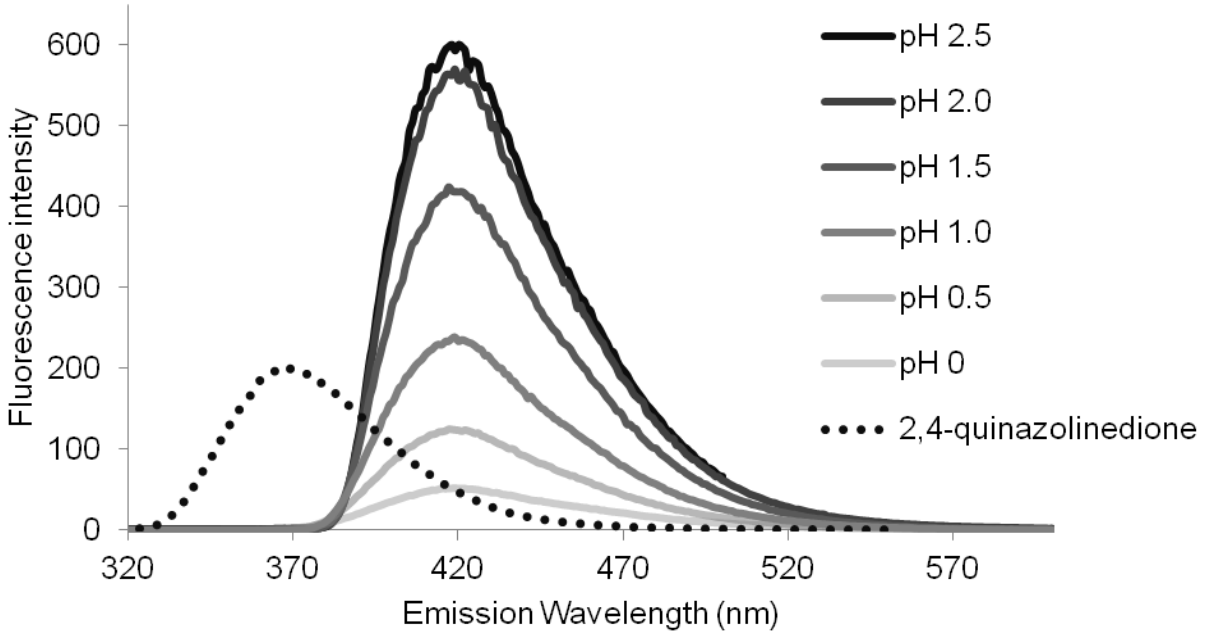

Figure 3. Fluorescence spectra of 40 mM 2-aminobenzoic acid. Spectra at pH ≤ 2.5 are shown by solid lines where the darkest line is pH 2.5 and the lightest line is pH 0. The spectrum for 10 μM 2,4-quinazolinedione is shown for pH 2 (dotted line). The fluorescence intensity of 2-aminobenzoic acid decreased with decreasing pH. At pH > 2.5, the fluorescence intensisty of 2-aminobenzoic acid is greater than or equal to that at pH 2.5 (data not shown). The fluorescence spectra of 2,4-quinazolinedione at varying pH values are not shown because the spectrum does not change with pH. The excitation wavelength was 312 nm.

Following derivatization, Lundquist et al. (1993) employed additional extraction and purification steps to isolate cyanate specific to their sample matrix (blood plasma), which were unnecessary steps for seawater samples. This simplification permitted HPLC analysis immediately following derivatization and greatly reduced the potential for contamination and low recovery. However, we had to contend with a large excess 2-aminobenzoic acid peak which would have been eliminated using the extraction procedures of Lundquist et al. (1993). As a zwitterion, 2-aminobenzoic acid is protonated, neutral, or negatively charged, depending on the solution pH. At neutral pH, such as the mobile phase employed by Lundquist et al. (1993), 2-aminobenzoic acid is negatively charged (pK_a 4.85), but at very low pH, 2-aminobenzoic acid is

protonated (pK_a 2.17) and has a much lower fluorescence quantum yield (Figure 3) than the negatively charged and neutral species. By reducing the aqueous mobile phase component pH to 0.5, we significantly reduced the magnitude of the 2-aminobenzoic acid peak and obtained excellent separation of 2-aminobenzoic acid and 2,4-quinazolinedione (Figure 4). Consequently, we replaced the neutral pH 70:30 water/methanol mobile phase of Lundquist et al. (1993) with a low pH (< 1) mobile phase. The pH tolerance of most C18 columns, including that used by Lundquist et al. (1993), is not appropriate for a mobile phase of this pH, so we employed a poly(styrene-divinylbenzene) column which is stable to a pH of 0. Trifluoroacetic acid (pKa 0.2) was chosen to adjust the aqueous phase pH over other acids, such as phosphoric acid, because it did not require a salt buffer and was less corrosive to the instrument.

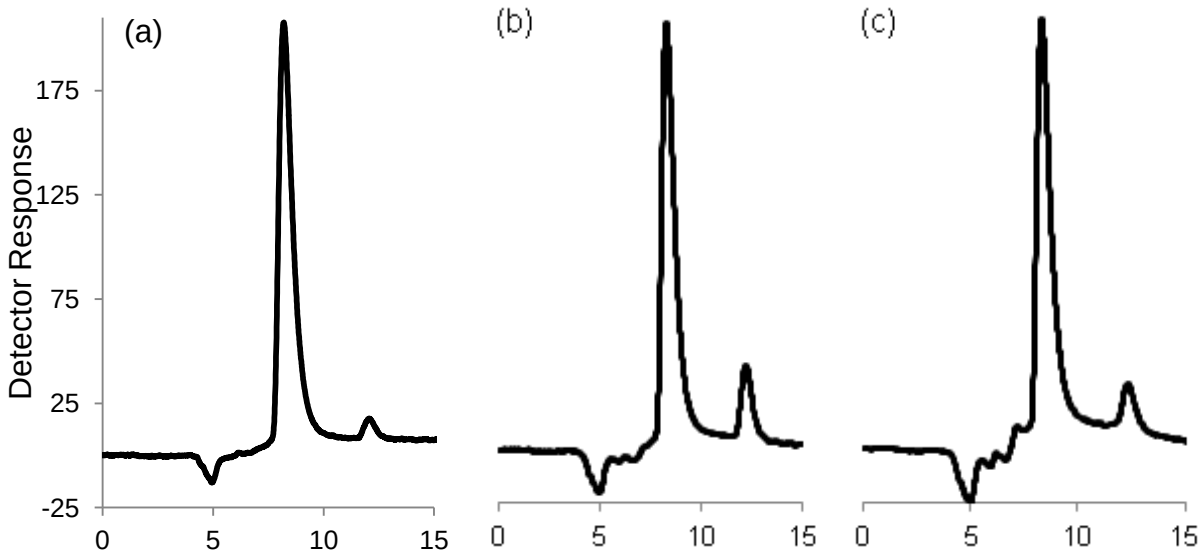

Figure 4. Sample chromatograms. Shown are (a) a reagent blank (relative SD (RSD) 3%), (b) a 50 nM standard (RSD 1.5%), and (c) a sample from the Elizabeth River (21.4 nM, RSD 1.9%) (c) using MeOH in the mobile phase. In all panels, the negative peak at 5 minutes is the solvent, the peak at 8 minutes is excess 2-aminobenzoic acid, and the peak at 12 minutes is the 2,4-quinazolinedione (cyanate) peak.

Mobile phase composition and flow rate were optimized to achieve full peak separation and short retention times. Separation was first achieved using an isocratic mobile phase of 86:14 5% TFA/acetonitrile (ACN) and a flow rate of 110 µL/min.

Environmental Concentrations

Cyanate concentrations ranged from 16 to 40 nM in samples collected from surface waters and at the depth of the fluorescence maximum along the CBM transect where salinities ranged from 16.4 to 27.8 (Table 3). In the coastal water samples salinities were higher: 31.8 and 33.2 at the surface and depth of maximum fluorescence, respectively. Cyanate concentrations in coastal North Atlantic waters were substantially lower: 1.44 nM in surface waters and 0.93 nM at the depth of the fluorescence maximum. Our LOD of 0.4 nM was sufficient for quantification of cyanate concentrations in all CBM and coastal samples, although the concentrations in coastal samples were very close to the detection limit. The absolute recovery was 98%, and the analytical recovery was 99% for both sets of samples, but the relative average deviation was 4% for samples in the CBM (n=2) and the relative standard deviation was 24% for the coastal samples (n=3) where cyanate concentrations were very close to the analytical detection limit. The measurements reported here from the Chesapeake Bay mouth and the North American mid-Atlantic continental shelf are the first measurements of cyanate concentrations from natural waters.

Table 3. Cyanate concentrations for representative Chesapeake Bay Mouth stations and one North Atlantic station.

		Depth 1			Depth 2		
Latitude (ºN)	Longitude (ºW)	Depth (m)	Salinity[1]	[OCN^-] (AD) (nM) [2]	Depth (m)	Salinity[1]	[OCN^-] (AD) (nM) [2]
36.987	76.163	1.9	18.1	30.0 (1.21)	12.1	27.8	26.6 (0.43)
37.013	76.152	1.3	18.6	27.3 (2.14)	5.1	19.4	16.6 (0.34)
37.046	76.137	1.4	16.4	29.7 (0.46)	4.0	17.6	34.7 (1.03)
37.072	76.113	1.4	16.7	41.1 (0.79)	8.7	26.1	33.8 (3.03)
37.833[3]	74.579	4.9	31.8	1.44 (0.41)	15.8	33.2	0.93 (0.18)

[1]Salinity measured in natural samples is a unitless value that roughly corresponds to parts per thousand.

[2][OCN^-] shown are the average of two replicates with the exception of the coastal station. Average deviation (AD) in parentheses.

[3]For the coastal station (final row), [OCN^-] is an average of three replicates.

CHAPTER III

SOURCES OF CYANATE TO MARINE SYSTEMS AND AN INITIAL SURVEY OF CYANATE DISTRIBUTION AND UPTAKE IN THE NORTH ATLANTIC

PREFACE

Part of the content of this Chapter is submitted to Environmental Science and Technology Letters. Due to size limitations of Environmental Science and Technology Letters, the Chapter presented here has been modified to expand the body of the manuscript and include supplemental information in the main text.

INTRODUCTION

Nitrogen (N) limits phytoplankton growth in most marine environments. Consequently, identifying sources and sinks of bioavailable N is critical for estimating oceanic primary and secondary productivity. While many dissolved organic nitrogen (DON) compounds are known to be bioavailable, much of that pool is uncharacterized (Sipler and Bronk 2015). Recently it was discovered that some microbes have the genetic capacity to take up and metabolize cyanate (OCN^-), perhaps the simplest DON compound. Genes encoding intracellular cyanate decomposition and a cyanate-specific transporter have been identified in marine cyanobacteria (Kamennaya and Post 2013; Palenik et al. 2003; Rocap et al. 2003). In addition, isolates of *Synechococcus* (WH8102), *Prochlorococcus* (MED4), the harmful dinoflagellate, *Prorocentrum donghaiense*, and some heterotrophic bacteria have been cultured using cyanate as the sole N source (Guilloton et al. 1993; Hu et al. 2012; Kamennaya and Post 2011), and cyanate was recently shown to support nitrification as both a reductant and N source in chemoautotrophic bacterial cultures (Palatinszky et al. 2015).

Prochlorococcus and *Synechococcus* account for two thirds of present day oceanic primary production (Bryant 2003), therefore cyanate utilization by these two groups could be globally significant and its biogeochemistry may affect global primary and secondary production. It has been hypothesized that the evolution of *Prochlorococcus* strains has been

driven by the availability of different N sources. Because *Prochlorococcus* have streamlined genomes containing only the genes necessary for survival (Bryant 2003; Garcia-Fernandez et al. 2004), it is likely that *Prochlorococcus* strains living in the modern ocean and containing cyanate-related genes utilize this compound in the environment.

Cyanate is produced by urea decomposition (Dirnhuber and Schutz 1948) and by decomposition of carbamoyl phosphate, an intermediate in numerous biochemical pathways (Jones 1963, Appendices B and C). As a simple molecule with chemical linkages common in organic matter, cyanate is likely produced by other largely unexplored biotic and abiotic processes in aquatic systems such as pyrimidine, protein and peptide decomposition. However, the abundance and distribution of cyanate and its reactivity in marine environments is unknown because, until recently, we lacked a sensitive method to quantify it. Cyanobacterial cyanate hydratase appears to have evolved early (Kamennaya and Post 2011) suggesting cyanate could have served as an N source for cyanobacteria living on the pre-oxygenated Earth (Allen and Jones 1964). Cyanate may have formed on the prebiotic Earth by electric discharges in the presence of the prebiotic gases N_2, CO_2, and H_2 (Danger et al. 2012; Yamagata and Mohri 1982), and it is possible that cyanate played important roles in early Earth biogeochemistry (Falkowski 1997), contributing to the abiotic synthesis of pyrimidines (Ferris et al. 1968), adenosine diphosphate (ADP) (Yamagata 1999), N-carbarmoyl amino acids (Commeyras et al. 2005), and peptides (Danger et al. 2006). Understanding cyanate cycling in the modern ocean may therefore give important clues to both present day and early Earth N cycling.

I have developed a method to measure cyanate in seawater (Widner et al. 2013), and here I provide the first observations of: 1) cyanate distributions in present day North Atlantic coastal waters, 2) cyanate production through biotic and abiotic processes, and 3) cyanate uptake by natural microbial communities.

MATERIALS AND METHODS

Sample Collection and Analysis of N compounds in the coastal North Atlantic

Samples and *in situ* field data were collected during a research cruise on the NOAA vessel, *R/V Henry B. Bigelow*, in the coastal North Atlantic Ocean, August 8-23, 2012 (Figure 5). Water samples were collected using twelve Niskin bottles mounted to a CTD rosette. Samples

for cyanate, urea, nitrate, nitrite, and ammonium analyses were filtered by gravity through a 0.2 µm membrane Millipore filter attached directly to the Niskin bottle and collected in duplicate sterile 15 mL polypropylene tubes. Three, 1 mL aliquots were transferred from the polypropylene tubes to acid-cleaned, combusted 4 mL amber glass vials for cyanate analysis. The remaining contents of the 15 mL tubes were stored at -20 °C for later analysis of urea, nitrate, nitrite, and ammonium concentrations.

Urea, nitrate, and nitrite concentrations were measured on an Astoria Pacific nutrient autoanalyzer using standard methods (Parsons et al. 1984). Ammonium was analyzed using the manual phenol-hypochlorite method (Solorzano 1969). Samples for cyanate analysis were derivatized at sea < 48 hours after collection and stored at -20 °C until they were quantified using high performance liquid chromatography (HPLC) (Widner et al. 2013). The method detection limits were 80, 70, 70, 40, and 0.4 nM for urea, nitrite, nitrate, ammonium, and cyanate analyses, respectively.

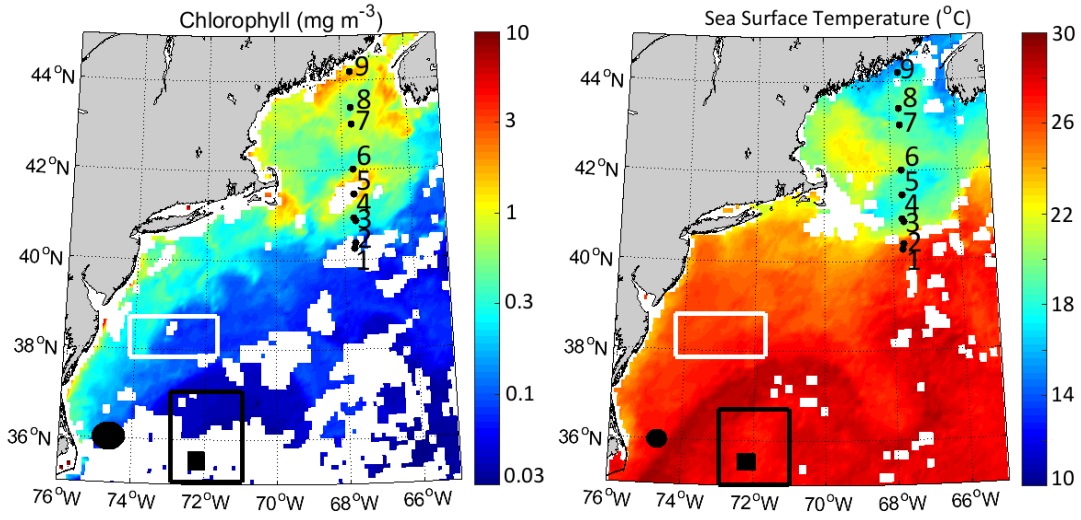

Figure 5. Station Locations for Chapter III. Mid-Atlantic Bight station (circle), Oligotrophic station (square), and the Gulf of Maine Transect stations (1-9), are superimposed on averages of satellite-derived sea surface chlorophyll (left) and temperature (right) during the sampling period for the August 2012 cruise. Six aerosol samples and three rain samples collected using the NADP sampler were collected inside the white box and three aerosol samples and two rain samples collected using the funnel were collected inside the black box.

Sample Collection and Analysis of N Compounds in a North Atlantic Oligotrophic Gyre

Samples and hydrographic data from the North Atlantic oligotrophic gyre were collected on August 9, 2014 aboard the *R/V Hugh Sharp* at 72.2 °West longitude and 31.5 °North latitude (Figure 5). Samples were collected using Niskin bottles mounted on a CTD rosette. Samples for cyanate, urea, nitrate, nitrite, and ammonium analysis were filtered using a peristaltic pump through a 0.2 µm membrane Millipore filter attached with cleaned silicone hosing to the Niskin bottle and filtrate was collected in sterile 15 mL polypropylene tubes for nitrate, nitrite, and urea, 2 mL sterile polypropylene tubes for cyanate, and 15 mL polypropylene tubes pre-conditioned with the orthophthaldialdehyde (OPA) reagent for ammonium analysis (Holmes et al. 1999). To minimize ammonium contamination from filtration, the filtration apparatus was plastic, and the filter was rinsed with 2 L of site water before sample collection began. Filtration is believed by many to contaminate nanomolar ammonium samples, but I consistently measured sample fluorescence equal to the reagent blank, and I consider filtration necessary to stabilize samples for short-term storage in the refrigerator. Nutrient samples were stored at 4 °C until analysis within 48 hours of collection for nitrate, nitrite, and urea and 24 hours for ammonium. Cyanate samples were stored at -80 °C until analysis within 1 year of collection.

Urea, nitrate, and nitrite were analyzed on an Astoria Pacific nutrient autoanalyzer according to the manufacturer's specifications and using standard colorimetric methods (Parsons et al. 1984). A waveguide was used for nitrate and nitrite to increase the sensitivity of these analyses (Zhang 2000). Ammonium was analyzed using the OPA method (Holmes et al. 1999) with modifications outlined by Taylor et al. (2007). Samples for cyanate analysis were thawed then derivatized immediately before quantification by HPLC (Widner et al. 2013). Detection limits were 80, 10, 10, 10, and 0.4 nM for urea, nitrate, nitrite, ammonium, and cyanate, respectively.

Atmospheric Deposition Measurements

Nine aerosol and five rain water samples were collected during the August 2014 cruise aboard the *R/V Hugh Sharp* (Figure 5). Aerosol and rainwater samplers were mounted on a platform above the ship's wheelhouse as far as possible from overhanging structures, masts, and cables. Samples were collected when the ship was steaming into the prevailing wind to avoid contamination from the ship's stacks and when there was minimal risk of contamination due to sea spray.

Aerosol samples were collected using a sampler equipped with a cascade impactor (Tisch Series 235) loaded with six acid-cleaned (0.5 N hydrochloric acid) Whatman 41 cellulose filters designed to capture particles in two size fractions (less than and greater than 1 μm) (Baker et al. 2003; Baker et al. 2007). One quarter of each filter was leached using 750 mL of nanopure water. The leachate was filtered (0.4 μm polycarbonate) and stored according to the methods described above for nutrient and cyanate analysis.

Two rainwater samples were collected using an automated N-Con Systems NADP rain water sampler and three rain water samples were collected using a trace-metal clean polyethylene funnel attached to a 2L low density polyethylene (LDPE) bottle by a Teflon collar (Sedwick et al. 2007). The rain collection funnel and bottle were removed from their mountings immediately after rainfall ceased and samples were filtered and stored as described above.

Photochemical Experiments

Water samples for the photochemical experiments were collected from three different water systems: the Dismal Swamp (freshwater site) on December 5, 2012, the Elizabeth River (estuarine site) on January 16, 2013, and the Virginia Beach oceanfront (coastal oceanic site) on January 13, 2013 (Table 1). Water was filtered through a 0.2 μm Supor filter using a vacuum pump pressure of less than 5 mm Hg, the salinity was determined using a refractometer, and samples were stored in amber glass bottles until irradiation on January 16, 2013. Samples were irradiated in a solar simulator which mimicked springtime noon sunlight in the UV range between 295 and 365 nm (Helms et al. 2008; Minor et al. 2006). Nine quartz tubes for each water type were prepared, 3 of which were wrapped in aluminum foil, and placed in the solar simulator. After 2, 4, and 8 hours , duplicate quartz tubes and a dark tube were removed from the solar simulator to measure cyanate concentrations. The absorbance of each sample at 300 nm was determined using an Agilent 8453 UV-Vis Diode Array Spectrophotometer to account for differences between samples of different matrices. Photoproduction rates were normalized to the sample absorptivity at 300 nm (Bushaw-Newton and Moran 1999). Here, I report both absolute and normalized photoproduction rates (Table 1).

Culture Experiments

Cultures of two diatoms (*Thalassiosira pseudonana* and *Thalassiosira oceanica*) and one cyanobacterium (*Synechococcus* FWRI isolate CCFCW 502) were grown on f/2 media (Guillard

1975) with sodium silicate added for diatom cultures in quadruplicate bottles. All cultures were incubated in batch in loosely capped 1 L acid-washed and combusted borosilicate bottles under fluorescent lighting (39.5 uE m^{-2} s^{-1}) supplied on a 12 h light/ 12 h dark cycle. *T. pseudonana* and *Synechococcus* were incubated at 21 °C and *T. oceanica* was incubated at 25 °C. The *Thalassiosira* cultures were axenic prior to the experiment, but I microscopically confirmed the presence of bacteria after the cultures had incubated for one week. Non-autofluorescent bacteria were present in the *Synechococcus* cultures both before and during the experiment. *In vivo* fluorescence and cyanate concentrations were monitored daily for 17 days and then biweekly for 40 additional days. When cultures reached senescence, as determined by *in vivo* fluorescence, two culture bottles were placed in 24 hour darkness, while the other two bottles were maintained under the original light/dark cycle. At each time point, each culture bottle was tightly capped and gently inverted 3 times and then a 15 mL aliquot was removed using a sterile pipette to measure *in vivo* fluorescence on a Turner TD-700 Fluorometer equipped with a PN 7000-962 optical filter kit (436 nm excitation, 680 nm emission). This sample was then filtered through a 0.2 µm sterile Supor filter, and the filtrate was transferred to a sterile polypropylene tube and stored at -80 °C until cyanate analysis. Abiotic controls consisting of sterile f/2 media in acid-washed, combusted borosilicate bottles were also incubated and sampled at each time point for cyanate.

Nitrogen Uptake

Uptake of N from NH_4^+, NO_3^-, NO_2^-, urea, and cyanate was measured at 3 depths at a station in the oligotrophic North Atlantic during a cruise aboard the *R/V Hugh Sharp* (72.2 °W, 31.5 °N, Figure 5) using stable isotopes as tracers. Incubations were initiated with the addition of 100 nM of highly enriched (96-99%) ^{15}N-labeled substrate. Samples were incubated for two hours at simulated *in situ* temperature and light conditions in a flow-thru deck incubator under neutral density screens. After two hours, incubations were filtered through pre-combusted GF/F filters. Particulate isotope enrichment was measured using a Europa 20/20 isotope ratio mass spectrometer equipped with an automated N and C analyzer. Uptake rates were calculated using a mixing model (Montoya et al. 1996; Mulholland et al. 2006; Orcutt et al. 2001). When ambient substrate concentrations were below detection, as was the case at most depths for urea, ammonium, and nitrite, a value one half that of the detection limit was used to calculate the uptake rate. This may have caused an over-estimation of some uptake rates.

Satellite Data

Sea surface temperature data are from MODIS, and sea surface chlorophyll data are from SeaWIFS and MODIS-Aqua obtained from the Ocean Biology Processing Group at the Goddard Space Flight Center, Greenbelt, MD. Both are averages over the cruise dates (August 8-23, 2012).

Gulf of Maine Section Plots

The Gulf of Maine section plots were constructed using Ocean Data View (Schlitzer, R., Ocean Data View, http://odv.awi.de, 2014).

RESULTS AND DISCUSSION

Vertical profiles of cyanate were measured in the North Atlantic Ocean on the continental slope near the Mid-Atlantic Bight (MAB, Figure 5). Cyanate, urea, nitrite, and ammonium concentrations exhibited surface minima, consistent with biological consumption in the photic zone, and subsurface maxima, indicative of excess production over consumption at the base of the photic zone (Figure 6). Profiles of this shape are generally thought to reflect the balance of biological consumption in surface waters, production in subsurface waters as a result of remineralization, and oxidation to nitrate below the nitracline (Gruber 2008). Therefore, I infer that cyanate is biologically labile. Because cyanate exhibited vertical distributions similar to urea, ammonium, and nitrite, it is likely that, cyanate production and consumption processes are similar to or linked with those N compounds at the Mid-Atlantic Bight. Profiles of ammonium and nitrite generally reflect rates of removal through phytoplankton uptake in surface waters and ammonification and ammonium and nitrite oxidation (nitrification) in subsurface waters and rates of production through excretion and organic matter degradation (Gruber 2008; Lomas and Lipschultz 2006). Recent evidence suggests that cultured nitrifying bacteria can also oxidize cyanate when ammonium is unavailable (Palatinszky et al. 2015). If this process happens in the environment, it may partially explain the subsurface cyanate maximum as well as the depletion of cyanate below approximately 200 m. The gradual depletion of cyanate in deep waters, is likely due to abiotic and/or biotic degradation of cyanate to ammonium followed by nitrification. Although maximal cyanate concentrations were lower than those of urea, ammonium, and nitrite,

cyanate utilization and remineralization can still be quantitatively important if its production and consumption are tightly coupled as has been shown for ammonium (Gruber 2008).

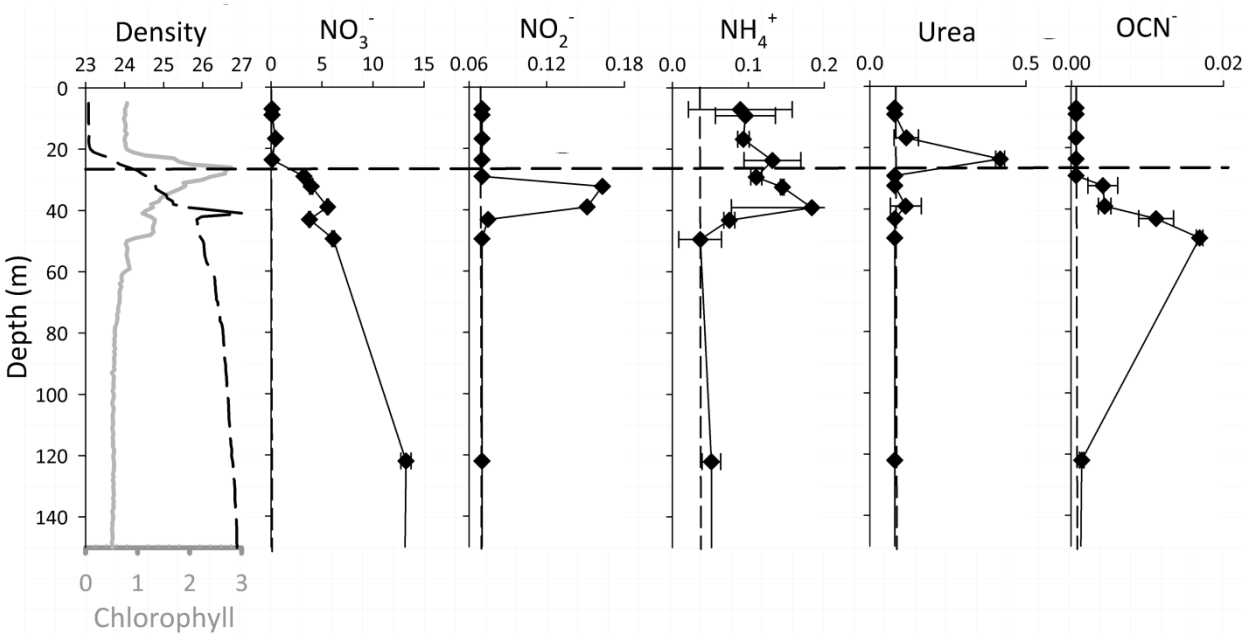

Figure 6. Cyanate Distribution at the Mid-Atlantic Bight. Vertical profiles of density (black dashed line, sigma theta, kg m^{-3}), chlorophyll *a* (grey solid line, mg m^{-3}), nitrate (NO_3^-) (μM), nitrite (NO_2^-) (μM), ammonium (NH_4^+) (μM), urea (μM), and cyanate (OCN^-) (μM) from a Mid-Atlantic Bight station. The dashed vertical lines are the method detection limits (S/N=3), and the dashed horizontal line indicates the depth of the chlorophyll maximum. Concentrations below the detection limit were plotted as equal to the detection limit. Error bars are ± 1 standard deviation.

To determine whether the relationship between cyanate distributions and those of other simple N compounds is consistent across a highly productive coastal environment, cyanate, ammonium, nitrite, and nitrate distributions were examined with respect to salinity, temperature and chlorophyll *a* concentrations in a physically, biologically, and chemically heterogeneous shallow coastal region in the Gulf of Maine (GOM). Vertical profiles were measured at nine stations along a south to north transect from the continental shelf slope, across Georges Bank

(GB) and the GOM to the coast of Nova Scotia (Figures 5 and 7, Appendix E). Cyanate was generally more abundant on GB and in the GOM than in the more oligotrophic Gulf Stream-influenced slope waters. At stations on the slope and interior GOM basin, there were cyanate peaks below the chlorophyll maximum similar to what was observed in the MAB (Figure 7). However, on GB and at the nearshore station, elevated surface cyanate concentrations were coincident with weak stratification and high surface chlorophyll *a* concentrations, and on GB, cyanate and chlorophyll *a* concentrations were also high near the bottom suggesting a possible sedimentary source of cyanate (Figure 7). At these stations ammonium, nitrite, and nitrate were depleted in surface waters (Figure 7).

To help explain the vertical distributions of cyanate concentrations, I evaluated cyanate production from organic matter degradation. In the *Thalassiosira* cultures, cyanate concentrations increased linearly as biomass decreased during late stationary phase. Cyanate production slowed and stopped when cultures were placed in the dark but continued to increase in cultures supplied light (Figure 8 A-D), suggesting that cyanate was produced by a light-sensitive process such as N release by senescent diatoms. Cyanate production continued at the same rate in the *T. pseudonana* cultures during senescence and when the cultures began growing exponentially again after 40 days without additional nutrient amendments or transfer (Figure 8A). Cyanate did not accumulate in the *Synechococcus* cultures possibly because they didn't produce it or because it was taken up at rates similar to production. Tight coupling between production and consumption has been observed for other reduced N compounds (Gruber 2008).

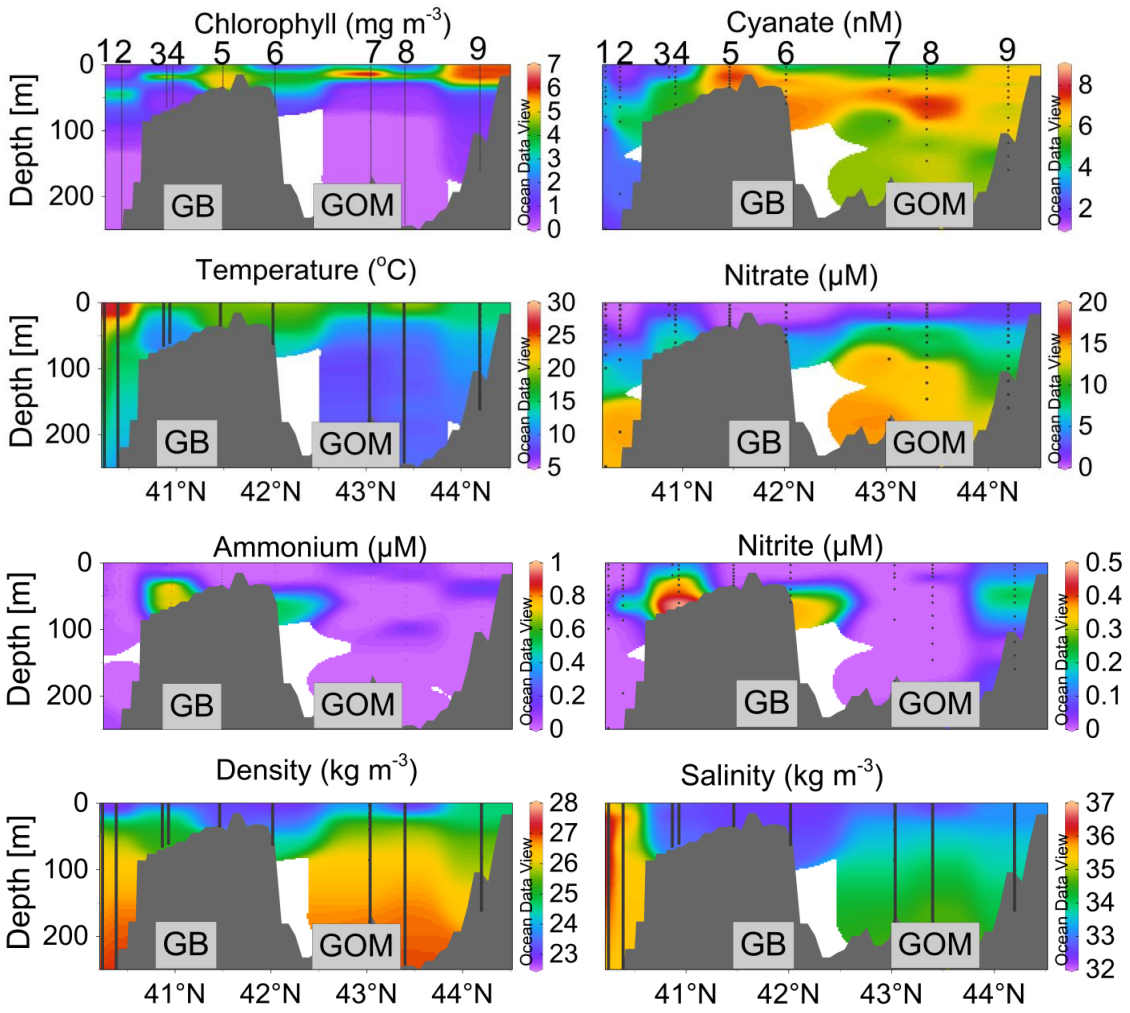

Figure 7. Cyanate and Dissolved Inorganic Nitrogen Distributions in the Gulf of Maine.Chlorophyll *a* (mg m^{-3}), temperature (^{o}C), cyanate (nM), nitrate (µM), ammonium(µM), nitrite (µM), density (sigma theta, kg m^{-3}), and salinity (kg m^{-3}) along a transect in the Gulf of Maine here the colored contours represent interpolations of the given parameters between data points and data points are represented by grey lines and dots for continuous and discrete profiles, respectively. To the left is the offshore station (station 1, Figure 5) and to the right is the nearshore station (station 9, Figure 5). The Gulf of Maine (GOM) and Georges Bank (GB) are indicated in grey boxes. See Appendix E for cyanate, nitrate, ammonium, and nitrite concentrations.

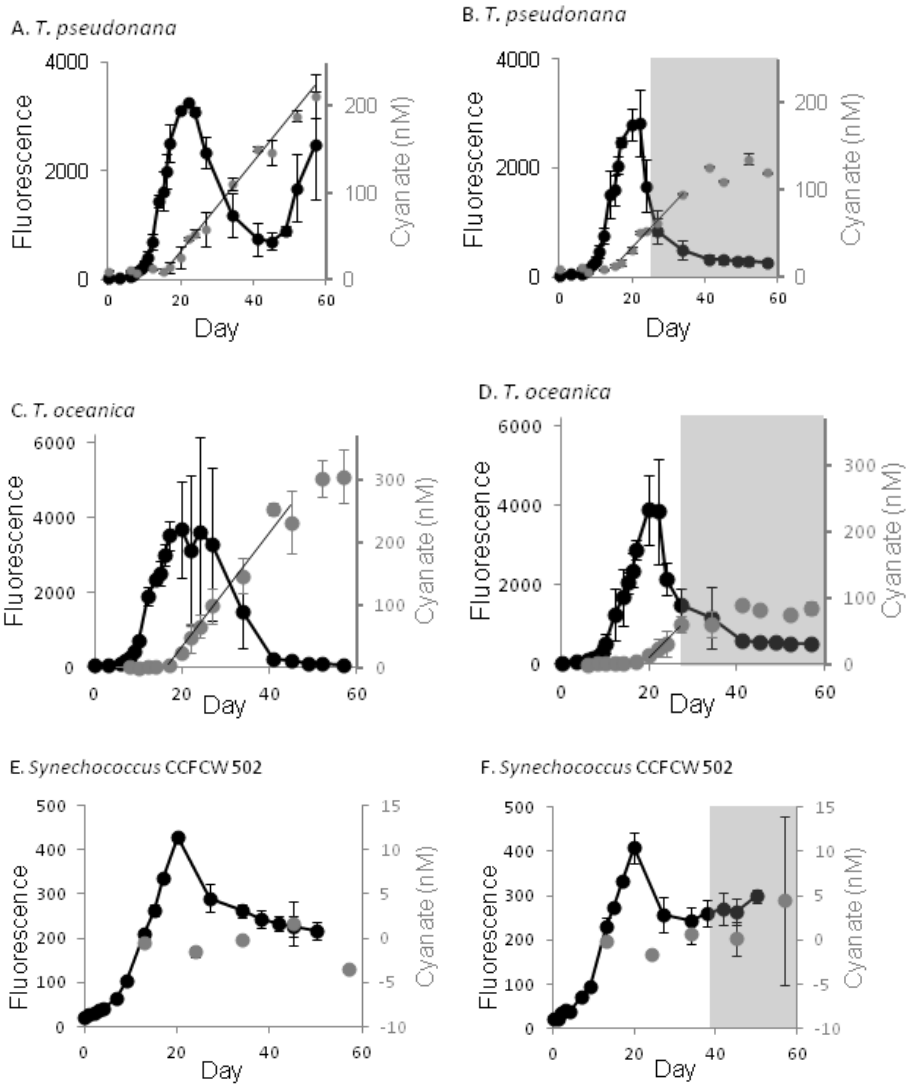

Figure 8. Cyanate Production in Phytoplankton Cultures. The cultures were *Thalassiosira oceanica* (A and B), *Thalassiosira pseudonana* (C and D), and *Synechococcus* CCFCW 502 (E and F). Cultures maintained on a 12 hour light/dark cycle for the entire experiment are shown in panels A, C, and E, and cultures that were transferred to 24 hour darkness after reaching stationary phase are shown in panels B, D, and F where the shaded area indicates when the cultures were placed in the dark. *In vivo* fluorescence was used as a proxy for biomass and is shown in black, and cyanate concentrations corrected for sterile controls are shown in grey. Error bars are ± 1 standard deviation (n=2). Cyanate production rates during the linear portions were 5.0, 4.5, 9.1, and 6.5 nM d^{-1} in *T. pseudonana* cultures in the light and dark and *T. oceanica* cultures in the light and dark, respectively (R^2 0.97, 0.97, 0.93, and 0.94, respectively; all slope p-values <0.0001).

The vertical zonation of microbial communities with respect to light, physical gradients, and availability of nitrogenous substrates results in separation of nutrient regeneration processes by depth and the sequential accumulation of N cycle intermediates within and below the euphotic zone (Meeder et al. 2012). In vertical profiles collected from the MAB (Figure 6), the cyanate maximum was below that of urea indicating that cyanate might be produced from urea decomposition, analogous to the observation that nitrite accumulates below the ammonium maximum as a result of nitrification (Meeder et al. 2012). There is currently no known mechanism for biotic conversion of urea to cyanate, but abiotic decomposition of biologically produced urea and carbamoyl phosphate have been proposed as sources of cyanate production in marine systems (Kamennaya et al. 2008). Because C-N linkages are so common in organic matter it is also likely that there are many other pathways of cyanate production and decomposition, both biotic and abiotic, that remain to be discovered. Phytoplankton are also known to release labile metabolic intermediates when stressed (Bronk and Steinberg 2008), and so it is possible that *T. pseudonana* and *T. oceanica* directly released cyanate or that they released urea or carbamoyl phosphate which then degraded to cyanate either abiotically or through unknown biotic pathways. Direct phytoplankton release could explain the light-dependence of cyanate production in *Thalassiosira* cultures and the elevated cyanate concentrations correlated with high chlorophyll fluorescence on GB and at the nearshore end of the GOM transect. Organic matter degradation could also explain this trend and that of cyanate accumulation below the subsurface chlorophyll maxima.

Atmospheric N deposition (AND) can provide N for new production and contribute to eutrophication in the coastal ocean (Howarth and Marino 2006). Gaseous isocyanic acid (HOCN) is released by fossil fuel combustion (Nicholls and Nelson 2000), biomass burning (Roberts et al. 2011), and atmospheric photoproduction (Roberts et al. 2011). This isocyanic acid could be deposited to marine systems through precipitation (wet deposition) and through direct contact of aerosol particles and gases with the ocean surface (dry deposition). I measured wet and dry deposition of cyanate to the seasonally oligotrophic western North Atlantic which is known to receive large inputs of atmospheric N. Cyanate was below the limit of detection (0.4 nM) and urea was less than 1 μM in all and most rain water samples, respectively although dissolved inorganic nitrogen was present at micromolar concentrations in both wet and dry deposition samples (C. Sookhdeo pers. comm.). Isocyanic acid is rapidly hydrolyzed in clouds,

resulting in a lifetime of two hours to five days, depending on cloud encounter rates (Barth et al. 2013) and so any cyanate present in the air mass over land would likely have degraded to ammonium before deposition and so its absence from rain water is not entirely unexpected.

I observed cyanate photoproduction rates ranging from 0.4 to 14 nM h^{-1} (Figure 9, Table 4). These rates were similar in magnitude to previously reported ammonium and amino acid photoproduction rates (Mopper et al. 2015). Photoproduction of cyanate could have contributed to the elevated surface cyanate concentrations on GB and at the nearshore end of the GOM transect, particularly if biotic uptake was lower than photoproduction as has been observed for other simple organic compounds (Kieber et al. 1989). Alternatively, GOM coastal waters experience dense algal blooms which could produce large amounts of labile dissolved organic matter including cyanate and/or cyanate precursors. Cyanate production from degrading organic matter could occur within dense algal blooms, just below them, or in the sediments where they are deposited. Cyanate can then accumulate in place or nearby, depending on the rate of its production and circulation patterns. High cyanate concentrations near the coast relative to continental slope waters south of GB (Figure 7) could also indicate terrestrial cyanate sources, including urban, industrial, and agricultural runoff and decomposition of N compounds therein (such as urea and organic matter) to cyanate (Dirnhuber and Schutz 1948; Glibert et al. 2006). Cyanate is not monitored in industrial or municipal wastewater discharges (Johnson 2015) so it is not known whether they are significant sources of cyanate to receiving waters.

When I compared cyanate uptake rates with those of nitrate, nitrite, ammonium, and urea, I found that cyanate contributed up to 10% of total N uptake, and cyanate uptake rates were comparable to those of nitrate and nitrite but lower than those of ammonium and urea which together accounted for > 50% of total N uptake (Figure 10, Table 5). As for other N compounds, cyanate uptake was higher near the surface corresponding to lower cyanate concentrations (< 1 nM) than at the chlorophyll fluorescence maximum where cyanate concentrations were highest (Figure 10A). Cyanate turnover times were 1.6 and 76 hours in surface waters and at the chlorophyll maximum, respectively, which were shorter than turnover times calculated for nitrate and nitrite (Table 5).

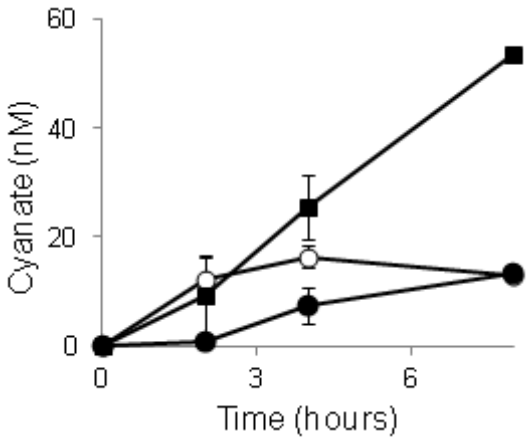

Figure 9. Cyanate Photoproduction. The samples irradiate were sterile (0.2 μm filtered) fresh (open circles), estuarine (squares), and coastal oceanic (closed circles). The cyanate concentrations shown are the concentration measured in each sample less the cyanate concentration in the corresponding dark control. Error bars are ± 1 standard deviation (*n*=2).

Table 4. Cyanate Photoproduction Rates.

	Latitude (°N)	Longitude (°W)	Salinity	Production Rate (nM h^{-1})			Normalized Production Rate (nM m h^{-1})[1]		
				1[2]	2	3	1	2	3
Great Dismal Swamp	36.600	76.382	0	5.6 (0.7)	2.3 (0.1)	-1.4 (0.4)	0.1 (0.0)	0.05 (0.0)	-0.02 (0.0)
Elizabeth River	36.886	76.319	20	4.4 (0.0)	8.4 (3.2)	14 (0.1)	5.5 (0.0)	10.4 (4.1)	17.5 (0.1)
Virginia Beach	36.903	75.988	29	0.4 (0.4)	3.4 (1.4)	2.6 (0.5)	2.4 (2.2)	20.9 (8.6)	15.8 (3.2)

[1] Normalized rates were the production rate normalized to the absorbance at 300 nm.
[2] Rates were calculated for the first two hours (1), second 2 hours (2), and final 4 hours (3).

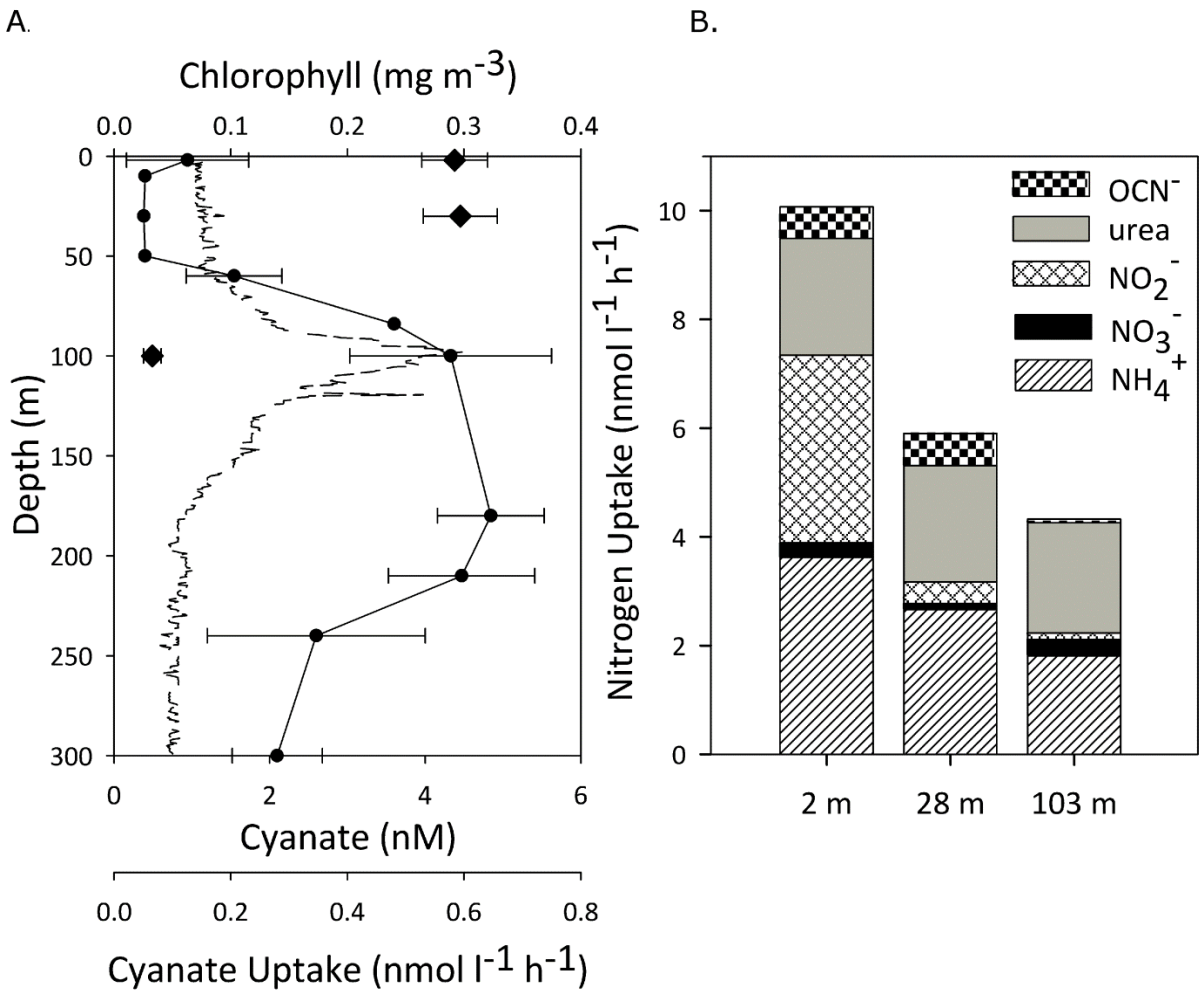

Figure 10. Cyanate and Total Nitrogen Uptake in at the North Atlantic Oligotrophic Station. A) Cyanate uptake (diamonds), cyanate concentration (circles), and chlorophyll fluorescence (dashed line). Error bars are ± 1 standard deviation (n=3). B) Total N uptake at each depth as the sum of ammonium (diagonal lines), nitrate (solid black), nitrite (hatched), urea (solid grey), and cyanate (black and white checked) uptake.

Table 5. Concentration, Uptake Rates, and Turnover Times of N compounds at the Oligotrophic Station.

Depth (m)		Nitrate	Nitrite	Ammonium	Urea	Cyanate
	Concentration (nM)	29.0	b.d.l.[1]	b.d.l.	b.d.l.	0.9
2	Uptake (nmol l^{-1} h^{-1})	0.3(0.1)[2]	3.5(0.6)	3.6(0.2)	2.1(0.2)	0.6(0.1)
	Turnover Time (h)	109.9	NA[3]	NA	NA	1.6
	Concentration (nM)	b.d.l.	36.0	b.d.l.	b.d.l.	b.d.l.
28	Uptake (nmol l^{-1} h^{-1})	0.1(0.1)	0.4(0.1)	2.7(1.8)	2.1(1.0)	0.6(0.1)
	Turnover Time (h)	NA	90.8	NA	NA	NA
	Concentration (nM)	691.0	46.0	b.d.l.	b.d.l.	5.0
103	Uptake (nmol l^{-1} h^{-1})	0.3(0.0)	0.1(0.1)	1.8(0.3)	2.0(1.0)	0.1(0.0)
	Turnover Time (h)	2217	402.9	NA	NA	76.1

[1] b.d.l. signifies a concentrations below the method detection limit.
[2] Standard deviations (n = 3) are in parentheses.
[3] Turnover times could not be calculated when concentrations were below the limit of detection.

The distribution of cyanate and the similarity in magnitude of production and community uptake rates relative to those of other dissolved N compounds suggests that cyanate is an important component of nitrogen cycling in coastal marine environments and that its production and consumption are tightly coupled. Here I provide the first comprehensive set of measurements comparing the distributions of cyanate to those of other biogeochemically important N compounds in the ocean. I also demonstrate for the first time that cyanate can be produced via decomposition of phytoplankton and photoproduction, and that cyanate uptake is quantitatively important in the environment. However, many questions remain regarding the biotic and abiotic sources and sinks of cyanate in disparate marine environments, the organisms and biochemical pathways that produce and consume cyanate in the present day ocean, regional and seasonal trends in cyanate biogeochemistry, and its possible role in the evolution of life.

CHAPTER IV

CYANATE DISTRIBUTION AND UPTAKE IN NORTH ATLANTIC COASTAL WATERS

PREFACE

The content of this Chapter is submitted for publication in *Limnology and Oceanography*.

INTRODUCTION

Nitrogen (N) limits phytoplankton growth and primary productivity in much of the world's oceans, yet the majority of the dissolved organic nitrogen (DON) pool remains uncharacterized and therefore the biogeochemical reactivity of most DON compounds unknown (Sipler and Bronk 2015). Cyanate (OCN^-) is arguably the simplest organic N compound, and it is a source of N for marine microbial communities (B. Widner et al. unpubl.). Genes for cyanate metabolism evolved early suggesting cyanate could have contributed to cyanobacterial evolution. These genes were likely more common in ancestral cyanobacteria than they are today (Kamennaya and Post 2011).

In modern cyanobacteria, cyanate uptake and intracellular decomposition is encoded by an ABC-type cyanate-specific transporter (*cynABD*) (Espie et al. 2007) and a cyanate lyase (*cynS*) which catalyzes bicarbonate-dependent decomposition of cyanate to ammonium (NH_4^+) and carbon dioxide (CO_2) (Anderson et al. 1990). *cynABDS* was identified in cultured strains of the marine cyanobacteria *Prochlorococcus* and *Synechococcus* (Palenik et al. 2003; Rocap et al. 2003) and later identified in natural cyanobacterial populations from diverse geographical regions including the Red Sea, Southern Ocean, Mediterranean Sea, Indian Ocean (Kamennaya and Post 2013), and temperate North Pacific Ocean (A. Post pers. comm.) leading to the hypothesis that cyanate may serve as a N source for these ubiquitous organisms. A second cyanate lyase, *cynH*, has been identified in cyanobacteria (Kamennaya and Post 2011), and a putative cyanate transporter, *cynX*, has been identified in some environmental microorganisms, including an aquatic bacterium, *Chromobacterium violaceum*, and a marine ammonium oxidizing bacterium, *Nitrosococcus oceani* (Anderson et al. 1990; Carepo et al. 2004; Klotz et al. 2006; Pao et al. 1998). To our knowledge, no cyanate transporter has been identified in

eukaryotes, but *cynS* has been identified in species of animals, plants, and fungi as well as some bacteria (Guilloton et al. 2002) and archaea (Spang et al. 2012).

The marine phytoplankton *Prochlorococcus* MED4, *Synechococcus* WH8102, and *Prorocentrum donghaiense* have been cultured on cyanate as the sole N source (Hu et al. 2012; Kamennaya et al. 2008; Palenik et al. 2003), as has an ammonium oxidizing archaea, *Nitrososphaera gargensis*, which also utilized cyanate as the sole reductant, oxidizing cyanate N to nitrite (Palatinszky et al. 2015). Bacteria that have been grown on cyanate as the sole N source include *Escherichia coli* (Guilloton and Karst 1987), *Pseudomonas fluorescens* (Dorr and Knowles 1989), and *Methylobacterium thiocyanatum* (Wood et al. 1998). Cultures of *Synechococcus sp.* PCC6301 took up cyanate C (Espie et al. 2007), and coastal microbial populations had a high affinity for cyanate, similar to those measured for ammonium, nitrate, and urea (Mulholland and Lomas, 2008; Chapter III). Using a newly developed sub-nanomolar assay we measured cyanate concentrations from 0.9 to 40 nM in samples from the Chesapeake Bay and Mid-Atlantic Bight (Widner et al. 2013), and on the North Atlantic continental shelf and slope cyanate accumulated below the deep chlorophyll maximum (DCM) but was depleted in surface and deeper waters (Chapter III), a distribution that has also been observed for nitrite and ammonium (Gruber 2008) and is suggestive of net consumption in surface waters and production below.

In this study, we measured cyanate concentrations in coastal waters at 35 stations from Cape Hatteras to Nova Scotia including stations in the Mid-Atlantic Bight, Gulf of Maine, and Georges Bank. We also measured cyanate concentrations and N- and C- specific cyanate uptake during four cruises to the study region in three seasons, and we evaluated trends in uptake rate by season, geographical region, and depth.

METHODS

Study Site and Sample Collection

Cyanate uptake was measured in samples collected during cruises aboard the NOAA Ship *Delaware II* during May 26 - June 9, 2010, November 6-21, 2010, June 3-15, 2011, and aboard the NOAA Ship *Henry B. Bigelow* during August 8-23, 2012 at stations selected at random as part of the NOAA Ecological Monitoring (EcoMon) program. Randomized sampling was

advantageous for this study because these were the first measurements of cyanate uptake and a more focused sampling strategy may have biased the results. Cyanate concentrations were measured during the August 2012 cruise at stations selected nonrandomly by the EcoMon program to monitor nutrient distributions and fluxes within important basins and at major estuarine outflows. The region sampled was a portion of the North American North Atlantic continental shelf and slope between Cape Hatteras and Nova Scotia (65-76°W, 35-45 °N). The study site is characterized by three distinct ecoregions: the Mid-Atlantic Shelf (MAS), the Gulf of Maine (GOM), and Georges Bank (GB; Figure 11). Water samples were collected and vertical profiles of temperature, salinity, chlorophyll fluorescence, and photosynthetically active radiation (PAR) were measured to a maximum depth of 500 m using a CTD mounted to a 12 Niskin rosette. Euphotic depth was calculated as the depth at which PAR was 1% of surface irradiance, and mixed layer depth (MLD) was defined as a sigma-t change of 0.125. Chlorophyll inventory was calculated using trapezoidal integration of the continuous chlorophyll profile collected by the CTD.

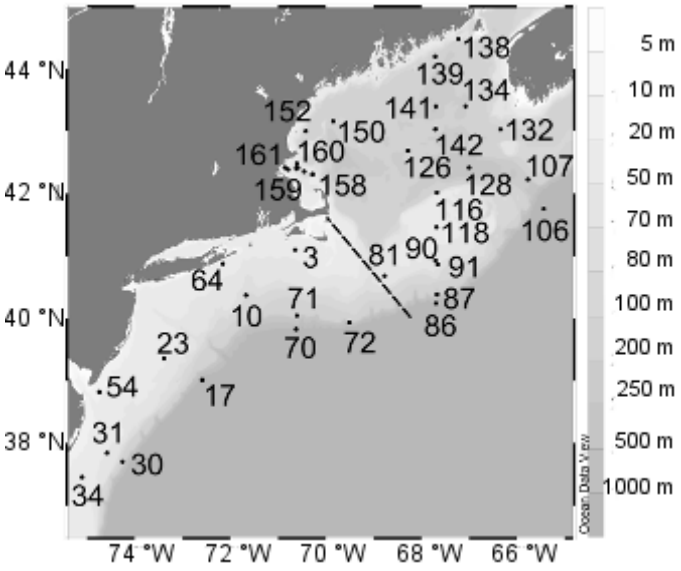

Figure 11. Distribution stations from August 2012. The dotted line represents the division between the Mid-Atlantic Shelf (MAS) and Gulf of Maine/Georges Bank (GBGOM) study regions, and the shading represent bathymetry.

Water samples for nitrate, nitrite, ammonium and cyanate analyses were collected from the Niskin bottles by gravity filtering (0.2 μm Millipore filter) water directly into duplicate polypropylene conical tubes (15 ml) for ammonium and single polypropylene conical tubes (15 ml) for nitrate and nitrite. Sub-samples were then transferred from the polypropylene tubes into 3 amber glass vials (4 ml) for cyanate analysis. The remaining samples were frozen and stored at -20 °C until analysis.

Nutrient and Chlorophyll a Analysis

Nitrate and nitrite and were analyzed on an autoanalyzer using standard methods (Parsons et al. 1984). Ammonium was measured using the phenol hypochlorite method (Solorzano 1969). Detection limits were 70, 70, and 40 nM for nitrate, nitrite, and ammonium, respectively. The nitracline depth was calculated as the middle depth between the first sample with a concentration > 100 nM and the sample above it (Dore and Karl 1996). Chlorophyll *a* samples were collected onto GF/F filters (0.7 μM) and analyzed fluorometrically (Welschmeyer 1994).

Cyanate Analysis and Modifications to Method

Cyanate was derivatized at sea in the amber vials and stored at -20 °C until analysis using high performance liquid chromatography (HPLC) with modifications to the Widner et al. (2013) method. We encountered some anomalously high and variable data that was likely the result of sample contamination. We believe this occurred at sea as the derivatization process requires manipulation steps during which the samples could have been exposed to airborne contaminants. We therefore recommend sample storage at -80 °C and derivatization in a more controlled laboratory environment.

Derivatized samples contain 6 N hydrochloric acid which damaged the HPLC autosampler after repeated use leading to irregular injection volume, injection of bubbles, and costly instrument repairs. To ameliorate this problem, we neutralized the samples by adding 10 N sodium hydroxide (0.72 mL) to 0.9 mL derivatized sample in a 2 ml combusted amber vial. A precipitate formed upon addition of NaOH, and so, when the samples reached room temperature we inverted them 5 times and waited for the precipitate to settle to the bottom prior to injection on the HPLC. The needle height was adjusted to prevent injection of the precipitate, and the autosampler chiller was turned off to prevent sample stratification from uneven cooling. We found that derivatized, neutralized samples were stable up to 72 hours at room temperature. The

mobile phase was adjusted to 70:30 5% TFA/ 100% methanol, and the flow rate and sample injection volume were adjusted to 200 µL/min and 400 µL, respectively.

All cyanate, nitrate, nitrite, and ammonium concentrations can be found in Appendix F, and a link to the CTD data can be found in Appendix G.

Uptake Methods

Cyanate uptake was measured in water collected from the surface and the DCM depth on each cruise. Whole water from each depth was transferred from Niskin bottles into 10 L carboys from which 500 ml PETG incubation bottles were filled for tracer experiments. When weather conditions did not permit deployment of the CTD rosette, surface water was collected from the ships' flow-through systems which were located at depths of approximately 3.7 and 5 m on the bows of the NOAA Ships *Delaware* and *Bigelow*, respectively, and were cleaned with 5% bleach or flushed with freshwater before each cruise for the *Delaware* and *Bigelow*, respectively. Uptake experiments were initiated by amending incubation bottles with $^{15}N^{13}C$ - labeled potassium cyanate ($KO^{13}C^{15}N$). Our intent was to make trace additions (2-10%) to avoid perturbing the community and thereby obtain realistic rates of *in situ* cyanate uptake (Mulholland et al. 2009). In May/June 2010, marine cyanate concentrations were unknown, so we added 100 nM $KO^{13}C^{15}N$ so that tracer additions of cyanate were the same as those used to measure ammonium, nitrite, nitrate, and urea uptake (M. R. Mulholland pers. comm.). Prior to the November 2010 cruise, we made the first measurements of cyanate in a Chesapeake Bay estuary and found that concentrations were < 50 nM (Chapter II). Consequently, on the remaining cruises, we decreased tracer additions to 30 nM. This addition was greater than 10% of the *in situ* cyanate concentrations during the 4th cruise and so it is possible that uptake was stimulated by the tracer addition in some or all of our experiments.

Bottles were incubated in one of two deck incubators equipped with flow-through surface seawater to maintain surface water temperature and neutral density screens to reduce incident light to approximately 55% and 30% of ambient. After two hours, each sample was filtered through a combusted GF/F filter (0.7 µM), rinsed with filtered seawater, placed in a sterile cryovial, and stored at -20 °C. Upon return to the laboratory, filters were dried at 40 °C, pelletized in tin capsules, and analyzed on a Europa 20/20 isotope ratio mass spectrometer equipped with an automated N and C analyzer. Uptake rates were calculated using a mixing model (Montoya et al. 1996; Mulholland et al. 2006; Orcutt et al. 2001). On cruises where

cyanate concentrations were not measured (May/June 2010, November 2010, June 2011), the average cyanate concentration from August 2012 (3 nM) was used to calculate cyanate uptake rates. Limits of detection (LOD) were calculated as the uptake rate calculated when the atom percent enrichment was equal to the LOD of the mass spectrometer (3 x the standard deviation of 7 standards of 12.5 µg N/ 100 µg C). Because the LOD was influenced by incubation time and particulate N and C concentrations, we calculated an individual LOD for each experiment and used that number to determine if the corresponding rate was below the LOD (BDL). The average LODs were 0.02 and 0.03 nmol l^{-1} h^{-1} for N and C uptake, respectively and ranged from < 0.01 to 0.13 and < 0.01 to 0.05 nmol l^{-1} h^{-1} for N and C, respectively. In statistical calculations uptake rates that were BDL were reported as 0.01 nmol l^{-1} h^{-1}.

Calculation of cyanate production from abiotic urea decomposition

Abiotic urea decomposition to cyanate and cyanate decomposition to NH_4^+ are first order reactions (Equations (1) and (2)) (Amell 1956; Dirnhuber and Schutz 1948; Hagel et al. 1971).

$$\text{urea} \rightarrow \text{cyanate} + NH_4^+ \quad (1)$$

$$\text{cyanate} \rightarrow NH_4^+ + CO_2 \quad (2)$$

Hypothetical cyanate production from abiotic urea decomposition was calculated using two methods. For both methods, we assumed a urea concentration of either the mean or maximum observed by Filippino et al. (2011) in the Mid-Atlantic Bight (0.1 and 0.6 µM, respectively). First, a cyanate production rate was calculated using the urea decomposition rate constant that Hagel et al. (1971) developed in a sodium nitrate solution with ionic strength 0.25 at 25 °C (k, 5.04e-8 min^{-1}) according to Equation (3).

$$\text{rate} = k * [\text{urea}] \quad (3)$$

Then a new k was calculated from the NH_4^+ production experiments of Kamennaya and Post (2008) and utilized to calculate urea decomposition to cyanate. Because one mole of urea produces one mole of NH_4^+ during decomposition (Equation 2) and another mole of NH_4^+ is produced following the decomposition of the cyanate produced (Equation 3), the abiotic NH_4^+ production rate can be calculated from Equation (4) where $rate_{urea}$ is the rate of urea decomposition (Equation 2), $rate_{cyanate}$ is the rate of cyanate decomposition (Equation 3), and $rate_T$ is the total rate of NH_4^+ production from urea. To make this calculation, we assumed that abiotic decomposition of urea and cyanate were the only processes consuming urea, producing

and consuming cyanate, and producing NH_4^+ and that the rates of reverse reactions were negligible.

$$rate_{cyanate} + (2 \times rate_{urea}) = rate_T \qquad (4)$$

Kamennaya and Post (2008) measured production of NH_4^+ from 20 µM urea and cyanate in solutions of abiotic Sargasso seawater. NH_4^+ production from urea and cyanate was 8.3 and 19.3 nmol l^{-1} h^{-1}, respectively. We used these production rates and Equation (1) to calculate a cyanate production rate constant (k) of 0.00028 h^{-1} from 20 µM urea. This rate constant was substituted into Equation (1) to calculate a hypothetical cyanate production rate in the Mid-Atlantic Bight based on urea concentrations observed there by Filippino et al. (2011).

Statistics

All statistical analyses were performed using Matlab software. In order to test differences between cyanate uptake by season, region, and depth, we performed 3 separate 3-way ANOVAs for N-specific uptake, C-specific uptake, and uptake C:N ratio where the factors were cruise (May/June 2010, November 2010, June 2011, and August 2012), region (Mid-Atlantic Shelf and Georges Bank/Gulf of Maine, and depth (surface and DCM). We included interaction terms in the ANOVAs and used a Type III Sum of Squares because of uneven sample sizes. The assumption of normality of residuals was not met, so we created a randomized F distribution with 10,000 iterations to calculate the p value (Manly 1997). P values that met the criterion of $\alpha < 0.05$ were considered significant.

RESULTS

Cyanate Distribution

The study region was heterogeneous physically, chemically, and biologically. Surface temperature and salinity ranged from 5 to 25 °C and 32 to 36, respectively. Using temperature-salinity (TS) diagrams (Figure 12) and bathymetric features, we organized stations into three categories: Shelf, Slope, and Basin stations. Shelf stations were located on the continental shelf, excluding deep stations in the interior Gulf of Maine, and ranged in salinity from 32 to 34.3. Slope stations were located in relatively deep waters on the continental slope and were more saline than Shelf stations ranging in salinity from 34 to 37. Stations located in the interior Gulf of Maine with a maximum depth of at least 200 m were classified as Basin stations because

physical and bathymetric features in the Gulf of Maine cause this continental shelf sea to have characteristics of both Shelf and Slope stations (Townsend et al. 2006).

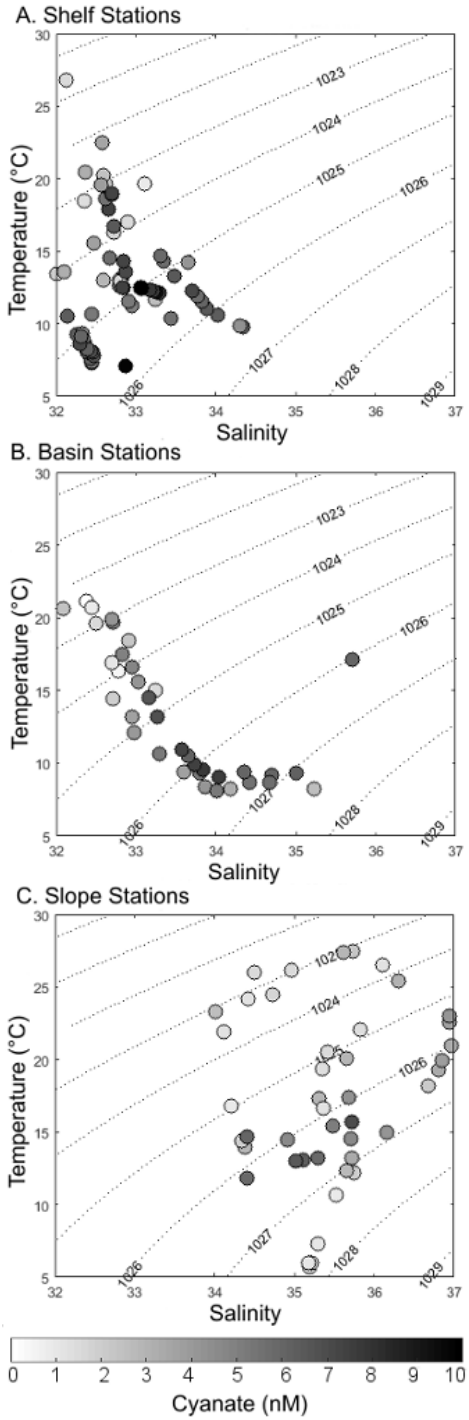

Figure 12. Temperature-Salinity diagrams of each station category. Shelf (A), Basin (B), and Slope (C) stations are depicted. Shading corresponds to cyanate concentration (nM). Some data are reproduced from Chapter III.

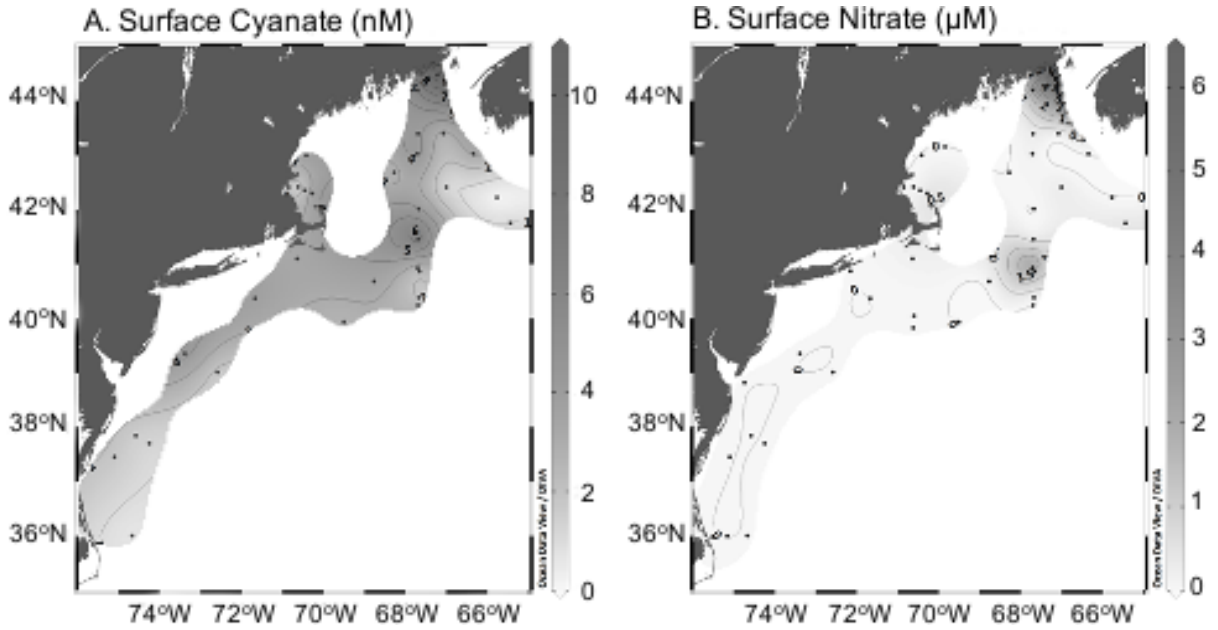

Figure 13. Surface cyanate and nitrate concentrations for August 2012. The black dots are stations, and the contours interpolate between them. White space is where no data was available. Some data are reproduced from Widner et al. 2013 and Chapter III.

In surface waters, cyanate concentrations were higher nearshore than offshore, and cyanate was slightly elevated on shallow Georges Bank and near the Bay of Fundy (Figure 12) where the water column was well-mixed and chlorophyll was elevated at the surface (Chapter III, this Chapter). At the majority of stations, cyanate was depleted in surface waters (Figure 13) and accumulated below the DCM (Figures 14 & 15). This was especially true at Slope stations where cyanate concentrations decreased below the subsurface maximum (Figures 12A & 14D). At Basin stations, cyanate decreased below the subsurface maxima but remained detectable (~5 nM) at the bottom of the water column (Figures 12C & 14D). Cyanate profiles were more variable at Shelf stations than at Basin and Slope stations, probably because of the increased physical, bathymetric, and biological heterogeneity of these stations. At some Shelf stations there was a subsurface cyanate maximum as observed at Slope and Basin stations (Figures 12B, 14A), whereas at other Shelf stations, the water column was well-mixed and cyanate was uniformly distributed with depth (Figures 12B & 14B). At other Shelf stations cyanate accumulated to maximum levels near the bottom of the water column (Figures 12B and 14C),

possibly due to the shallowness of the water column relative to the DCM depth or to a sediment cyanate source.

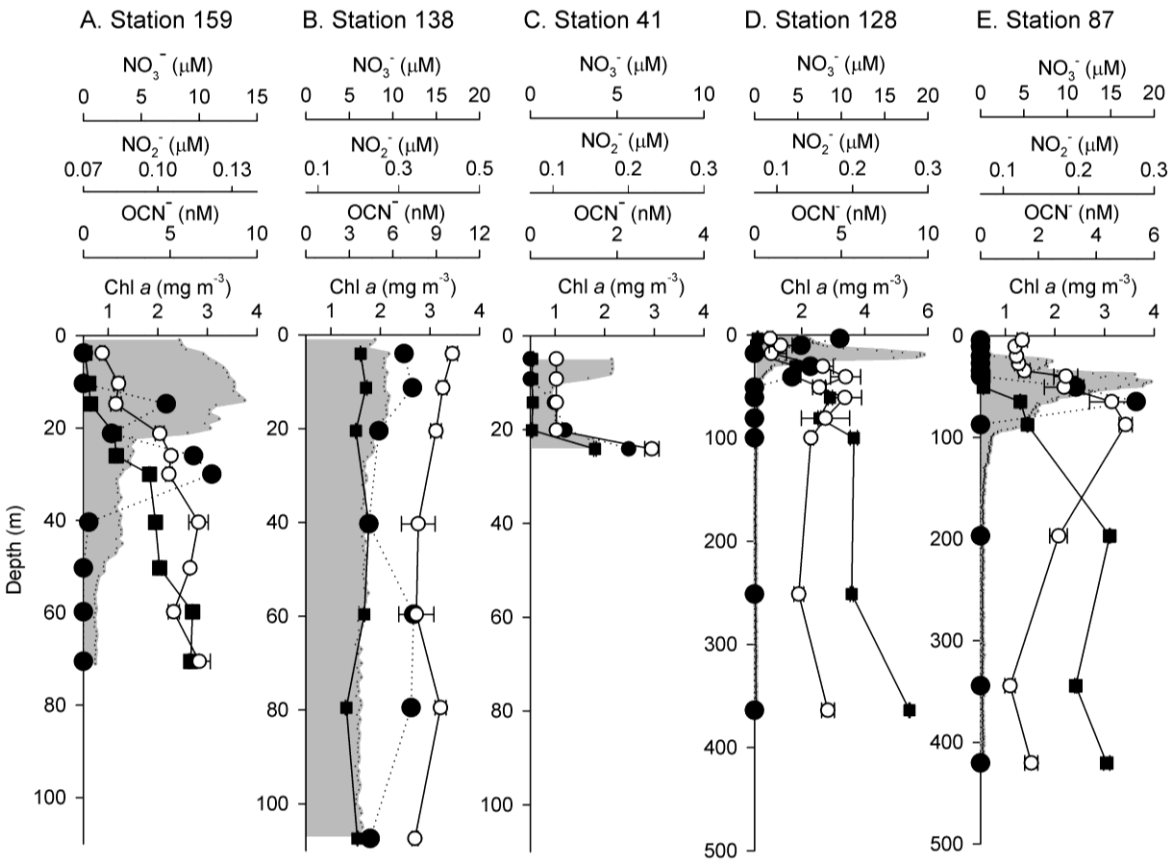

Figure 14. Representative profiles of N and chlorophyll *a*. Profiles are shown for shelf (A-C), basin (D), and slope (E) stations depicting chlorophyll *a* (chl *a*, shaded region), cyanate (OCN^-, open circles), nitrite (NO_2^-, closed circles), and nitrate (NO_3^-, squares). Error bars are ± 1 standard deviation (n =3).

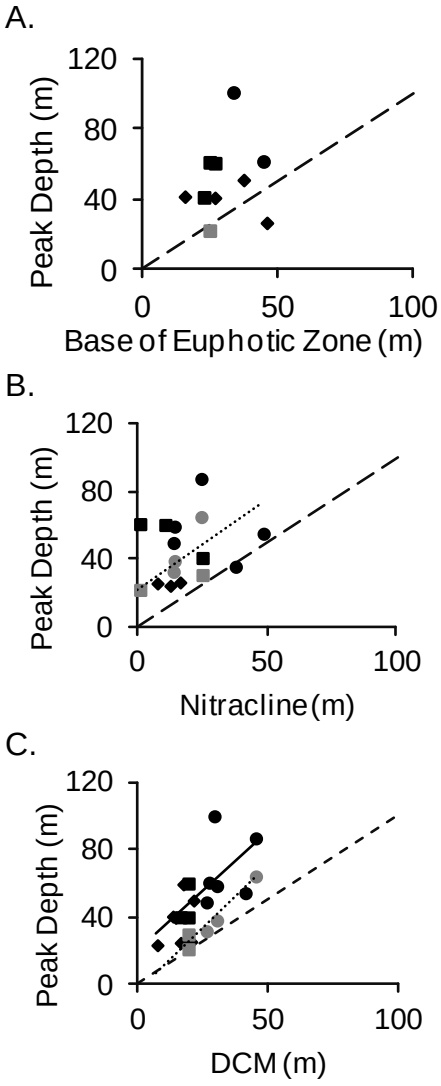

Figure 15. Correlations between the depth of the cyanate and nitrite peaks and euphotic depth (A), nitracline (B), and deep chlorophyll maximum (DCM) (C)depths. Cyanate and nitrite maximum depths are depicted in black and grey, respectively, for Basin stations (squares), Shelf stations (diamonds), and Slope stations (circles). Dashed lines represent a 1 to 1 relationship and solid and dotted lines represent statistically significant correlations for cyanate (y = 1.4 + 20, $p = 0.010$, $R^2 = 0.47$ for panel C) and nitrite (y= 1.1 + 22, $p = 0.055$, $R^2 = 0.42$ for panel B and y = 1.5 - 3.8, $p = 0.001$, $R^2 = 0.95$ for panel C), respectively for criteria $\alpha = 0.1$. Some data are reproduced from Chapter III.

Because the cyanate maximum was below the DCM, similar to the typical profiles of other labile, regenerated N compounds such as ammonium and nitrite (Gruber 2008), we compared vertical profiles of cyanate to these compounds as well as nitrate. We were unable to directly compare the cyanate maximum with the ammonium maximum because ammonium maxima were not observed at many stations, possibly due to our high detection limit (0.04 μM). The cyanate maximum (CM) was generally deeper than the primary nitrite maximum (PNM), euphotic depth, nitracline, and DCM (Figure 15). The depth of the cyanate maximum was not correlated with euphotic or nitracline depth, but it was loosely correlated with the DCM depth (R^2 = 0.47, p = 0.010, Figure 15C) independent of station type. The maximum cyanate concentration for each station was correlated with depth-integrated chlorophyll *a* in the overlying water (Figure 16A, R^2 = 0.79, p < 0.001) at Basin and Shelf stations but not at Slope stations. Cyanate was not directly correlated with chlorophyll *a* concentrations (Figure 16B). The maximum nitrite concentration for each station was not significantly correlated with depth-integrated chlorophyll *a* in the euphotic zone (Figure 16A, R^2 = 0.52, p = 0.081) for criteria α = 0.05, probably due to the small sample size.

Cyanate Uptake

Cyanate uptake was observed on all four cruises (Figure 17, Tables 6-9). N uptake from cyanate was higher on average than C uptake from cyanate (1.3 ±1.9 and 0.4 ± 0.6 nmol l^{-1} h^{-1}, respectively, paired t-test, p < 0.001) suggesting that cyanate was used primarily as an N source. Despite low data density in this heterogeneous study region, 3-way ANOVAs revealed significant differences between: 1) cruises for N uptake (F = 5.4, p = 0.001, R^2 = 0.12), C uptake (F = 5.9, p = 0.001, R^2 = 0.14), and C:N uptake from cyanate (F = 16.2, p < 0.001, R^2 = 0.27); 2) regions for C uptake (F = 3.7, p = 0.049, R^2 = 0.03) and C:N uptake from cyanate (F = 14.7, p < 0.001, R^2 = 0.08); and 3) the interaction between cruise and region for C:N uptake from cyanate (F = 10.5, p < 0.001, R^2 = 0.18). No significant differences were found between: 1) regions for N uptake, 2) depth for N and C uptake and C:N uptake from cyanate; or 3) any of the other interaction terms.

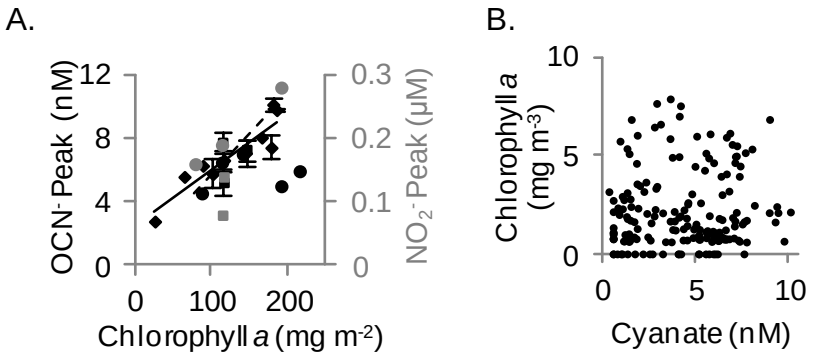

Figure 16. Relationship between cyanate concentration and chlorophyll *a*. A) The maximum concentrations of cyanate and nitrite at each station where a well-resolved cyanate or nitrite subsurface maximum was found. Maximum cyanate and nitrite concentrations are depicted in black and grey, respectively, for Basin (squares), Shelf (diamonds), and Slope (circles) stations. The maximum cyanate and nitrite concentrations were significantly correlated with chlorophyll inventory for all stations for $\alpha = 0.05$ and 0.1, respectively ($y = 0.02x + 3.7$, $p = 0.007$, $R^2 = 0.37$ for cyanate and ($y = 0.001x + 0.01$, $p = 0.081$, $R^2 = 0.52$ for nitrite, dashed line), but the correlation for cyanate was stronger when slope stations were excluded ($y = 0.04 + 2.5$, $p < 0.001$ $R^2 = 0.79$, solid line) and there was no significant correlation for Slope stations alone. B) There was no direct correlation between chlorophyll *a* and cyanate concentrations. Some data are reproduced from Chapter III. Error bars for cyanate are ± 1 standard deviation ($n = 3$).

C uptake from cyanate was significantly higher in August 2012 than in May/June 2010 (Table 10), while N uptake from cyanate was significantly higher in May/June 2010 and June 2011 than in November 2010 (Table 10). C:N uptake from cyanate was significantly higher in November 2010 than during the other three cruises (Table 10). Both C uptake and the C:N ratio from cyanate uptake were significantly higher in the MAS than GBGOM, while there was no significant difference in N uptake from cyanate by region (Table 10). The C:N uptake ratio was significantly higher during the November 2010 cruise in the MAS region than during any of the other cruises and regions (Table 10). This is likely a result of the extremely low N uptake rates from cyanate in November 2010 and higher cyanate C uptake rates on the MAS independent of cruise.

Although there was no significant difference between N uptake, C uptake, or C:N uptake from cyanate between DCM and surface waters, at 65% of stations, N uptake from cyanate at the surface exceeded that at the DCM, at 73% of stations, cyanate C uptake at the DCM exceeded that measured at the surface, and the cyanate C:N uptake ratio was higher at the DCM than at the surface at 69% of stations (Figure 18). Cyanate uptake was not correlated with $NO_3^-+NO_2^-$ concentration, chlorophyll concentration (Figure 19), cyanate concentration (August 2012 only), temperature, or salinity (data not shown) except where temperature reflected seasonality. However, the highest rates of both N and C uptake from cyanate occurred at relatively low NO_3+NO_2 concentrations (Figures 19A and B).

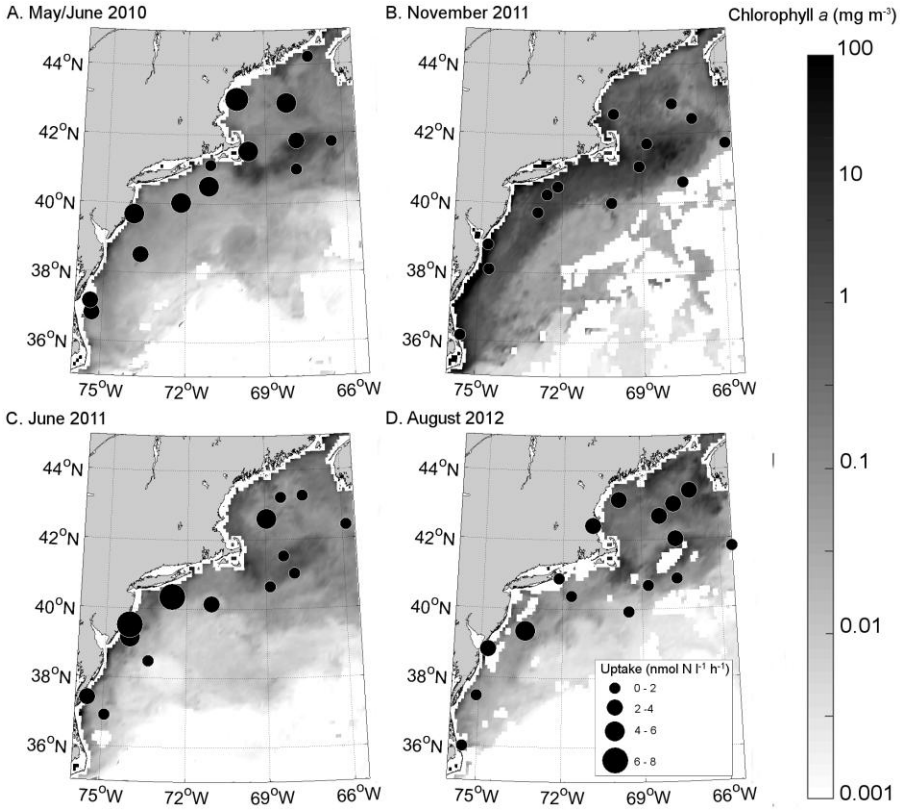

Figure 17. Binned uptake data from all four cruises at the surface. The circle sizes correspond to the binned N-specific uptake rate. Cruises are May/June 2010 (A), November 2010 (B), June 2011 (C), and August 2012 (D). The greyscale represents sea surface chlorophyll (mg m^{-3}).

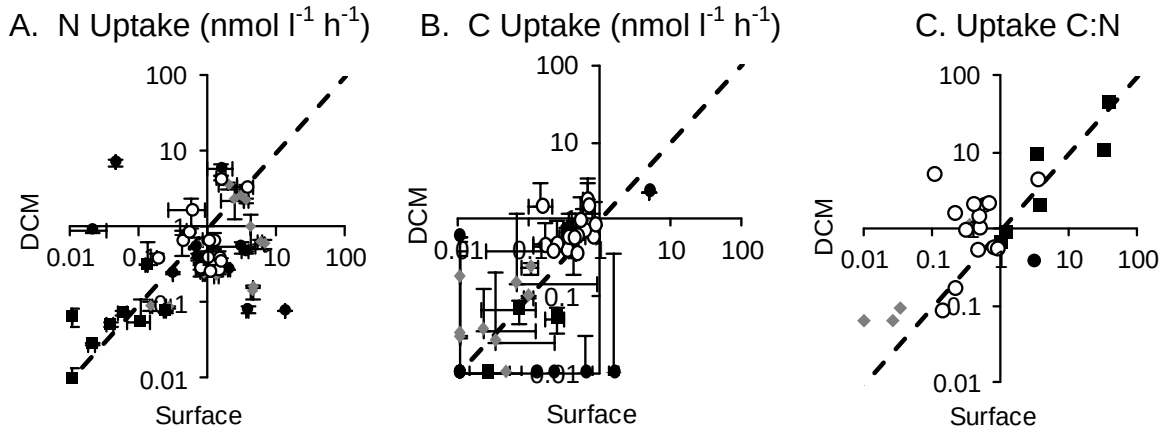

Figure 18. Cyanate uptake at the surface and deep chlorophyll maximum (DCM). A) N uptake, B) C uptake, and C) C:N of cyanate uptake depicted by cruise: May/June 2010 (grey diamonds); November 2010 (black squares); June 2011 (black circles); and August 2012 (open circles). Error bars are ± 1 average deviation (panels A and B only). The dashed line is the 1:1 line where surface and chlorophyll maximum rates would be equal. Uptake rates below their respective detection limit were plotted as 0.02 nmol l^{-1} h^{-1}.

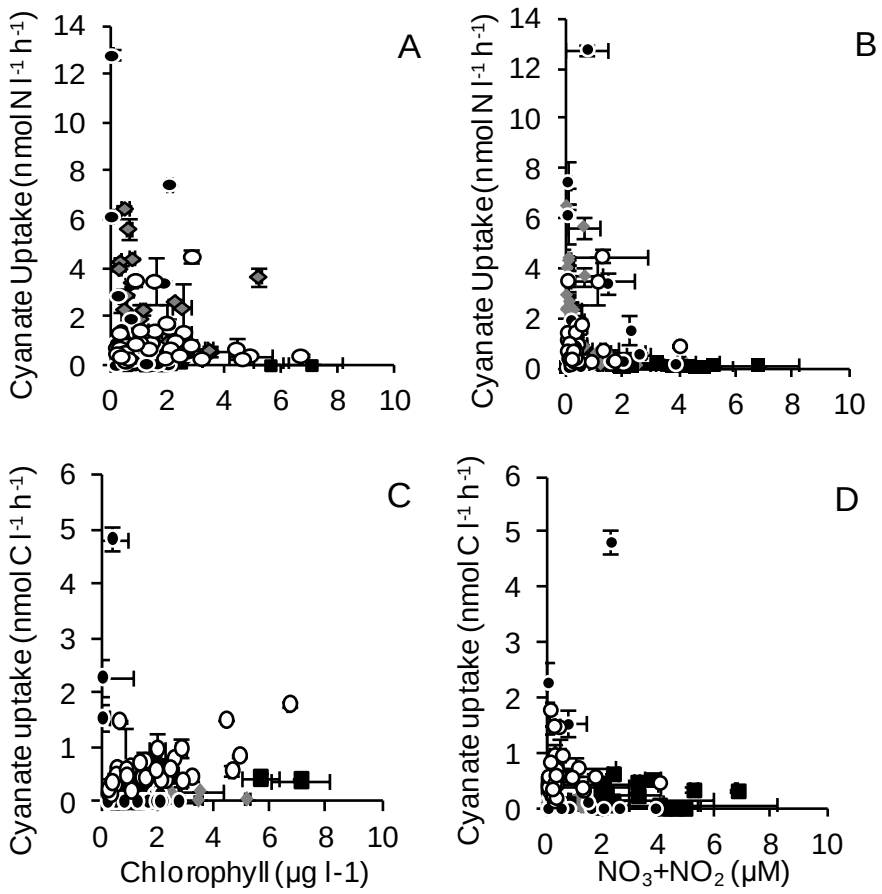

Figure 19. Correlation between N- and C- specific cyanate uptake and NO_3^-+NO_2^- and chlorophyll *a* for all cruises: May/June 2010 (grey diamonds), November 2010 (black squares), June 2011 (black circles), and August 2012 (open circles). Error bars are ± 1 average deviation.

Table 6. Water properties and cyanate uptake rates (N and C) in May/June 2010. All samples were collected on the NOAA ship *Delaware II.* Standard deviations are in parentheses. Standard deviations of 0.00 or 0.0 indicate that the standard deviation was < 0.01 or 0.1, respectively.

Latitude (°N)	Longitude (°W)	Region	Depth (m)	Chl *a* (µg/L)	Temperature (°C)	Salinity	NO_3+NO_2 (µM)	Cyanate uptake (nmol l^{-1} h^{-1}) N	C	C:N
41.109	-71.109	MAS	2	0.3(0.0)	13.36	31.5	1.21(0.37)	0.14(0.00)	b.d.l.	N/A
36.812	-75.373	MAS	2.6	0.5(0.0)	18.10	33.3	b.d.l.	2.33(0.79)	0.06(0.01)	0.03
41.524	-69.677	GOM	2.7	0.7(0.1)	13.45	31.1	0.09(0.06)	4.40(0.03)	0.04(0.02)	0.01
43.022	-70.099	GOM	2.7	0.5(0.1)	14.97	30.6	b.d.l.	6.49(0.09)	0.02(0.02)	0.00
38.516	-73.690	MAS	2.8	0.3(0.0)	14.54	32.1	0.07(0.00)	1.28(0.10)	b.d.l.	N/A
39.690	-73.972	MAS	2.8	0.6(0.1)	16.53	30.0	0.61(0.59)	5.66(0.43)	b.d.l.	N/A
41.806	-67.813	GB	2.8	1.0(0.1)	12.46	32.1	0.26(0.31)	1.94(0.52)	b.d.l.	N/A
44.230	-67.261	GOM	2.8	0.7(0.0)	9.80	32.1	0.90(0.03)	0.26(0.02)	0.09(0.02)	0.36
37.145	-75.449	MAS	2.9	0.5(0.0)	17.98	31.3	b.d.l.	2.91(0.03)	0.10(0.04)	0.03
40.983	-67.842	GB	2.9	2.7(0.6)	9.63	33.0	1.38(0.46)	0.70(0.01)	b.d.l.	N/A
41.772	-66.462	GB	3	2.2(0.0)	9.88	32.1	0.63(0.07)	0.84(0.03)	b.d.l.	N/A
40.026	-72.222	MAS	3.1	0.3(0.0)	13.11	32.2	0.07(0.16)	4.29(0.19)	b.d.l.	N/A
40.497	-71.183	MAS	3.2	0.3(0.0)	14.47	32.4	b.d.l.	4.01(0.11)	b.d.l.	N/A
42.897	-68.159	GOM	3.4	0.7(0.0)	12.52	31.7	b.d.l.	3.44(0.18)	0.03(0.01)	0.01
40.983	-67.842	GB	10.7	3.5(0.8)	9.22	32.3	1.06(0.30)	0.58(0.17)	0.17(0.00)	0.30
41.772	-66.462	GB	11.2	2.0(0.0)	8.91	32.2	1.93(0.09)	0.25(0.00)	b.d.l.	N/A
41.109	-71.109	MAS	11.8	0.6(0.1)	11.57	31.5	2.49(2.84)	0.09(0.01)	b.d.l.	N/A
42.897	-68.159	GOM	13.1	1.1(0.1)	11.98	31.7	0.26(0.23)	2.31(0.19)	0.03(0.01)	0.01
37.145	-75.449	MAS	15.3	2.2(0.0)	13.97	31.5	0.11(0.08)	2.65(0.03)	0.24(0.00)	0.09
36.812	-75.373	MAS	19.2	2.5(0.3)	12.41	31.7	b.d.l.	2.38(1.04)	0.14(0.01)	0.07
39.690	-73.972	MAS	22.1	3.5(0.1)	8.27	31.5	1.29(1.48)	0.65(0.04)	b.d.l.	N/A
44.230	-67.261	GOM	22.4	0.7(0.1)	7.96	32.3	4.08(0.04)	0.09(0.00)	0.10(0.01)	1.10

Table 6. Continued

Latitude (°N)	Longitude (°W)	Region	Depth (m)	Chl *a* (µg/L)	Temperature (°C)	Salinity	NO_3+NO_2 (µM)	Cyanate uptake (nmol l^{-1} h^{-1}) N	C	C:N
41.524	-69.677	GOM	25.7	2.2(0.1)	6.44	31.8	4.25(0.33)	0.16(0.00)	0.02(0.03)	0.06
43.022	-70.099	GOM	26.7	1.1(0.1)	6.46	31.5	1.42(0.16)	0.61(0.09)	0.04(0.01)	0.06
38.516	-73.690	MAS	28.5	1.1(0.1)	8.34	32.8	2.46(1.68)	0.23(0.01)	b.d.l.	N/A
40.497	-71.183	MAS	31.7	2.0(0.1)	8.43	32.6	b.d.l.	1.03(0.48)	0.03(0.02)	0.03
41.806	-67.813	GB	31.9	5.2(0.1)	10.26	32.4	0.65(0.65)	3.68(0.36)	0.03(0.03)	0.01
40.026	-72.222	MAS	32	1.0(0.1)	9.16	32.5	0.15(0.14)	0.14(0.03)	b.d.l.	N/A

Table 7. Water properties and cyanate uptake rates (N and C) All samples were collected on the NOAA ship *Delaware II.* Standard deviations are in parentheses. Standard deviations of 0.00 or 0.0 indicate that the standard deviation was < 0.01 or 0.1, respectively.

Latitude (°N)	Longitude (°W)	Region	Depth (m)	Chl *a* (µg/L)	Temperature (°C)	Salinity	NO_3+NO_2 (µM)	Cyanate uptake (nmol l^{-1} h^{-1}) N	C	C:N
42.421	-66.999	GOM	2.3	0.5(0.1)	10.5	32.6	4.88(0.04)	0.02(0.00)	0.01(0.01)	0.34
38.778	-74.719	MAS	2.5	7.1(1.1)	13.7	32.1	b.d.l.	b.d.l.	0.40(0.02)	N/A
39.730	-72.903	MAS	3	0.4(0.0)	14.6	32.9	3.98(4.23)	0.06(0.01)	0.07(0.05)	1.24
36.142	-75.580	MAS	3	1.5(0.4)	16.3	31.5	b.d.l.	b.d.l.	0.34(0.06)	N/A
41.682	-65.775	GB	3	1.9(0.4)	11.4	32.4	1.87(0.02)	0.04(0.00)	0.03(0.03)	0.69
42.856	-67.775	GOM	3.4	1.0(0.0)	10.8	33.0	5.20(0.15)	0.10(0.03)	0.34(0.05)	3.45
41.729	-68.779	GOM	3.5	2.5(0.0)	10.4	32.5	3.20(0.10)	0.12(0.00)	0.48(0.03)	3.91

Table 7. Continued

Latitude (°N)	Longitude (°W)	Region	Depth (m)	Chl *a* (µg/L)	Temperature (°C)	Salinity	NO_3+NO_2 (µM)	Cyanate uptake (nmol l^{-1} h^{-1}) N	C	C:N
40.599	-67.437	GB	4	0.8(0.2)	13.7	32.1	3.22(0.83)	0.23(0.01)	0.24(0.07)	1.02
40.251	-72.567	MAS	3.7*	1.2(0.1)	14.5	32.5	1.91(1.04)	b.d.l.	0.17(0.00)	N/A
40.486	-72.180	MAS	3.7*	1.8(0.1)	13.8	31.8	2.05(0.33)	b.d.l.	0.31(0.04)	N/A
40.025	-70.147	MAS	3.7*	0.7(0.2)	16.0	31.5	4.35(0.48)	0.05(0.02)	b.d.l.	N/A
41.061	-69.081	GOM	3.7*	1.5(0.0)	12.6	31.8	2.31(3.59)	0.04(0.01)	0.14(0.06)	3.46
42.590	-70.051	GOM	3.7*	1.0(0.1)	10.6	32.5	6.78(0.06)	0.08(0.06)	0.33(0.01)	3.84
38.069	-74.657	MAS	3.7*	0.6(0.0)	15.7	32.3	0.71(0.32)	0.14(0.02)	0.09(0.03)	0.69
38.778	-74.719	MAS	9	5.6(0.6)	13.7	32.1	1.97(1.95)	b.d.l.	0.44(0.08)	N/A
36.142	-75.580	MAS	10	1.8(0.2)	16.3	31.5	0.20(0.08)	0.07(0.02)	0.71(0.01)	10.49
41.729	-68.779	GOM	14.8	2.1(0.3)	10.4	32.5	2.33(0.18)	0.32(0.13)	0.63(0.01)	1.96
40.599	-67.437	GB	15	0.7(0.1)	16.6	34.6	1.63(0.43)	0.08(0.00)	0.05(0.02)	0.65
39.730	-72.903	MAS	22	0.6(0.0)	14.7	32.9	2.20(0.76)	0.08(0.00)	0.07(0.02)	0.88
42.421	-66.999	GOM	23	0.5(0.0)	10.3	32.6	4.57(0.19)	0.03(0.00)	b.d.l.	N/A
41.682	-65.775	GB	36	1.2(0.0)	10.5	32.6	4.16(0.28)	0.05(0.00)	b.d.l.	N/A
42.856	-67.775	GOM	46	2.1(0.2)	10.5	33.2	3.74(0.28)	0.06(0.02)	0.53(0.04)	9.17

* Sample collected from ship's flow through system.

Table 8. Water properties and cyanate uptake rates (N and C) in June 2011. All samples were collected on the NOAA ship *Delaware II*. Standard deviations are in parentheses. Standard deviations of 0.00 or 0.0 indicate that the standard deviation was < 0.01 or 0.1, respectively.

Latitude (°N)	Longitude (°W)	Region	Depth (m)	Chl *a* (µg/L)	Temperature (°C)	Salinity	NO_3+NO_2 (µM)	Cyanate uptake (nmol l^{-1} h^{-1}) N	C	C:N
42.395	-65.852	GOM	2	0.4(0.1)	9.7	31.0	1.53(0.38)	0.29(0.01)	b.d.l.	N/A
40.145	-71.081	MAS	2.5	0.7(0.0)	17.0	33.3	0.13(0.13)	1.94(0.04)	b.d.l.	N/A
42.610	-68.953	GOM	2.6	1.8(0.1)	11.2	31.9	1.42(0.00)	3.41(0.43)	0.12(0.01)	0.0
40.638	-68.844	GB	2.7	0.6(0.1)	13.1	32.3	b.d.l.	0.67(0.04)	b.d.l.	N/A
41.020	-67.912	GB	2.7	1.5(0.1)	10.8	32.3	b.d.l.	0.64(0.00)	b.d.l.	N/A
39.173	-74.108	MAS	2.8	0.8(0.0)	20.0	30.0	b.d.l.	3.62(0.06)	0.61(0.73)	0.2
40.351	-72.558	MAS	3	0.2(0.0)	15.7	31.5	b.d.l.	2.89(1.92)	b.d.l.	N/A
38.489	-73.403	MAS	3	0.2(0.0)	20.7	34.8	0.09(0.04)	b.d.l.	b.d.l.	N/A
36.897	-74.938	MAS	3	2.0(0.1)	22.9	30.5	b.d.l.	0.04(0.00)	0.21(0.01)	4.9
37.395	-75.573	MAS	3	0.4(0.0)	22.2	29.6	2.25(0.00)	1.52(0.62)	4.83(0.24)	3.2
39.523	-74.119	MAS	3	0.0(0.0)	17.6	30.1	0.71(0.73)	12.8(0.22)	1.54(0.24)	0.1
41.524	-68.311	GB	3	1.4(0.1)	11.3	32.3	3.83(1.61)	0.18(0.00)	b.d.l.	N/A
43.265	-67.513	GOM	3.7*	0.5(0.1)	12.7	31.9	0.74(0.57)	0.12(0.03)	b.d.l.	N/A
42.395	-65.852	GOM	14	0.8(0.0)	5.8	31.3	0.42(0.48)	0.25(0.01)	b.d.l.	N/A
40.145	-71.081	MAS	34	2.0(0.0)	12.8	33.7	1.97(0.00)	0.29(0.00)	b.d.l.	N/A
42.610	-68.953	GOM	17.5	2.0(0.0)	10.9	31.9	0.38(0.36)	1.67(0.30)	0.14(0.01)	0.1
40.638	-68.844	GB	14	2.7(0.2)	9.5	32.4	0.17(0.20)	0.49(0.01)	b.d.l.	N/A
41.020	-67.912	GB	41	2.2(0.0)	10.3	32.3	b.d.l.	0.42(0.05)	b.d.l.	N/A
39.173	-74.108	MAS	13.6	1.3(0.0)	13.0	30.9	0.07(0.17)	0.57(0.01)	0.60(0.02)	1.1
40.351	-72.558	MAS	30	1.6(0.1)	6.8	32.3	b.d.l.	0.08(0.01)	b.d.l.	N/A
38.489	-73.403	MAS	63	1.9(0.0)	12.6	34.4	2.54(0.42)	0.58(0.10)	b.d.l.	N/A
36.897	-74.938	MAS	25	0.2(0.0)	9.2	32.7	0.34(0.4)	0.95(0.09)	b.d.l.	N/A

Table 8. Continued

Latitude (°N)	Longitude (°W)	Region	Depth (m)	Chl *a* (µg/L)	Temperature (°C)	Salinity	NO_3+NO_2 (µM)	Cyanate uptake (nmol l^{-1} h^{-1}) N	C	C:N
37.395	-75.573	MAS	15	2.0(0.2)	14.0	31.7	b.d.l.	7.48(0.86)	b.d.l.	N/A
39.523	-74.119	MAS	14	0.0(0.0)	12.9	30.8	b.d.l.	6.15(1.11)	2.29(0.35)	0.4
41.524	-68.311	GB	40	1.2(0.1)	10.4	32.2	0.46(0.39)	0.08(0.00)	b.d.l.	N/A

* Sample collected from ship's flow through system.

Table 9. Water properties and cyanate uptake rates (N and C) in August 2012. All samples were collected on the NOAA ship *Henry B. Bigelow*. Standard deviations are in parentheses. Standard deviations of 0.00 or 0.0 indicate that the standard deviation was < 0.01 or 0.1, respectively.

Latitude (°N)	Longitude (°W)	Region	Depth (m)	Chl *a* (µg/L)	Temperature (°C)	Salinity	NO_3+NO_2 (µM)	Cyanate uptake (nmol l^{-1} h^{-1}) N	C	C:N
40.371	-71.671	MAS	2.7	0.5(0.4)	23.9	31.8	b.d.l.	0.40(0.00)	0.32(0.03)	0.79
39.358	-73.387	MAS	3	1.5(3.5)	26.4	31.2	1.08(1.35)	3.49(0.97)	0.75(0.17)	0.21
37.456	-75.101	MAS	4	0.2(0.7)	26.8	31.2	0.22(0.10)	0.74(0.09)	0.16(0.05)	0.21
35.985	-75.521	MAS	3	1.3(1.1)	23.6	34.2	b.d.l.	1.15(0.07)	0.57(0.05)	0.49
38.821	-74.740	MAS	3.1	2.6(1.4)	21.3	31.8	0.30(0.00)	1.38(0.10)	0.80(0.03)	0.58
40.874	-72.154	MAS	5	0.5(0.2)	22.6	30.9	0.12(0.00)	0.18(0.00)	0.61(0.05)	3.50
39.933	-69.507	MAS	2.7	0.3(0.7)	23.0	32.4	1.27(0.11)	0.73(0.04)	0.33(0.08)	0.46
40.681	-68.770	GB	4.1	0.3(1.3)	22.7	31.6	0.22(0.01)	1.34(0.11)	0.14(0.05)	0.11
40.867	-67.659	GB	3.7	0.5(0.5)	20.1	32.4	0.24(0.00)	0.55(0.29)	0.49(0.04)	0.90

Table 9. Continued

Latitude (°N)	Longitude (°W)	Region	Depth (m)	Chl *a* (µg/L)	Temperature (°C)	Salinity	NO_3+NO_2 (µM)	Cyanate uptake (nmol l^{-1} h^{-1}) N	C	C:N
41.756	-65.441	GB	3.4	0.2(0.5)	24.2	34.3	0.18(0.02)	0.50(0.03)	0.23(0.12)	0.46
42.015	-67.676	GB	4.1	1.4(0.9)	19.6	32.4	0.31(0.00)	0.93(0.09)	0.45(0.01)	0.48
42.687	-68.280	GOM	3.7	1.0(1.0)	20.5	31.9	0.37(0.17	0.97(0.16)	0.64(0.09)	0.67
43.400	-67.077	GOM	3.7	1.5(1.4)	18.5	32.7	b.d.l.	1.44(0.11)	0.44(0.00)	0.31
43.029	-67.711	GOM	4.4	2.8(0.8)	16.6	32.8	0.23(0.18)	0.83(0.10)	0.98(0.18)	1.18
43.157	-69.847	GOM	4.2	1.0(1.5)	21.9	31.5	0.28(0.18)	1.45(0.22)	0.20(0.07)	0.14
42.417	-70.854	GOM	4.2	2.3(1.0)	19.6	31.1	0.07(0.11)	1.01(0.24)	0.40(0.20)	0.40
40.371	-71.671	MAS	15	2.1(0.7)	16.8	32.3	b.d.l.	0.70(0.26)	0.40(0.05)	0.57
39.358	-73.387	MAS	14	0.8(3.5)	24.9	31.6	b.d.l.	3.52(0.21)	0.59(0.00)	0.17
37.456	-75.101	MAS	26.4	3.2(0.3)	14.2	33.5	0.23(0.16)	0.29(0.05)	0.46(0.05)	1.61
35.985	-75.521	MAS	17	1.3(0.7)	23.4	35.8	0.30(0.08)	0.69(0.18)	0.72(0.01)	1.04
38.821	-74.740	MAS	8.4	4.9(0.4)	15.3	34.4	0.08(0.04)	0.41(0.09)	0.85(0.03)	2.06
40.874	-72.154	MAS	17.8	6.7(0.4)	18.1	31.8	0.08(0.03)	0.41(0.04)	1.80(0.04)	4.42
39.933	-69.507	MAS	30.5	1.9(0.3)	14.8	34.3	1.68(0.56)	0.30(0.03)	0.59(0.05)	1.94
40.681	-68.770	GB	20.3	0.6(0.3)	12.8	32.7	0.39(0.08)	0.29(0.03)	1.49(0.01)	5.20
40.867	-67.659	GB	19.8	2.0(1.8)	12.6	32.7	0.51(0.12)	1.76(0.77)	0.97(0.27)	0.55
41.756	-65.441	GB	27.6	0.9(0.9)	16.1	35.2	3.98(0.00)	0.90(0.01)	0.48(0.02)	0.53
42.015	-67.676	GB	24.2	2.4(0.4)	17.8	32.5	0.28(0.00)	0.42(0.09)	0.61(0.07)	1.46
42.687	-68.280	GOM	15.8	4.4(0.7)	14.9	35.5	0.21(0.09)	0.69(0.39)	1.50(0.01)	2.17
43.400	-67.077	GOM	25	0.3(0.4)	15.2	33.1	0.15(0.16)	0.37(0.03)	0.36(0.04)	0.97
43.157	-69.847	GOM	17.7	2.9(4.5)	12.6	32.3	1.23(1.67)	4.50(0.29)	0.39(0.12)	0.09
42.417	-70.854	GOM	13.2	4.6(0.3)	12.4	31.7	0.85(0.09)	0.27(0.03)	0.58(0.09)	2.11

Table 10. Means associated with ANOVAs + Tukey significance for cyanate uptake. Interaction means are only shown for region and cruise because depth was not significant for anything. Tukey test p-values are indicated by symbols below the table.

	N uptake (nmol l-1 h-1)			C uptake (nmol l-1 h-1)			Uptake C:N		
Cruise	GBGOM	MAS	Cruise Total	GBGOM	MAS	Cruise Total	GBGOM	MAS	Cruise Total
May/June 2010	1.4(1.7)	2.0(1.8)	1.9(1.8)*	0.0(0.0)	0.0(0.1)	0.0(0.1) $^{\alpha}$	0.1(0.2) $^{\eta}$	0.0(0.0) $^{\lambda}$	0.1(0.2) $^{\nu}$
November 2010	0.1(0.1)	0.0(0.0)	0.1(0.1) *†	0.2(0.2)	0.3(0.2)	0.2(0.2)	2.4(2.6) $^{\theta}$	17.9(17.7) $^{\eta, \theta, \iota, \kappa, \lambda, \mu, \nu}$	9.5(14.1) $^{\gamma, \delta, \varepsilon}$
June 2011	0.7(1.0)	2.8(3.7)	1.8(2.9) †	0.0(0.0)	0.7(1.4)	0.4(1.0)	0.0(0.0) $^{\iota}$	0.7(1.5) $^{\mu}$	0.5(1.1) $^{\delta}$
August 2012	1.1(1.0)	1.0(1.1)	1.1(1.0)	0.6(0.4)	0.6(0.4)	0.6(0.4) $^{\alpha}$	1.0(1.2) $^{\kappa}$	1.3(1.3) $^{\nu}$	1.2(1.3) $^{\varepsilon}$
Region Total	1.0(1.3)	1.6(2.4)		0.3(0.4) $^{\beta}$	0.4(0.8) $^{\beta}$		0.9(1.6) $^{\zeta}$	4.0(10.2) $^{\zeta}$	

* $p = 0.0017$; † $p = 0.0048$; $^{\alpha}$ $p = 0.0006$; $^{\beta}$ $p = 0.0480$; $^{\gamma}$ $p < 0.0001$; $^{\delta}$ $p < 0.0001$; $^{\varepsilon}$ $p < 0.0001$; $^{\zeta}$ $p = 0.0002$; $^{\eta}$ $p < 0.0001$; $^{\theta}$ $p < 0.0001$; $^{\iota}$ $p < 0.0001$; $^{\kappa}$ $p < 0.0001$; $^{\lambda}$ $p < 0.0001$; $^{\mu}$ $p < 0.0001$; $^{\nu}$ $p < 0.0$

Cyanate Production from Urea

Using the rate constant of Hagel et al. (1971), we calculated that the rate of abiotic cyanate production from urea at the Mid-Atlantic Bight could be 0.0004 nmol l^{-1} h^{-1} and up to 0.002 nmol l^{-1} h^{-1} based on previously reported average and maximum urea concentrations in this region (Filippino et al. 2011). However, building upon the work of Kamennaya and Post (2008) and assuming that the urea decomposition rate is independent of its concentration, the rate of abiotic cyanate production from urea could have been as high as 0.03or 0.20 nmol l^{-1} h^{-1} for the mean and maximum urea concentrations, respectively.

DISCUSSION

During August, 2012, cyanate concentrations in coastal waters in the Gulf of Maine, Georges Bank, and mid-Atlantic Bight ranged from below the limit of detection (0.4 nM) to 11 nM (Figure 11, Appendix G). Nanomolar concentrations are typical for small biologically labile reduced N compounds (Sipler and Bronk 2015), and absolute concentrations reflect the balance of production and consumption. For example, while ammonium is frequently at the limit of analytical detection in surface waters, it typically accounts for a large fraction of the total N utilization and its production and consumption are tightly coupled (Bronk and Steinberg 2008; Mulholland and Lomas 2008). Cyanate concentrations were generally higher nearshore than offshore, suggesting either a terrestrial source or higher production rates nearshore where organic matter and bacterial and phytoplankton biomass are also higher (Pan et al. 2011). Overall, cyanate concentrations were lower in coastal waters than in the Chesapeake Bay and its estuaries (17 to 41 nM and up to 100 nM (Widner et al. 2013)) and slightly higher closer to shore than on the slope which may indicate a terrestrial or estuarine source of cyanate to coastal systems. Typically estuarine dissolved N and DOM concentrations are higher than in coastal waters as a result of natural and anthropogenic processes in these highly productive systems. Consequently, estuaries can be a large source of both N and DOM to coastal ecosystems (Raymond and Spencer 2015; Seitzinger and Harrison 2008).

Cyanate likely enters marine systems through both allochthonous and autochthonous sources. Cyanate may be produced in riverine, estuarine, and terrestrial systems from degrading organic matter and photoproduction (Chapter III). In situ production of cyanate has been

demonstrated in phytoplankton cultures and primary production and degradation of sinking organic matter has been used to explain vertical distributions of cyanate in marine systems (Chapter III). As such, variability in cyanate concentrations may be related to the trophic status of the system, as has been observed for other N compound (Gruber 2008). Terrestrial processes may also input cyanate to coastal regions and these include release of cyanate or its precursors from urban runoff and wastewater and industrial and agricultural discharges (Boening and Chew 1999; Dirnhuber and Schutz 1948; Glibert et al. 2006; Kamennaya et al. 2008). However, a comprehensive investigation of cyanate sources was beyond the scope of this study.

Surface cyanate concentrations were not always correlated with chlorophyll *a* concentrations (Figure 14, Chapter III) which suggests that cyanate production is either temporally or spatially uncoupled from phytoplankton biomass or that consumption of cyanate exceeds its production in sunlit waters where chlorophyll *a* concentrations are highest. An exception was that cyanate concentrations were high in surface waters at the northernmost station sampled in the Gulf of Maine (Figure 13B) and on Georges Bank (Chapter III) where chlorophyll *a* concentrations were also high. These areas experience persistently high chlorophyll *a* concentrations and frequent phytoplankton blooms (Townsend et al. 2006), which can result in rapid release and accumulation of DON in surface waters (Boneillo and Mulholland 2014; Egerton et al. 2014; Mulholland et al. 2009). Deep water in the Gulf of Maine originates from the Slope, which introduces water through the Northeast Channel below 75 m, and the Scotian Shelf, which introduces water at the surface (Townsend 1998). In the stratified summer months, tidal upwelling transports deep water to the surface at the northern edge of the Gulf of Maine (Townsend et al. 1987). This nitrate-rich plume flows southwest parallel to the coastline and fuels phytoplankton growth including that of the harmful bloom-forming *Alexandrium* sp. In August 2012, we observed elevated nitrate concentrations at the northern edge of the Gulf of Maine suggestive of such an upwelling plume (Figures 12 and 13 and Chapter III). However, the elevated cyanate concentrations in the same water cannot be explained by upwelling because deep Gulf of Maine waters had lower cyanate concentrations. It is more likely that high surface cyanate concentrations were produced by the high *in situ* productivity there.

The vertical distribution of cyanate was similar to those of ammonium and nitrite (Figure 14, Chapter III) with a surface minimum, subsurface maximum, and a minimum below the nitracline suggesting uptake by phototrophs in the euphotic zone, production by organic matter

degradation at the base of the photic zone, and oxidation in deeper water below (Gruber 2008). At most stations, the subsurface cyanate peak was substantially deeper than the DCM, PNM, nitracline, and euphotic depths (Figure 15) and deeper than is typical for the nitrite and ammonium maxima with respect to the DCM, nitracline, and euphotic depth (Dore and Karl 1996; Mackey et al. 2011). So, while the depth of the cyanate maximum probably depends on the balance between multiple depth-dependent consumption and production processes, we do not yet fully understand what those processes are and how they are affected by other vertical gradients in the sea. Overall the cyanate maximum appears to be analogous to the PNM suggesting it is an intermediate in organic matter degradation. However, the processes involved in the formation of the PNM are better understood as are its relationship with the DCM depth and the depth of the nitracline (Adornato et al. 2005; Dore and Karl 1996; Kiefer et al. 1976; Lomas and Lipschultz 2006).

The correlation between the maximum cyanate concentrations in vertical profiles and depth-integrated chlorophyll concentrations (Figure 16) suggests that cyanate is likely a product of organic matter degradation and dependent on the sinking flux of phytoplankton from surface waters. To the best of my knowledge, no other study has examined the correlation between the maximum concentrations of a decomposition product in subsurface waters with the total overlying phytoplankton biomass. The maximum nitrite concentration was significantly correlated with depth-integrated chlorophyll *a* concentrations only for the criteria $\alpha = 0.1$, but this most likely relects the small sample size and low sampling resolution. Nitrite is also produced from phytoplankton biomass either by direct release or as an intermediate species in nitrification (Ward 2008) and might be expected to be correlated with overlying phytoplankton biomass.

At most Slope and Basin stations, cyanate was depleted below the subsurface maximum. This indicates that cyanate production is slow at depth or that cyanate is consumed by processes at depth which may include abiotic degradation or biologically-mediated transformation. Cyanate abiotically degrades to ammonium (Kamennaya et al. 2008) which can then be oxidized to nitrate. Abiotic degradation of cyanate to ammonium is slow in seawater, which could explain why cyanate concentrations below the cyanate maximum were not as low at the shallower Basin stations in the Gulf of Maine and the Shelf stations compared to Slope stations. It would also explain the broad tail below the cyanate maximum at some Slope stations. In slope waters,

cyanate can mix into the vast deep ocean reservoir where it can slowly degrade, whereas in the basin of the Gulf of Maine, physical removal of water is slow (Townsend et al. 2006), so cyanate may accumulate. Elevated bottom water cyanate concentrations on the Shelf may reflect a sediment source of cyanate potentially by oxidation of sedimentary thiocyanate or cyanide (Kamyshny et al. 2013).

Abiotic urea decomposition has been proposed as a mechanism of cyanate production in marine systems (Kamennaya et al. 2008), and in vertical profiles collected from the Mid-Atlantic Bight the cyanate maximum was below that of urea (Chapter III) indicating that cyanate could have been produced from urea decomposition, analogous to the observation that nitrite accumulates below the ammonium maximum as a result of ammonium oxidation (Meeder et al. 2012). Although abiotic cyanate production from urea decomposition was slow when calculated using Hagel et al.'s (1971) hypothetical rate constant (~ 0.001 nmol l^{-1} h^{-1}), the rate calculated based on ammonium production from urea and cyanate in sterile, particle-free Sargasso seawater (~ 0.1 nmol l^{-1} h^{-1}) (Kamennaya et al. 2008) was similar in magnitude to typical rates of urea regeneration (Bronk et al. 1998; Cho and Azam 1995; Mulholland and Lomas 2008). Cyanate has also been shown to be produced by spontaneous decomposition of carbamoyl phosphate (Allen and Jones 1964, see Appendices B and C) which could be released from cells by sloppy feeding and cell lysis. While there are no known biological pathways of cyanate production from urea or other organic compounds, aside from carbamoyl phosphate (Allen and Jones 1964), it is likely that cellular or extracellular pathways exist as carbon-nitrogen linkages are common in all biological systems.

N-specific cyanate uptake rates ranged from below the limit of detection (0.02) to 12.8 nmol l^{-1} h^{-1} which is similar in magnitude to reported rates of uptake of other dissolved inorganic and small organic N compounds (Mulholland and Lomas 2008). At the majority of stations, cyanate uptake was ~1% of total N uptake, but at some stations it was as high as 13% of total measured N uptake (which included NO_3^-, NO_2^-, NH_4^+, urea, cyanate, and dissolved free amino acids; M.R. Mulholland, pers. comm.). Overall cyanate uptake was a lower fraction of total N uptake in this coastal system than at an oligotrophic N. Atlantic station (Chapter III). However, natural microbial populations from the Mid-Atlantic continental shelf had a high affinity and high maximum uptake rates for cyanate (Widner unpubl.) suggesting that microbes are capable of taking up cyanate at high rates under a range of environmental concentrations. It is possible

that cyanate uptake is episodic following sporadic cyanate inputs (Espie et al. 2007) or varies temporally and with physiological state as is the case for other N compounds (Mulholland and Lomas 2008).

Seasonality and spatial heterogeneity resulted in large differences in temperature, water column structure, community structure, biomass, nutrient availability, mixing, and light availability between cruises (Tables 6-9). Cyanate N uptake was higher during the summer cruises when the water column was generally stratified and mixed layer DIN concentrations were low. Picoeukaryotes and cyanobacteria, which are known to utilize cyanate (Kamennaya and Post 2013; Palenik et al. 2003; Rocap et al. 2003), comprise a large fraction of the phytoplankton community during late summer (Pan et al. 2011; Townsend et al. 2006) and regenerated N compounds typically fuel productivity at this time of year when the water column is stratified (Lalli and Parsons 1997). During November cyanate uptake rates were lower. This is a time of year when winter mixing typically results in increased availability of upwelled NO_3^- and the phytoplankton community is typically dominated by large eukaryotes (Pan et al. 2011) in which cyanate-related genes have not yet been identified.

C uptake from cyanate was generally low suggesting that cyanate was used primarily as an N source by microbes. However, C uptake from cyanate and hence the C:N uptake ratio from cyanate were both higher during November than during the summer and in microbial assemblages collected from the DCM relative to those collected from well-lit surface waters. Like urea, cyanate contains reduced N and oxidized C which are converted to NH_4^+ and CO_2 intracellularly (Anderson et al. 1990; Berges and Mulholland 2008). Most microbes readily incorporate NH_4^+-N, but only autotrophs are able to reduce and fix CO_2. If cyanate-derived CO_2 is not rapidly fixed it diffuses out of the cell resulting in higher N than C incorporation, which may explain why we observed statistically higher overall uptake of N than C. Cyanate C could be used to augment photosynthetic C uptake, but low light during winter and at the depth of the DCM would have limited light-mediated C assimilation, and primary productivity was significantly higher at the surface compared to the DCM in this study region (M.R. Mulholland, unpubl.).

C uptake in excess of N could also result from the occurrence of a dissimilatory nitrogen process coupled with C fixation. Recent evidence indicates that ammonium oxidizers may oxidize urea-N and fix urea-C (Alonso-Sáez et al. 2012). Since ammonium oxidation is

dissimilatory, this process would result in excess C uptake relative to N. We speculate that a similar process might be at work for cyanate. *CynS* has been identified in an ammonium oxidizing archaeon from a microbial mat (Spang et al. 2012), *cynX* has been identified in a marine ammonium oxidizing bacterium (Klotz et al. 2006), and an ammonium-oxidizing archaeon, *Nitrososphaera gargensis*, has been grown on cyanate as the sole source of N and reductant (Palatinszky et al. 2015). *CynS* is also widespread in nitrite oxidizing bacteria, and Palatinszky et al. (2015) demonstrated that a nitrite oxidizing bacteria, *Nitrospira moscoviensis*, decomposed cyanate when it was supplied at millimolar concentrations. The resultant NH_4^+ was then available for ammonium oxidation and subsequent nitrite oxidation by *N. moscoviensis*. However, no cyanate uptake transporter has been identified in nitrite oxidizers and it is unknown whether this process occurs at the nanomolar cyanate concentrations observed in marine and estuarine systems to date. If cyanate is an intermediate species in nitrification, the subsurface cyanate maximum could reflect vertical zonation of this process relative to cyanate production pathways.

To date, *cynA* and *cynX* have only been identified in bacteria (Kamennaya and Post 2013; Pao et al. 1998), and *cynA* expression has been primarily observed in cyanobacteria, largely *Prochlorococcus*. It has been suggested that eukaryotic phytoplankton are also capable of utilizing cyanate (Berg et al. 2008; Hu et al. 2012; Wurch et al. 2011; Zhuang et al. 2015), but cyanate uptake has not been conclusively demonstrated for these organisms and no cyanate transporter has been identified in their genomes or in any eukaryotic genome published to date. Our study region was not dominated by *Prochlorococcus* as this genus is less abundant in coastal waters and north of 40 °N (Partensky et al. 1999). There are coastal strains of *Synechococcus* (Scanlan et al. 2009), but no cyanobacterial *cynA* was amplified from samples collected during the May/June 2010 cruise at stations where cyanate uptake was observed (A. Post, pers. comm.). Although failure to detect cyanobacterial *cynA* does not unequivocally confirm its absence, these results combined with the dominance of eukaryotic phytoplankton in this system (Pan et al. 2011) suggest that cyanate was likely taken up by eukaryotes.

Decomposition of cyanate converts 1 mole each of HCO_3^- and cyanate to two moles of CO_2, and it has been suggested that CynS may function as a carbon concentrating mechanism (CCM) in photosynthetic organisms (Guilloton et al. 2002). The highest cyanate concentrations observed to date in marine environments are three orders of magnitude lower than typical

oceanic CO_2 concentrations (Emerson and Hedges 2008), and the half-saturation constants of phytoplankton RuBisCo (range from 6 to 185 μM) are three to five orders of magnitude higher than the highest cyanate concentrations in marine and estuarine waters (Badger et al. 1998; Widner et al. 2013, this study, Chapter III). So, even if cyanate uptake were energetically favorable in comparison to other CCMs, this process would not likely generate enough CO_2 to be assimilated by RuBisCo at a similar rate to HCO_3^--derived CO_2.

Overall, we have demonstrated that cyanate has a biological distribution over a large coastal region, cyanate is taken up in surface waters, and that cyanate is likely produced by organic matter degradation resulting in a subsurface cyanate maximum and higher cyanate concentrations below productive surface waters where phytoplankton biomass is also high. As for other N compounds, the subsurface cyanate maximum is likely due to the balance between its production and consumption: cyanate is taken up in surface waters, produced as a result of decaying organic matter in subsurface waters, and oxidized slowly at depth.

CHAPTER V

CYANATE DISTRIBUTION AND UPTAKE ABOVE AND WITHIN THE EASTERN TROPICAL SOUTH PACIFIC OXYGEN DEFICIENT ZONE

INTRODUCTION

Simple, reduced, organic nitrogen compounds are potentially important sources of nitrogen for assimilation and energy in marine systems (Alonso-Sáez et al. 2012; Palatinszky et al. 2015; Sipler and Bronk 2015) and yet much is still unknown about the cycling of these compounds. Cyanate (OCN^-) is perhaps the simplest organic N compound and has only recently been measured in marine systems (Widner et al. 2013). OCN^- is produced from algal degradation, photochemical reactions, and abiotic urea degradation (Dirnhuber and Schutz 1948; Kamennaya et al. 2008; Widner et al. submitted). Urea [$CO(N_2H_2)_2$] accounts for approximately one third of nitrogen uptake across all aquatic systems and is released to marine systems by bacteria, fecal pellet leaching, sloppy feeding, zooplankton excretion, atmospheric deposition and anthropogenic sources such as wastewater and fertilizer (Bronk and Steinberg 2008; Glibert et al. 2006; Mulholland and Lomas 2008; Sipler and Bronk 2015). Both urea and OCN^- are taken up and produced by marine microbes and therefore have distributions that are biologically controlled, similar to those of ammonium (NH_4^+) and nitrite (NO_2^-) (Gruber 2008; Chapter II; Chapter III). Urea uptake represents 27.7 ±19.0 % of measured N uptake across all aquatic and marine systems (Sipler and Bronk 2015). We found that urea uptake accounted for up to 50 % of the total measured N uptake at a station in the oligotrophic North Atlantic Ocean while OCN^- uptake accounted for up to 10 % of total N uptake (Chapter III).

The genetic capacity for urea uptake and intracellular decomposition are widespread among marine microbes, and the gene for intracellular OCN^- decomposition, *cynS*, has been identified in plants, phytoplankton, bacteria, and archaea (Guilloton et al. 2002). In addition, a OCN^- transporter, *cynABD*, has been identified in some bacteria, including strains of the ubiquitous marine cyanobacteria *Prochlorococcus* and *Synechococcus* (Palenik et al. 2003; Rocap et al. 2003), and *cynA* expression has been observed in marine systems (Kamennaya and Post 2013). Cultured populations of *Synechococcus* WH8102 (Palenik et al. 2003), *Prochlorococcus* MED4 and SB (Berube et al. 2015; Kamennaya et al. 2008), and *Prorocentrum*

donghaiense (Hu et al. 2012) have been grown on OCN^- as the sole source of nitrogen, and more recently, OCN^- and urea have been shown to support nitrification (Alonso-Sáez et al. 2012; Palatinszky et al. 2015) and anaerobic ammonium oxidation (Babbin et al. submitted).

The region of the Eastern Tropical South Pacific (ETSP) adjacent to the Peruvian and Northern Chilean coastline is unique in that rapid coastal upwelling leads to high rates of primary productivity and consequently the largest tonnage fishery in the world (Pennington et al. 2006). Below these highly productive waters, decomposition of sinking particulate organic matter coupled with poor ventilation of subsurface waters leads to the formation of a permanent oxygen deficient zone (ODZ) where oxygen concentrations are below the limit of detection (10 nM) (Revsbech et al. 2009). Although the three major oceanic ODZs in the Eastern Tropical North and South Pacific and Arabian Sea account for just 0.1 % of the ocean's volume (Codispoti et al., 2001), they are biogeochemically significant because they account for a third of oceanic N losses (Codispoti 2007) and because oxygen deficient zones are projected to expand in the future based on global change scenarios (Stramma et al. 2008). These N losses occur via two dissimilatory anaerobic pathways - "canonical" denitrification, a heterotrophic process whereby oxidized nitrogen compounds are reduced to N_2, and anaerobic ammonium oxidation (anammox), a chemoautotrophic process by which NO_2^- and NH_4^+ are converted to N_2 (Devol 2008).

ODZs may be analogous in some ways to the ancient preoxygenated Earth and prebiotic ocean (Paulmier and Ruiz-Pino 2009). The genes for OCN^- assimilation are ancient, and it has been hypothesized that OCN^- may have been a key nitrogen source for early cyanobacteria in ancient oceans (Kamennaya and Post 2011). OCN^- is likely present in abiotic extraterrestrial environments (Cole et al. 2015) and may have been abundant on the prebiotic Earth (Jones and Lipmann 1960; Yamagata and Mohri 1982) where it could have contributed to the synthesis of pyrophosphates (Hagan et al. 2007; Miller and Parris 1964), pyrimidines (Ferris et al. 1968), adenosine diphosphate (ADP) (Yamagata 1999), and peptides (Danger et al. 2006; Danger et al. 2012) and have been linked to cyanobacterial evolution .

In this study, we measured OCN^- concentrations and OCN^- uptake in the ETSP within and above the ODZ. We compared the water column distribution and uptake of OCN^- to those of urea, NH_4^+, NO_2^-, and nitrate (NO_3^-) in the shallow oxic layer (urea distribution was not measured at all stations), the distributions of these compounds in the underlying waters, and rates

of uptake and $^{15}N_2$ production (Babbin et al. submitted) from OCN^-, urea, and NH_4^+ within the ODZ.

MATERIALS AND METHODS

Study Site, Sample Collection, and Cyanate and Nutrient Analysis

All measurements and samples were collected during a cruise aboard the *R/V Nathaniel B. Palmer* from June 27 - July 21, 2013. Stations were located in the ETSP between 10 and 18 °S and 70 and 86 °W (Figure 20). Stations along two transects, one approximately 200 nm offshore and roughly parallel to the coastline and the other along 17 °S from 79 to 86 °W at 1 ° intervals and two process stations (BB1 and BB2), were occupied during the cruise. Station BB2 was located within an area experiencing intense coastal upwelling but this intensity decreased farther offshore (Figure 1A). Temperature, salinity, *in situ* chlorophyll *a* fluorescence (chl *a*), photosynthetically active radiation (PAR, Biospherical), and oxygen (Seabird) were measured using a CTD mounted to a 24-bottle rosette (10 L Niskin bottles) except at station BB2 where they were measured using a CTD mounted to an *in situ* pump profiler. The location of the ODZ was verified using a highly sensitive STOX sensor (detection limit 10 nM). No oxic intrusions were observed within the ODZ as has been shown previously in this area (Revsbech et al. 2009; Tiano et al. 2014; Garcia-Robledo pers. comm.).

At station BB2, OCN^-, urea, NO_3^-, NO_2^-, and NH_4^+ profiles were collected using an *in situ* pump profiler at ~ 4 m resolution. At all other stations, OCN^- samples were collected from the Niskin bottles by gravity filtration through a 0.2 μm membrane filter (Millipore) into triplicate sterile 2 ml polypropylene microcentrifuge tubes (Thomas Scientific, catalog number 1219F50). OCN^- samples were stored at -80 °C until derivatization and analysis by high performance liquid chromatography (HPLC) according to Widner et al. (2013) and Chapter IV and urea samples were stored at -20 °C until analysis by nutrient autoanalyzer (Price and Harrison 1987). At all stations other than BB2, NO_3^- and NO_2^- samples were collected directly from Niskin bottles into 30 ml acid-washed high density polyethylene (HDPE) bottles and analyzed shipboard within 24 hours using a nutrient autoanalyzer. Unfiltered NH_4^+ samples were collected directly from Niskin bottles into 60 mL pre-conditioned HDPE bottles and

analyzed using the OPA method (Holmes et al. 1999). Limits of detection for NO_3^-, NO_2^-, NH_4^+, urea, and OCN^- were 70, 70, 50, 70, and 0.4 nM, respectively.

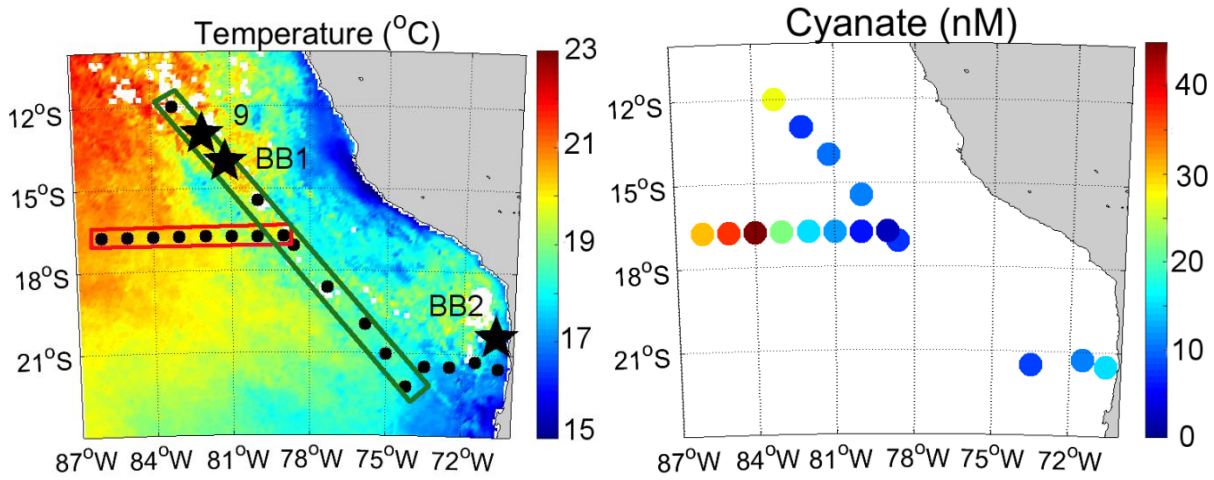

Figure 20. Station Map for the Eastern Tropical South Pacific. Locations of all CTD casts (circles) and stations 9, BB1, and BB2 (stars) overlie satellite-derived sea surface temperature (left). The longitudinal transect (Figures 21 and 22) and the transect parallel to the coastline (Figures 23 and 24) are shown in red and green boxes, respectively. Surface cyanate concentrations are shown in the right panel.

Oxic Uptake Methods

N uptake (NO_3^-, NO_2^-, NH_4^+, urea, and OCN^-) was measured at the surface and deep chl *a* maximum (DCM) at stations 9 and BB1; NH_4^+, urea, and OCN^- uptake were measured at station BB2. Oxygenated water samples collected from Niskin bottles mounted to the CTD rosette were transferred directly to 1 L PETG incubation bottles. Uptake experiments were initiated by adding highly enriched (98 %) ^{15}N-labeled NH_4^+, NO_3^-, NO_2^-, and $^{15}N^{13}C$-labeled urea and OCN^-. Substrate additions for oxic incubations were targeted to be between 2 and 10 % of the ambient concentrations of NH_4^+, NO_3^-, NO_2^-, urea, and OCN^- to yield reliable uptake rate measurements. When ambient concentrations were unknown prior to the initiation of experiments (urea and OCN^-) or were < 300 nM (sometimes true for NO_2^- and NH_4^+), 30 nM substrate additions were

made, which led to enrichments ≥ 10 % and may have stimulated uptake. Incubation bottles were placed in deck incubators equipped with flow-through seawater and 1, 2, or 4 neutral density screens to simulate *in situ* light conditions (55, 28, and 14 % of ambient incident light). Incubations were terminated after 2 hours by vacuum filtration (0.7 μm GF/F, ≤ 5 mm Hg) and filters were stored at -20 °C until analysis. Filters were dried at 40 °C, pelletized in tin capsules and analyzed on a Europa 20/20 isotope ratio mass spectrometer equipped with an automated N and C analyzer. Uptake rates were calculated using a mixing model (Montoya et al. 1996; Mulholland et al. 2006; Orcutt et al. 2001), and limits of detection were calculated as in Chapter IV.

Uptake kinetics of NH_4^+, urea, and OCN^- were measured at stations BB1 and BB2 by making ^{15}N-labeled substrate additions ranging from 10 to 1000 nM and incubating bottles for 2 hours as described above. To determine diurnal variability in OCN^- uptake in surface waters, OCN^- uptake experiments were conducted using water sampled from the ship's flow-through system at station BB2 and collected from a patch of water the ship followed using floating sediment traps as drogues. Diurnal uptake experiments were initiated approximately every 4 hours over a 27 hour period.

Anoxic Uptake Rates

Uptake rates were determined in anoxic, sub-euphotic waters at station BB2. To our knowledge, uptake rates have not been previously measured in anoxic waters below the euphotic zone. Anoxic samples were incubated in duplicate acid-washed, helium-purged, evacuated, 3.8 L, 2-mil thick, polyvinyl fluoride (PVF) opaque gas sampling bags with dual entry points: one a nickel-plated brass hose barb and the other a septum (Tedlar, Cole Parmer EW-01409-92). Water was transferred from Niskin bottles into the bags using teflon tubing attached to the barb. Any helium remaining in the bag after filling was removed by syringe through the septum port. To minimize oxygen contamination from air at the top of the Niskin bottle, Niskin bottles remained sealed until immediately prior to sampling, and only one bag was filled per Niskin bottle. Although these bags were used successfully on a previous cruise (Jayakumar et al. unpubl.), the batch of bags ordered for this cruise was unexpectedly fragile and even with careful handling, approximately 30 % of the bags ruptured leading to loss of replicates.

For all anoxic incubations, ambient concentrations of urea, NH_4^+, and OCN^- were below the limit of detection, and substrate additions ranged from 105 to 145 nM N consequently, rate estimates should be considered maximum rates. All bags were incubated in the dark at 11 °C in a cold room. Because some of the anoxic incubations included water from the secondary chl *a* maximum, uptake by phytoplankton may have been underestimated in dark incubations although PAR at the secondary chl *a* maximum was < 0.1 % of surface PAR. Because N uptake has not previously been measured in this environment and at such low biomass, each bag was sampled at multiple time points to determine the linearity of uptake over time and the optimal incubation length. Incubation times (12 to 48 hours) were longer than typical uptake incubations (McCarthy and Bronk 2008) because particle flux, and by extension microbial biomass and uptake rates, decreases exponentially with depth below the euphotic zone (Martin et al. 1987). Samples to measure uptake rates were collected using a peristaltic pump fitted with a GF/F (0.7 μm) housed in a swinnex filter holder. The filtrate was collected in a graduated cylinder to determine the volume filtered at each time point. Filters were stored at -20 °C until analysis as described above. Uptake rates were calculated in two ways. First, a rate was calculated for each time point using the standard method (hereon referred to as the standard calculation) described above for the oxic incubations and second, a rate was calculated by fitting a simple linear regression to N taken up over time for all replicate bags and time points (hereon referred to as the time series calculation), the typical method for calculating rates of dissimilatory nitrogen processes such as anammox (Dalsgaard et al. 2003) which was estimated in parallel incubations (Babbin et al. submitted) and with which we compare our uptake rates.

Ocean Color and Sea Surface Temperature

Ocean color and sea surface temperature data used in this study were produced with the Giovanni online data system, developed and maintained by the National Aeronautic and Space Administration Goddard Earth Sciences Data and Information Services Center (NASA GES DISC) (Acker and Leptoukh 2007).

RESULTS

Hydrographic Parameters and Dissolved N Distributions

Surface waters in the study region were characterized by cold, high chl *a* water nearshore and warmer, lower chl *a* water offshore (Figure 20A, data not shown). Surface OCN^- concentrations were highest at the northern- and western-most stations of the study region (Figure 20B) where high temperatures indicated that the water mass was influenced by the South Equatorial Current rather than the cold Peru current which flows along the coast (Pennington et al. 2006). Overall, OCN^- concentrations ranged from below the limit of detection (b.d.l.; 0.4 nM) to 45 nM above the oxycline where the mean concentration was 5.2 ± 8.5 nM (n = 286, where each n is the average of three replicates) and from b.d.l. to 10 nM in underlying anoxic waters where the mean concentration was 1.4 ± 1.8 (n = 69, where each n is the average of three replicates) (Figures 21-24).

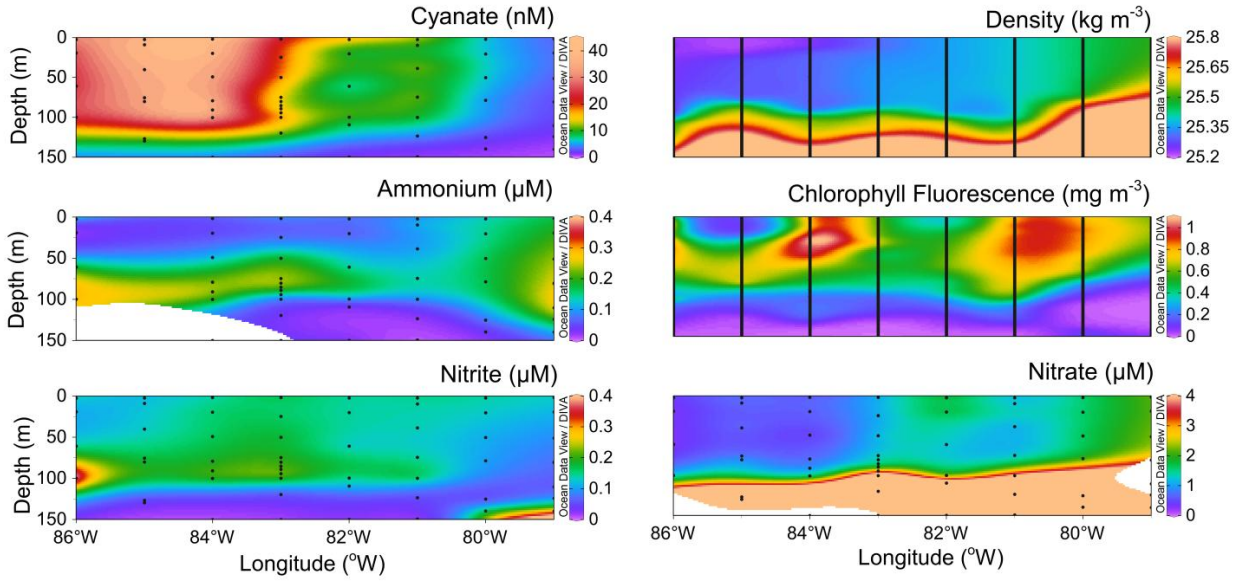

Figure 21. Hydrographic parameters in the upper 150 m along a longitudinal transect at 17 °S. Cyanate concentrations, density, and ammonium, chlorophyll *a* fluorescence, nitrite, and nitrate concentrations are shown. Black dots and lines represent sampling locations and the colored contours represent interpolations of the given parameters between those data points. See Figure 20 for station locations.

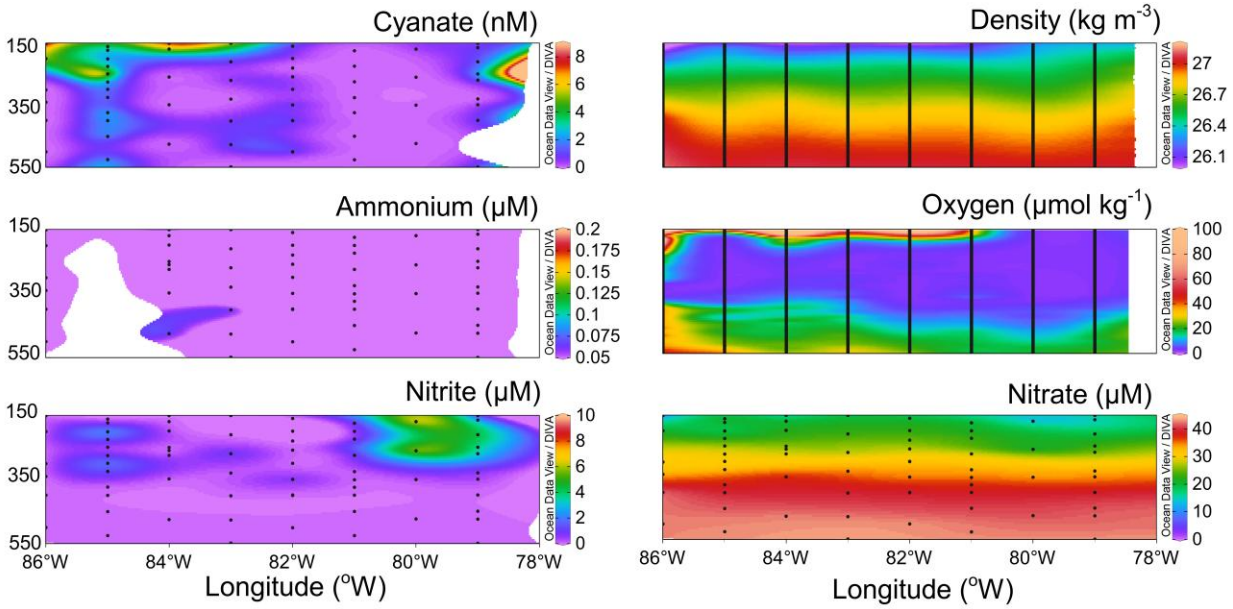

Figure 22. Hydrographic parameters between 150 and 500 m along a longitudinal transect at 17 °S. Cyanate concentrations, density, and ammonium, oxygen, nitrite, and nitrate concentrations are shown. Black dots and lines represent sampling locations and the colored contours represent interpolations of the given parameters between those data points. See Figure 20 for station locations.

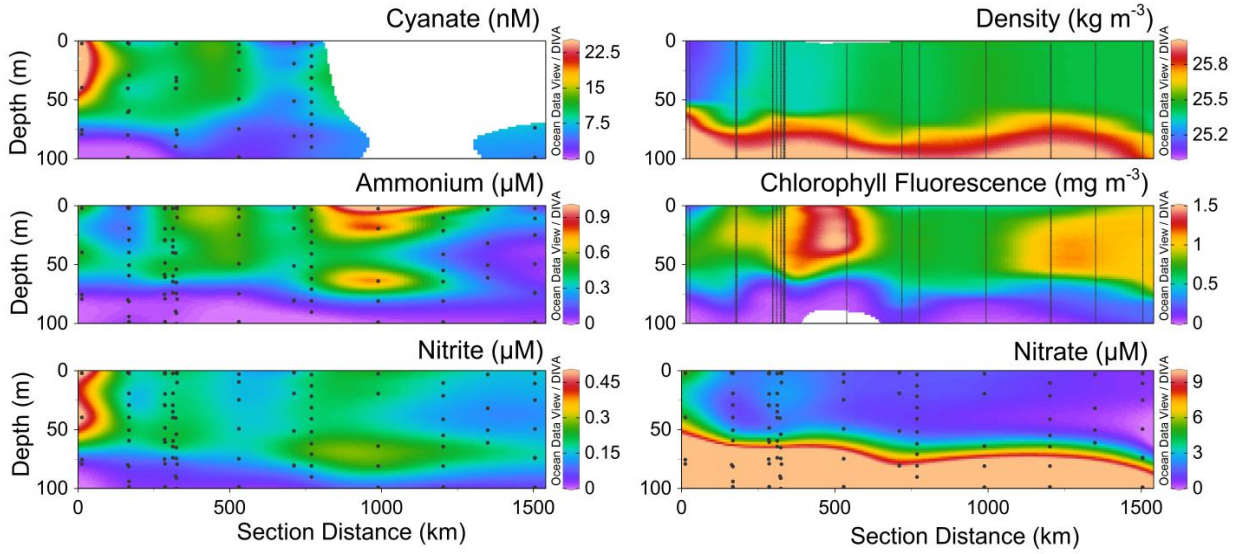

Figure 23. Hydrographic parameters in the upper 100 m along a transect parallel to the coastline. Cyanate concentrations, density, and ammonium, chlorophyll *a* fluorescence, nitrite, and nitrate concentrations are shown. Black dots and lines represent sampling locations and the colored contours represent interpolations of the given parameters between those data points. The left side (0 km) represents the northernmost station and the right side (1500 km) represents the southernmost station. See Figure 20 for station locations.

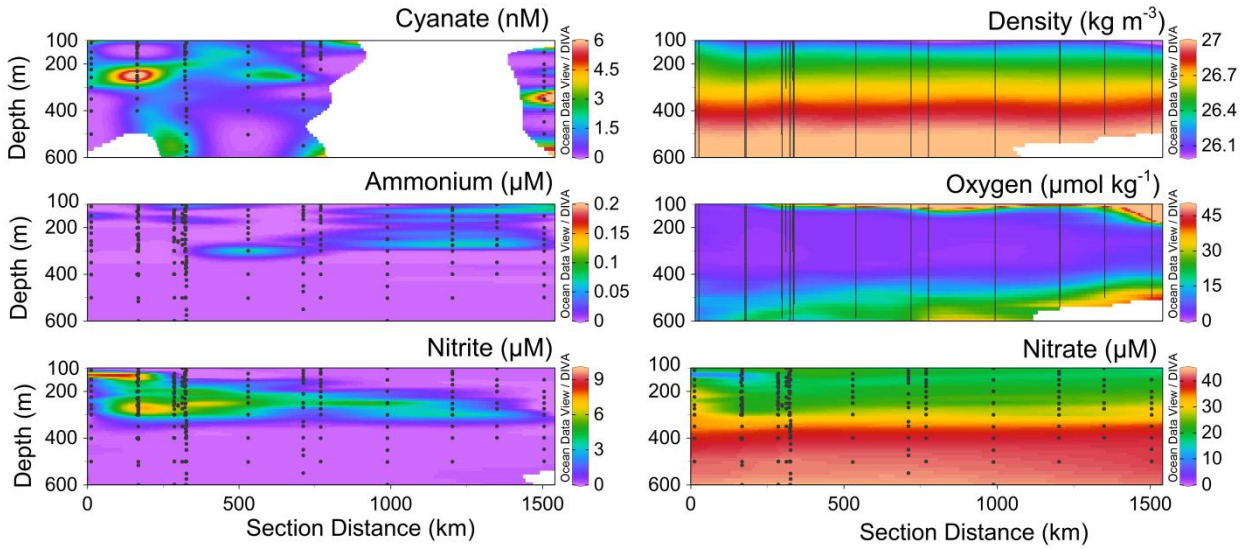

Figure 24. Hydrographic parameters between 100 and 600 m along a transect parallel to the coastline. Cyanate concentrations, density, and ammonium, oxygen, nitrite, and nitrate concentrations are shown. Black dots and lines represent sampling locations and the colored contours represent interpolations of the given parameters between those data points. The left side (0 km) represents the northernmost station and the right side (1500 km) represents the southernmost station. See Figure 20 for station locations

Along the longitudinal transect, density and NO_3^- concentrations above the pycnocline were higher in the east than in the west (Figure 21), likely indicating coastal upwelling which is common in this region (Pennington et al. 2006). In contrast, OCN^- concentrations above the pycnocline were highest in the western half of the transect and were the highest OCN^- concentrations observed in the study region (up to 45 nM, Figure 21). Above the pycnocline along the longitudinal transect, NH_4^+ and NO_2^- ranged from 0.3 to below the limit of detection (b.d.l.) and 0.4 to b.d.l. µM, respectively, with subsurface maxima below the chl *a* maximum (Figure 21).

Along the longitudinal transect, the ODZ thickened towards the coast, increasing from 40 m in thickness at the farthest west station to 370 m at the easternmost station (Figure 22). Secondary NO_2^- maxima (SNM) were present in the mid to upper ODZ, and an especially strong SNM was observed at the eastern end of the transect which corresponded to a decline in NO_3^-

concentrations compared to adjacent waters (Figure 22) indicating a zone of incomplete denitrification (Devol 2008). NH_4^+ concentrations were less than 0.1 μM or b.d.l. below the oxycline, and OCN^- concentrations were b.d.l. below the oxycline except for small patchy local maxima in the middle of the ODZ mainly in the western half of the transect (Figure 22).

Along the transect parallel to the coastline, density was lower at the northern end (Figure 23) delineating the influence of the warm South Equatorial Current in the North and the cold Peru current in the south, as is also visible from satellite-derived sea surface temperature (Figure 20A). Above the pycnocline, NO_3^-, NO_2^-, and OCN^- were highest at the northern end of the transect reaching concentrations of 5.5 μM, 0.6 μM, and 27 nM, respectively (Figure 23). NO_2^-, NH_4^+, and OCN^- concentrations were patchy above the pycnocline, probably due to low sampling resolution in highly productive waters with variable advection along the transect. There was a subsurface NO_2^- concentration maximum in the southern half of the transect (Figure 23).

On the transect parallel to the coastline, the ODZ was 100 to 300 m thick (thicker in the North) with a SNM throughout most of the transect (Figure 24). NO_2^- concentrations in the SNM were highest at the northern end (up to 10 μM), corresponding to a decrease in NO_3^- concentrations relative to adjacent waters (Figure 24), as was observed at the eastern end of the longitudinal transect (Figure 22). NH_4^+ concentrations were < 0.1 μM throughout the ODZ. OCN^- concentrations were patchy throughout the ODZ, likely due to low sampling resolution (Figure 24), and there were OCN^- concentration maxima at the northern and southern ends of the transect (6.8 and 6.4 nM). The maximum at the northern location was located between two SNMs at the same station including the highest NO_2^- concentration from the study region, but there was no SNM at the southern end where the other OCN^- maximum was observed (Figure 24). OCN^- concentrations were < 2 nM below 700 m at all stations (data not shown).

At station BB1 chl *a* was approximately 1 mg m^{-3} above 60 m with a slight maximum centered at 30 m (Figure 25A). The base of the euphotic zone (1% of surface PAR) was at 66 m (data not shown), the nitracline was at 60 m, and the ODZ extended from 190 to 370 m (Figure 25A). NO_3^- increased with depth below the pycnocline but decreased in concentration in the ODZ corresponding to an increase in NO_2^- concentrations (Figure 24B). OCN^- and NH_4^+ concentrations were highest at the surface, and there was a subsurface maximum in urea concentration. While urea and NH_4^+ concentrations peaked at approximately 0.6 μM, OCN^-

concentrations peaked at only 10 nM (Figures 24 C-E). OCN^- and NH_4^+ concentrations decreased to b.d.l. at the upper oxycline, although there was a small OCN^- peak within the ODZ (198 m, 3.6 nM).

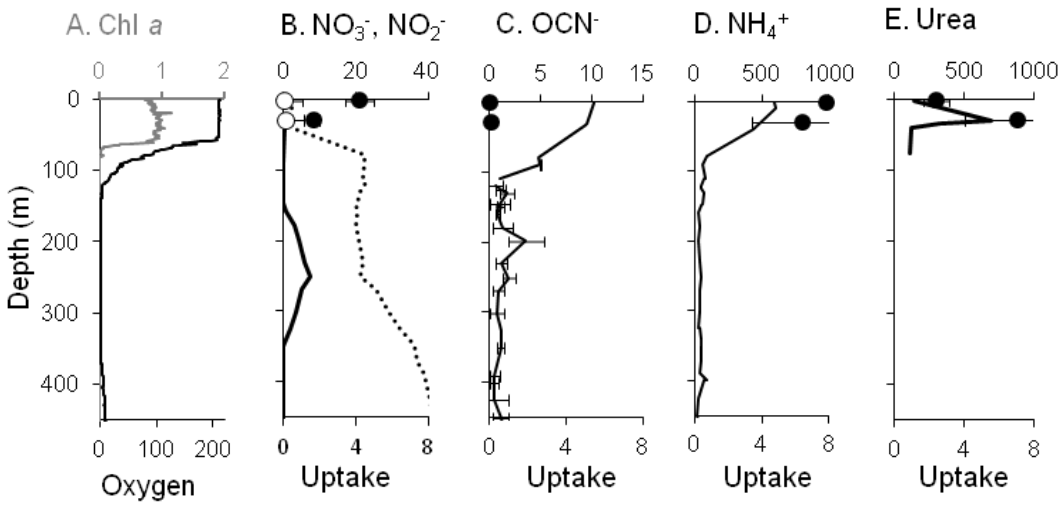

Figure 25. Vertical distributions and uptake rates for station BB1. A) Chlorophyll *a* Fluorescence (Chl *a*, mg m^{-3}) is shown in grey and oxygen concentrations (umol kg^{-1}) are shown in black. B) Nitrate (NO_3^-) and nitrite (NO_2^-) concentrations (μM) are shown with a dotted line and solid line, respectively, and uptake rates of NO_3^- and NO_2^- are shown with closed and open circles, respectively. In panels C-E concentrations (nM) of cyanate (OCN^-), ammonium (NH_4^+), and urea are depicted by the solid lines, and uptake rates of OCN^-, NH_4^+, and urea (nmol l^{-1} h^{-1}) are depicted with closed circles, Concentrations and uptake rates below the detection limit were plotted as equal to the detection limit (0.6 nM for OCN^-, 80 nM for urea, 50 nM for NH_4^+, and 70 nM for NO_2^- and NO_3^-). Error bars are ± 1 standard deviation for OCN^- concentrations (n = 3) and ± 1 average deviation for uptake rates (n = 2).

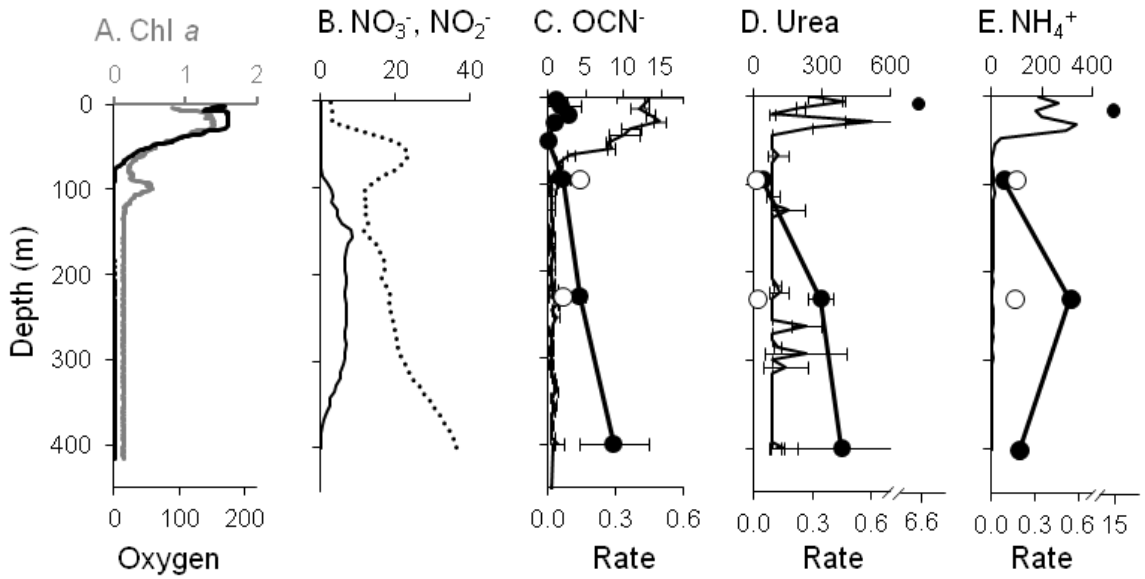

Figure 26. Vertical distributions, uptake rates, and anammox rates for station BB2. A) Chlorophyll *a* fluorescence (chl *a*, mg m^{-3}) is shown in grey and oxygen (μmol kg^{-1}) is shown in black. B) Nitrate (NO_3^- μM) is shown with a dotted line and nitrite (NO_2^-, μM) is shown with a solid line. In panels C-E concentration (nM) is depicted by the continuous solid line (samples collected every 4 m), uptake rate from the first time point (nmol l^{-1} h^{-1}) is depicted with closed circles, and rate of $^{15}N_2$ production from cyanate (OCN^-), urea, and ammonium (NH_4^+, nmol l^{-1} h^{-1}) is depicted by open circles. Concentrations and uptake rates below the detection limit were plotted as equal to the detection limit (0.6 nM for OCN^-, 80 nM for urea, and 10 nM for NH_4^+). Error bars are ± 1 standard deviation (concentration, $^{15}N_2$ production, n = 3) and ± 1 average deviation (uptake, n = 2). $^{15}N_2$ production rates and NO_3^-, NO_2^-, and oxygen profiles are reproduced from Babbin et al (submitted).

At station BB2 there were two chl *a* maxima, one in the oxic layer at 25 m and one in the ODZ centered around 99 m (Figure 26A) where PAR was < 0.1 % of surface irradiance (data not shown). The base of the euphotic zone (1 % of surface PAR) was at 40 m (data not shown) and the ODZ extended from 90 to 400 m (Figure 26A). As for BB1 and the transects, NO_3^- increased with depth below the pycnocline but then decreased in concentration in the ODZ corresponding to an increase in NO_2^- concentrations (Figure 26B). Vertical profiles of concentrations and uptake rates for OCN^-, urea, and NH_4^+ are shown in Figures 26 C - E. Although OCN^- concentrations were an order of magnitude lower than urea and NH_4^+ concentrations, the vertical profiles of all three were similar in shape with high surface concentrations, a subsurface minimum, and a maximum at 28 m. The OCN^-, urea, and NH_4^+ maxima were shallower than the primary NO_2^- maximum (PNM, 40 m) and deeper than the nitracline (25 m). Concentrations decreased to below detection near the base of the oxic layer, although the decrease in NH_4^+ and urea concentrations with depth was sharper than the decrease in OCN^- concentration.

Cyanate Uptake

OCN^- N uptake in surface waters and at the DCM at stations 9 and BB1 was less than 2 % of total measured N uptake (NH_4^+, urea, NO_3^-, NO_2^-, and OCN^-) (Figures 25 B-E and 27, Table 11), but the OCN^- turnover time was comparable to those of NH_4^+ and urea except at the surface at BB1 (Table 11). The majority of N taken up in the upper oxic water column was from NH_4^+ and urea, and the turnover times of these were less than 2 days for NH_4^+ and ≤ 8 days for urea (Table 11). At station BB2, OCN^- uptake at the surface and DCM was less than 1 % of NH_4^+ and urea uptake in the surface (Figure 26). OCN^- and urea C uptake was below the limit of detection at stations 9 and BB1.

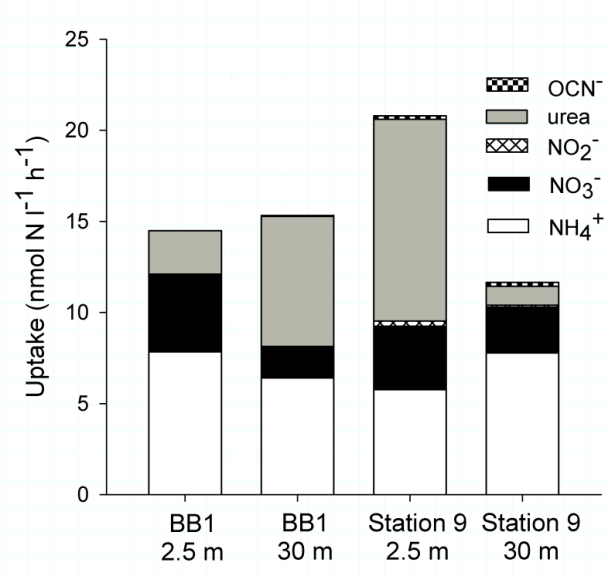

Figure 27. N uptake at two offshore stations. Total N uptake is the sum of ammonium (NH_4^+, white), nitrate (NO_3^-, black), nitrite (NO_2^-, hatched), urea-N (grey), and cyanate (OCN^-, black and white checked) uptake. See Table 11 for uptake rates including error.

Table 11. Uptake rates, turnover times, and ambient concentrations of nitrate (NO_3^-), nitrite (NO_2^-), ammonium (NH_4^+), urea, and cyanate (OCN^-) for stations BB1 and 9. Values below the limit of detection are indicated as b.d.l., and turnover times that could not be calculated because the uptake rate or concentration was b.d.l. are listed as N/A. Average deviations (n =2) are shown in parentheses. Uptake rates are in nmol N l^{-1} h^{-1}, turnover times are in days, and concentrations are in μM N.

Station	Latitude (°S)	Longitude (°E)	Depth (m)		NO_3^-	NO_2^-	NH_4^+	Urea	OCN^-
BB1	13.711	-81.390	2.5	Uptake	4.2(0.8)	0.04(0.0)	7.8(0.1)	2.4(0.7)	.01(0.0)
				Turnover Time	24	170	1.6	4.9	36
				Concentration	2.4	0.2	0.3	0.3	0.01
BB1	13.711	-81.390	30	Uptake	1.7(0.3)	0.1(0.1)	6.4(3.0)	7.1(3.1)	.05(0.0)
				Turnover Time	63	110	1.9	8.0	8.1
				Concentration	2.5	0.2	0.3	1.4	0.01
9	13.002	-82.198	2.5	Uptake	3.5(4.3)	0.3(0.1)	5.8(2.4)	11(2.7)	0.2(0.0)
				Turnover Time	13	15	0.9	2.3	2.3
				Concentration	1.1	0.1	0.1	0.6	0.01
9	13.002	-82.198	30	Uptake	2.5(3.3)	0.1(0.1)	7.8(0.8)	1.0(0.2)	0.2(0.2)
				Turnover Time	17	34	0.7	N/A	2.5
				Concentration	1.0	0.1	0.1	b.d.l.	0.01

OCN^- uptake did not reach Michaelis-Menten kinetics saturation at 1000 (BB1) or 600 (BB2) nM (Figure 28). Uptake kinetics could not be determined for urea or NH_4^+ at either station because concentrations of urea and NH_4^+ were 100 and 300 nM (for urea) and 300 and 600 nM (for NH_4^+) at BB1 and BB2, respectively, and uptake for both was saturated at these concentrations (data not shown). OCN^- C uptake was b.d.l. for all kinetics experiments. There was Significant diurnal variability in OCN^- uptake at station BB2 for both N and C uptake (Figure 29). Both volumetric and chl *a* -normalized N uptake were highest in the afternoon, but uptake was significantly higher on the second day (0.25 ± 0.12 nmol N l^{-1} h^{-1} at 16:20) than on the first day (0.04 ± 0.01 nmol N l^{-1} h^{-1} at 15:45) suggesting substantial daily variability as well. Volumetric and chl *a* -normalized C uptake was higher at night than during the day and also exhibited daily variability with higher uptake on the first day (0.3 ± 0.02 nmol C l^{-1} h^{-1} at 15:45) than on the second day (b.d.l. (< 0.02 nmol C l^{-1} h^{-1}) at 16:20).

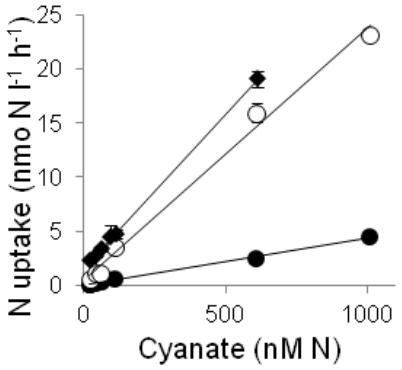

Figure 28. Cyanate uptake kinetics. Cyanate uptake at station BB1 in surface water (closed circles, R^2 = 0.9981) and at water collected from the DCM (open circles, R^2 = 0.9928), and at station BB2 in surface water (diamonds, R^2 = 0.9995). Error bars are ± 1 standard deviation (n = 2) where error bars not visible are smaller than the symbol.

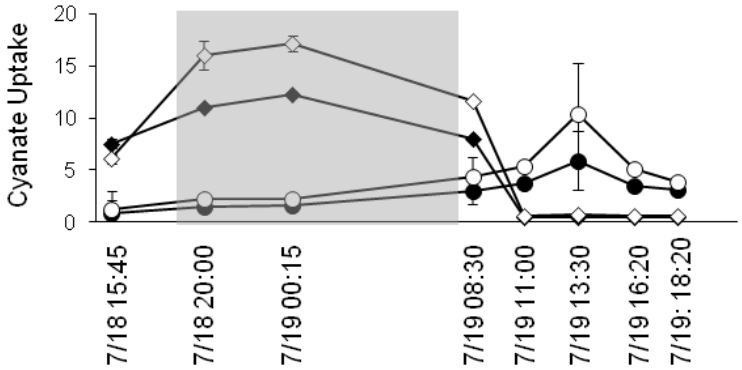

Figure 29. Diurnal cyanate uptake at station BB2. Samples were collected from the ship's seawater flow-through system on July 18 and 19, 2013 to measure cyanate uptake. N uptake rates are reported in nmol N l^{-1} h^{-1} (closed circles) and nmol N μg (Chl *a*)$^{-l}$ h^{-1} (open circles), and C uptake rates are reported in nmol C l^{-1} h^{-1} (closed diamonds) and nmol C μg (Chl *a*)$^{-l}$ h^{-1} (open diamonds). Error bars are ± 1 average deviation (*n*=2) and time is the mean of the incubation length for ~ 2 hour incubations. Carbon uptake rates that were b.d.l. are reported as equal to the average detection limit (0.02 nmol C l^{-1} h^{-1}).

At station BB2, OCN^-, urea, and NH_4^+ N was taken up just below the oxycline (95 m), at the SNM depth (230 m), and at the base of the ODZ (400 m) (Figures 27 C-E and 30, Table 12). Urea C uptake was b.d.l. at all ODZ depths, and OCN^- C uptake was b.d.l. at all depths and time points except for 95 m after 36 hours calculated using the standard calculation where the rate was 1.4 ±0.8 pmol C l^{-1} h^{-1}. Uptake of picomolar C was detectable because the uptake detection limit is inversely proportional to incubation time. NH_4^+ uptake was highest at the depth of the SNM, and urea and OCN^- uptake rates increased with depth within the ODZ and were highest at the base of the ODZ despite concentrations below detection for all three substrates throughout the ODZ (Figures 25 C-E). OCN^- uptake was of similar magnitude throughout the water column while urea and NH_4^+ uptake were 1 to 2 orders of magnitude higher at the surface than in the ODZ (Figures 26 D-E). In the ODZ, uptake rates of OCN^-, urea, and NH_4^+ were similar in magnitude to rates of $^{15}N_2$ production from those same compounds (Babbin et al. submitted, Figures 26 D-E). Uptake and $^{15}N_2$ production rates were similar at the top of the ODZ for all

three compounds, but uptake was significantly higher than $^{15}N_2$ production in the middle of the ODZ for all compounds.

For ODZ N uptake rates calculated using the standard calculation (Montoya et al. 1996; Mulholland et al. 2006; Orcutt et al. 2001), there were no significant differences between the first and second time points for all substrates (NH_4^+, OCN^-, and urea) and depths (95, 230, and 400 m), except for NH_4^+ at 95 m where uptake was significantly lower at the shorter time point (8 hours) compared to the longer time point (36 hours, Figure 30, Table 2), possibly indicating stimulation of uptake by substrate addition. However, uptake rates were linear for pooled replicate bags over the three time points as determined using the time series calculation (linear regression of N taken up over time for significance criterion $\alpha = 0.05$), except for OCN^- at 95 m and NH_4^+ at 400 m (Table 12). These deviations from linearity could have resulted from high variability between incubation bags, possibly caused by variable oxygen contamination or low sample size. For future studies of OCN^- N uptake where only one time point is logistically feasible, we recommend incubation lengths of 8 to 12 hours to maximize detectability but minimize bottle effects. To measure C uptake, incubation lengths should be > 36 hours.

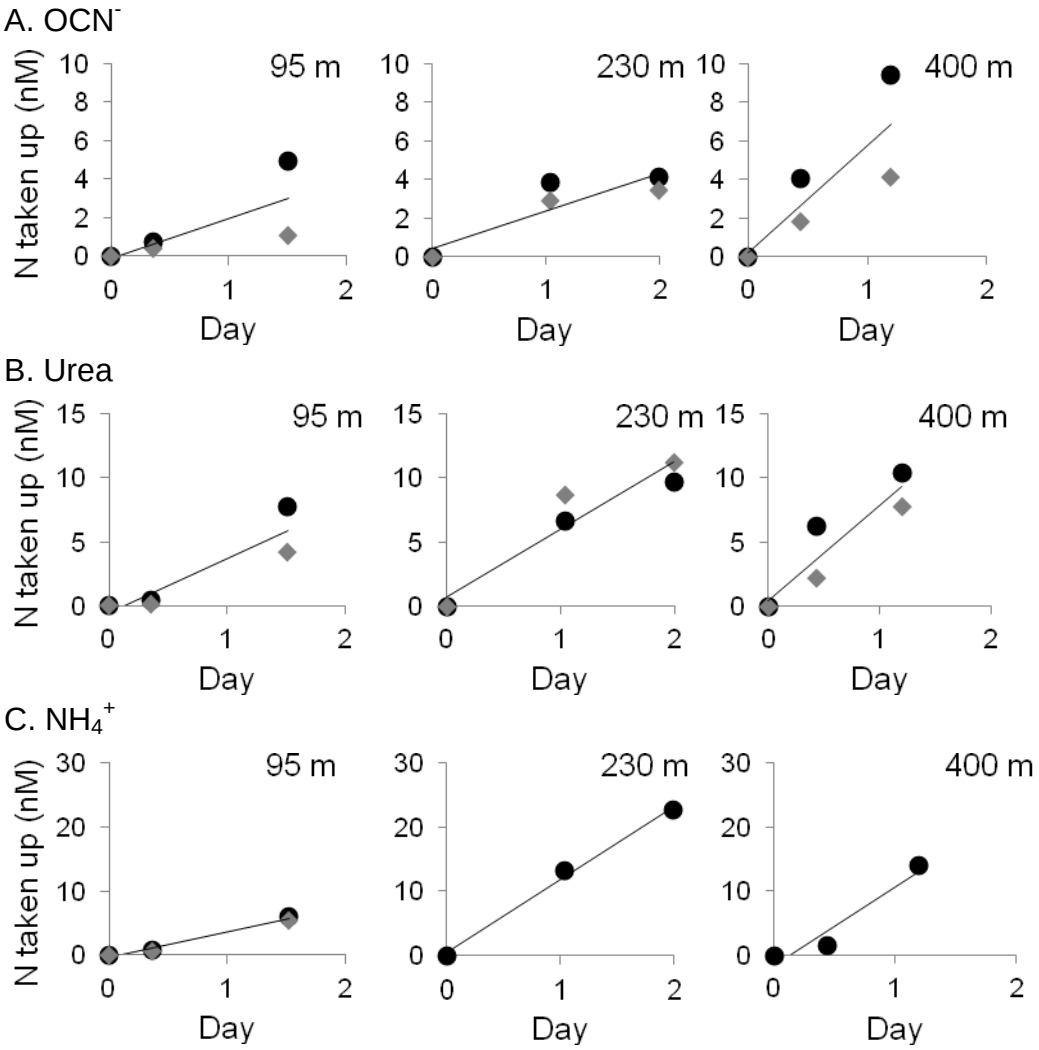

Figure 30. Uptake time series in the oxygen deficient zone. N taken up is shown for cyanate (OCN^-, A), urea (B) and ammonium (NH_4^+, C) at the first anoxic depth (95 m), at the secondary nitrite maximum (230 m), and just above the base of the ODZ (400 m). All incubations were performed at station BB2 in gas tight bags which were sampled at two time points. Replicate bags are represented by grey diamonds and black circles, and the uptake rate was calculated as the slope of the line of the average of all replicates (solid line). Statistical parameters and uptake rates are shown in Table 2.

Table 12. N uptake rates in the oxygen deficient zone at station BB2 calculated using the standard and time series calculations. For the standard calculation (Montoya et al. 1996; Mulholland et al. 2006; Orcutt et al. 2001), individual rates were calculated for each time point (A and B). Average deviations (n = 2 incubation bags) are shown in parentheses and p-values are the result of a two-tailed t-test where a bold value indicates a significant difference in uptake rate between time points A and B for $\alpha = 0.05$. For the time series calculation (Dalsgaard et al. 2003), standard errors (n = 6 or 3$^{\beta}$) are shown in parentheses, and p values shown in bold and italics indicate statistically significant linear uptake rates for α = 0.05 and 0.1 criteria, respectively. Statistical parameters that could not be calculated due to low number of replicates are given as N/A.

		Standard Uptake Calculation					Time Series Calculation		
	Depth (m)	Uptake (nmol N l^{-1} h^{-1})		Incubation Time (hours)		p	N Uptake (nmol N l^{-1} d^{-1})	R^2	p
		A	B	A	B				
OCN^-	95	0.07(0.03)	0.09(0.08)	8.6	36.3	0.78	0.08(0.04)	0.5689	*0.0755*
	230	0.14(0.02)	0.08(0.01)	25.9	47.9	0.11	0.08(0.03)	0.8182	**0.0100**
	400	0.13(0.00)	0.29(0.16)	10.5	28.8	0.77	0.23(0.03)	0.7309	**0.0242**
Urea	95	0.04(0.03)	0.18(0.07)	8.6	36.3	0.13	0.17(0.04)	0.8552	**0.0061**
	230	0.34(0.07)	0.24(0.03)	24.9	47.9	0.18	0.22(0.04)	0.917	**0.0019**
	400	0.45(0.31)	0.35(0.08)	10.5	28.8	0.70	0.31(0.04)	0.8638	**0.0053**
NH_4^+	95	0.09(0.00)	0.16(0.01)	8.8	36.5	**0.01**	0.16(0.04)	0.9847	< **0.0001**
	230$^{\alpha}$	0.20$^{\alpha}$	0.58$^{\alpha}$	24.9	47.9	N/A	0.47(0.04)	0.99	< **0.0001**
	400$^{\alpha}$	0.54$^{\alpha}$	0.36$^{\alpha}$	10.5	28.9	N/A	0.51(0.04)	0.93	*0.0716*

DISCUSSION

Oxic Processes

The shallow, euphotic oxic region sampled in the ETSP was characterized by NO_3^- in the low micromolar range, elevated OCN^- relative to deeper waters, patchy NO_2^- and NH_4^+, and high concentrations of chl *a*. Micromolar surface DIN concentrations are typical for this region due to the balance between inputs from nutrient-rich equatorial waters, thermocline shoaling, coastal upwelling, and drawdown from high productivity (Pennington et al. 2006). OCN^- concentrations were mostly uniform with depth above the pycnocline and below the limit of detection below the pycnocline with the exception of small maxima within the ODZ at some stations. OCN^- uptake was a small fraction of N uptake in the oxic water column (< 1 %), and OCN^- uptake was not saturated after addition of 1 μM substrate, but urea and NH_4^+ uptake were saturated for all substrate additions (up to 1 μM). From this we infer that OCN^- did not contribute significantly to N uptake in this system at this time of year.

OCN^- distributions were previously measured in the coastal North Atlantic between Cape Hatteras and the Gulf of Maine where they ranged from 0 to 25 nM (Chapters III and IV) however in the ETSP OCN^- concentrations were at or near the limit of analytical detection (Chapters III and IV). The North Atlantic study region is an N-limited temperate Western boundary area with a wide continental shelf and a mixed, seasonally dynamic phytoplankton community (Townsend et al. 2006), whereas the ETSP is a tropical Eastern boundary with a narrow continental shelf, coastal upwelling, general diatom dominance, and offshore iron limitation (Pennington et al. 2006). At stations on the continental shelf slope in the coastal North Atlantic, the OCN^- concentration was less than 2 nM at the surface and there was a OCN^- maximum below the DCM followed by a gradual decline in OCN^- concentration to below detection below 500 m (Chapters III and IV), whereas in this study, OCN^- concentrations were high (10 to 45 nM) in shallow waters and rapidly declined below the pycnocline with no subsurface maxima associated with the DCM. OCN^- profiles in the coastal North Atlantic were attributed to uptake in sunlit waters, production by degrading organic matter as it sank out of the euphotic zone, and oxidation at depth. In this study, increases in surface OCN^- concentrations along the western half of longitudinal 17 ^oS transect could have been a result of degradation of

chl *a* biomass as productive upwelled water moved offshore. High OCN^- concentrations above the pycnocline could also be explained by phytoplankton community composition. OCN^- is produced in senescing diatom cultures (Chapter III), to our knowledge sequenced diatoms do not have the genes for OCN^- utilization (Guilloton et al. 2002), and this system is typically dominated by diatoms (Pennington et al. 2006).

OCN^- N uptake rates at the surface and DCM were similar (1.7 ± 1.5 nmol l^{-1} h^{-1}, n = 29, 1 cruise) to those observed in the coastal North Atlantic Ocean (1.3 ± 1.9 nmol l^{-1} h^{-1}, n = 135, 4 cruises, Chapter IV). In both this study and the coastal North Atlantic, OCN^- uptake was a small fraction of total N uptake, while in the oligotrophic North Atlantic, OCN^- N was up to 10 % of total N uptake (Chapter III) indicating that OCN^- may be a quantitatively more important source of N in oligotrophic systems than in nutrient-rich coastal waters as suggested in previous studies (Kamennaya and Post 2013). Stations 9 and BB1 are on the edge of the Peruvian Coastal Upwelling region, which is typically dominated by diatoms which are thought to prefer NO_3^- as a N source (Pennington et al. 2006). In the present study, NO_3^- only accounted for 10- 29 % of total N uptake while the reduced forms of N, urea and NH_4^+, accounted for 8 - 53 % and 27 - 66 % of N uptake, respectively possibly indicating that these stations were outside the main upwelling region.

OCN^- N uptake was highest at midday, while OCN^- C uptake was highest at night (Figure 29) possibly indicating light dependence and inhibition of OCN^- N and C uptake, respectively, which may indicate different groups of organisms utilized OCN^- N and C. In the coastal North Atlantic, over four cruises where measurements were made during the afternoon, OCN^- N uptake predominated at the surface while OCN^- C uptake predominated at the DCM (Chapter IV). We attributed surface N uptake to phytoplankton and speculated that, at deeper depths, high uptake of C relative to N was because of light-inhibited dissimilatory oxidation OCN^- N and uptake of OCN^- C by chemoautotrophic nitrifiers. OCN^- can be used as a source of reductant by some ammonia oxidizers, and many NO_2^- oxidizers, including several marine strains, have the genes for OCN^- utilization (Palatinszky et al. 2015; Spang et al. 2012). Marine ammonia oxidation has been shown to be higher at night than during the day which may be attributed to reduced competition with phytoplankton (Smith et al. 2014) or photoinhibition of ammonia oxidation (Hooper and Terry 1974). A diurnal cycle of ammonia oxidation would explain the presence of archaeal ammonia oxidation genes and transcripts in surface waters when ammonia oxidation

was previously thought to be confined to the base of the euphotic zone (Church et al. 2010; Pedneault et al. 2014; Santoro et al. 2010). Our results may indicate that, in ETSP surface waters, OCN^- N is primarily taken up by photoautotrophs and that OCN^- is utilized as a source of reductant by ammonia oxidizers at night resulting in oxidation of OCN^- N and assimilation of OCN^- C.

Anoxic Processes

OCN^-, urea, and NH_4^+ uptake were also measured below the euphotic zone in the ODZ, and their uptake rates increased with depth exceeding rates of anammox attributed to those same substrates at the SNM (Babbin et al. submitted). Uptake rates at the base of the oxycline coincided with a small secondary chl *a* peak that could have been attributed to low light adapted *Prochlorococcus* which are typically found near the base of the oxycline and are known to be able to utilize OCN^- (Goericke et al. 2000; Kamennaya and Post 2013; Lavin et al. 2010). Nitrogen uptake is typically measured in sunlit waters where nitrogen limits phytoplankton growth and reproduction and consequently rates of primary production (Mulholland and Lomas 2008). To our knowledge, nitrogen uptake has not been measured in marine systems in the absence of phytoplankton biomass. However, important heterotrophic and chemoautotrophic biogeochemical processes take place in ODZs (Paulmier and Ruiz-Pino 2009) and the nitrogen uptake observed in this study may represent N assimilation supporting the growth of these organisms, some of which are autotrophs. Alternatively, our 30 nM additions could have stimulated NH_4^+, urea, and OCN^- uptake dependent on microbial community. Denitrifiers are more responsive to episodic nutrient additions than are anammox bacteria (Ward et al. 2009) however the extent to which either process is limited by N for assimilation is not clear. NO_3^- and NO_2^- are the abundant forms of nitrogen available for assimilation in ODZs, but assimilation of these oxidized forms is energetically expensive compared to reduced forms of N (Berges and Mulholland 2008; Mulholland and Lomas 2008).

NH_4^+ was taken up at rates equal to or greater than the rate of NH_4^+ consumption in support of the anammox reaction (Babbin et al. submitted). While it is most often assumed that N taken up in incubation experiments is assimilated, it could also reflect accumulation of intracellular NH_4^+ to support anammox. NH_4^+ concentrations were below the limit of analytical detection (50 nM) within the ODZ, as has been observed previously in marine ODZs, and these low concentrations have been attributed to consumption of NH_4^+ by anammox (Devol 2008). It

is presently thought that biological degradation of OCN^- and urea to NH_4^+ are intracellular processes (Miller and Espie 1994; Solomon et al. 2010). If this is the case, NH_4^+ produced from degradation of these compounds could be shunted to the anammox reaction assuming that anammox bacteria are capable of taking up OCN^- and urea as found by Babbin et al. (submitted). OCN^- degrades abiotically to NH_4^+ (Amell 1956; Kamennaya et al. 2008), and urea degrades abiotically to OCN^- (Dirnhuber and Schutz 1948). It is possible that NH_4^+ produced from OCN^- and urea extracellularly, whether biotically or abiotically, was rapidly taken up as NH_4^+ by the anammox bacteria. The $^{29}N_2$ excess concentration following the addition of ^{15}N- OCN^- increased linearly over 24 hours, and the rate of OCN^--supported anammox was not significantly different from that of traditional anammox (Babbin et al. submitted) suggesting that OCN^- may be used directly by anammox bacteria, and there may exist a "cyanammox" pathway. If this is a two-step process, this suggests that either the time-scales of our incubations were too long to detect the lag between NH_4^+ production from OCN^- or that anammox is the rate limiting step in the coupled reaction. In contrast to OCN^-, there was a 36 hour lag in urea-supported anammox during incubation experiments (Babbin et al. submitted). This suggests a slow conversion of urea to OCN^- or NH_4^+ followed by OCN^--supported or traditional anammox.

Because anammox is an intracellular process (van Niftrik et al. 2004), the chemoautotrophic bacteria capable of "cyanammox" could assimilate OCN^- C as CO_2 is released by cyanase. The ratio of NH_4^+ oxidized by the anammox pathway to C fixed by anammox bacteria is 15:1 (van Niftrik et al. 2004). For the rates of "cyanammox" at 95 and 230 m, the maximum OCN^- C uptake by anammox bacteria, assuming 100% efficiency of CO_2 assimilation, would have been 9.3 and 4.0 pmol l^{-1} h^{-1}, respectively. In fact, OCN^- C uptake at 95 m was b.d.l. after 8 hours but was 1.4 pmol l^{-1} h^{-1} after 36 hours which equates to a OCN^--derived CO_2 assimilation efficiency by anammox bacteria of 15% if anammox bacteria were the only autotrophs able to utilize OCN^-. At 95 m some OCN^- C could have been taken up by *Prochlorococcus* which is generally found in the secondary chl *a* maximum in ODZs (Figure 7A) (Lavin et al. 2010) and of which some strains can utilize OCN^- (Kamennaya and Post 2013; Rocap et al. 2003), resulting in a OCN^--C anammox bacteria assimilation efficiency of < 15%. At 230 m, OCN^- C uptake was b.d.l. (d.l. = 0.3 pmol l^{-1} h^{-1} for a 48 hour incubation) indicating a OCN^--derived CO_2 efficiency by anammox bacteria of less than 68%. Recovery < 100% could indicate that anammox bacteria lack a mechanism to efficiently fix CO_2 before it diffuses out of

the cell, that the majority of cyanase activity is not located inside anammox bacteria, or that C fixed by anammox bacteria is released from the cell during incubations.

OCN^-, urea, and NH_4^+ were taken up and supported anammox in the ODZ despite the fact that these compounds were below their limits of detection, suggesting that the community was "primed" for utilization of these compounds and that there is a tight coupling between production and consumption of these compounds. NH_4^+ is produced in ODZs by degradation of organic matter by denitrifiers (Devol 2008), and it is conceivable that OCN^- and urea are produced by similar pathways. Organic matter degradation could explain the OCN^- maxima observed at some stations within the ODZ, however particle flux and nutrient remineralization decrease exponentially with depth (Martin et al. 1987), and the anoxic OCN^- maxima were deeper than expected (300 m) for such a feature possibly indicating consumption of OCN^- in excess of production in the upper ODZ. In previous studies, the OCN^- maximum was similar in depth to the NO_2^- and NH_4^+ maxima and the nitracline indicating release by phytoplankton or production from degrading organic matter (Chapter IV; Post et al. unpubl.). However, measurements of OCN^- concentrations are still so limited as to preclude generalizations regarding rationalizations of its distribution in aquatic systems.

Urea is released to marine systems by microbes (Cho and Azam 1995) and zooplankton excretion (Sipler and Bronk 2015). Diurnal vertical migration (DVM) of zooplankton from the euphotic to the mesopelagic zone can contribute significantly to C and N export (Putzeys 2013). Assuming no change in zooplankton excretion rates during migration, Bianchi et al. (2014) calculated that NH_4^+ excreted by DVM may increase the percentage of N lost by the anammox pathway by 13% (Bianchi et al. 2014). However, zooplankton NH_4^+ excretion rates may decrease 4 to 5 fold in anoxic waters, sharply reducing the impact of DVM on anammox rates (Kiko et al. 2015). As a decomposition product of urea (Dirnhuber and Schutz 1948), OCN^- could form abiotically from urea excreted by DVM in the ODZ.

Overall, we have demonstrated that urea and ammonium were the dominant forms of N taken up in the euphotic zone in the study region, and OCN^- was not heavily utilized by the microbial community above the pycnocline. We identified a novel anoxic pathway of cyanate-supported anammox ("cyanammox") and made, to our knowledge, the first measurements of cyanate, urea, and ammonium uptake in an oxygen deficient zone.

CHAPTER VI

CONCLUSIONS

In this work I developed a nanomolar cyanate method appropriate for measuring its concentrations in estuarine and seawater samples. I applied the method to provide the first descriptions of cyanate distributions in the ocean and examine potential pathways of production and consumption in diverse marine environments. Cyanate concentrations were measured throughout the water column in the Chesapeake Bay and the Atlantic and Pacific oceans in oxic and anoxic waters. Using a custom-synthesized ^{15}N and ^{13}C labeled cyanate compound, I made the first measurements of cyanate N and C uptake across horizontal and vertical gradients, in three different seasons in North Atlantic coastal waters. Cyanate distribution and uptake measurements were compared along onshore and offshore gradients in both western and eastern boundary systems that included diatom- and picoplankton-dominated waters and in vertical profiles that included oxic and anoxic waters. The major findings of this research are as follows.

- Cyanate can be measured in estuarine and sea water at nanomolar levels (d.l. = 0.4 nM) by derivatization with 2-aminobenzoic acid to 2,4,-quinazolinedione and detection by fluorescence following high performance liquid chromatography.
- In the marine systems studied here, cyanate concentrations in seawater ranged from below the limit of detection to 45 nM; concentrations were usually < 5 nM.
- Cyanate distributions are non-conservative and biologically-driven.
    - Cyanate concentrations were low in environments dominated by cyanobacteria and picoeukaryotes who are known to take up cyanate.
    - Cyanate concentrations were higher in diatom-dominated systems and in regions with high rates of organic matter degradation because diatoms do not take up cyanate and cyanate is either released directly by diatoms or produced by degrading diatom-derived organic matter.
    - Cyanate was generally below detection below the euphotic zone except for patchy cyanate features within oxygen deficient waters where it was 5 - 8 nM.
- Cyanate is produced autochthonously in marine and estuarine systems.

    - Cyanate accumulated in senescent diatom cultures either by diatom release or degradation of dead cells.
    - Cyanate was produced photochemically.
    - Atmospheric deposition was not a source of cyanate in offshore systems.
- Cyanate N and C are taken up in the euphotic zone.
    - Cyanate N was a larger fraction of total N taken up at offshore oligotrophic stations in the Atlantic (10%) relative to nearshore systems in the North Atlantic and eastern tropical South Pacific, where cyanate was a very small fraction of N uptake (< 2%).
    - Cyanate N uptake was higher in surface waters than at the deep chlorophyll maximum, higher during the day than at night, and higher in spring and summer than in autumn in the coastal North Atlantic Ocean.
    - Cyanate C uptake was higher at the DCM than in surface waters, during the night relative to the day, and in the autumn relative to spring and summer.
- Cyanate N is taken up in ODZs at rates similar to ammonium and urea uptake.
- Cyanate also appears to contribute to N loss processes in the ocean, and I present the first evidence that in the eastern tropical South Pacific ODZ there is a cyanate-supported anammox ("cyanammox") pathway.

This work stemmed from "reverse genomics" in that the cyanate utilization pathway was identified in cyanobacterial genomes before cyanate uptake and assimilation were known quantities in natural systems. The discovery of a pathway for cyanate uptake and degradation in the genes of cultured strains of of the globally important cyanobacteria, *Prochlorococcus* and *Synechococcus* (Palenik et al. 2003; Rocap et al. 2003) led to the discovery of expressed cyanate genes in marine systems (Kamennaya and Post 2013). I then commenced this work to determine cyanate bioavailability using geochemical tools. Cyanobacterial cyanate utilization was most important in oligotrophic systems where *Prochlorococcus* is the dominant primary producer (Chapter III). However, the small sample size of this study precludes meaningful conclusions about the global significance of cyanate uptake in the vast oligotrophic gyres.

Since the inception of this project, our knowledge of cyanate has expanded to include dissimilatory nitrogen cycle processes. Using stable isotope techniques (^{15}N) as part of this work and in collaboration with Andrew Babbin (Babbin et al. submitted; Chapter V), we discovered

that cyanate can support anaerobic ammonium oxidation (cyanammox). Concurrently, it was demonstrated that cyanate can also support nitrification in place of ammonia in cultured organisms (Palatinszky et al. 2015; Spang et al. 2012).

Our current understanding of the marine cyanate N cycle is summarized in Figure 31 which includes pathways that are supported by direct measurements as well as those that are predicted by indirect measurements, culture studies, and genomes. Biomass burning and fossil fuel combustion produce isocyanic acid (Nicholls and Nelson 2000; Roberts et al. 2011) which rapidly degrades to ammonium and carbon dioxide in aqueous solution. Dry deposition of isocyanic acid may occur close to the combustion source in dry atmospheric conditions (Barth et al. 2013) but is unlikely to be a detectable source of cyanate to offshore waters. There may be natural and anthropogenic fluxes of cyanate from terrestrial to marine systems (Dirnhuber and Schutz 1948; Glibert et al. 2006; Koshiishi et al. 1997; Lin et al. 2008; Chapter II). Terrestrial and marine dissolved organic matter (DOM) may photodegrade to cyanate (Chapter III). Cyanate may be produced by algae (Chapter III) or by microbially-mediated degradation of organic matter (Chapters III-V), including urea and carbamoyl phosphate (Allen and Jones 1964; Dirnhuber and Schutz 1948; Kamennaya et al. 2008), and by heterotrophic bacteria. In the euphotic zone, cyanate can be taken up by cyanobacteria and other groups of phytoplankton (Berg et al. 2008; Kamennaya and Post 2013; Zhuang et al. 2015).

At the base of the euphotic zone, cyanate may be produced by organic matter degradation in sinking particles either directly or through abiotic degradation of urea (Chapters III-IV). Cyanate would then be consumed by one of three processes: 1) slow abiotic conversion to ammonium (Amell 1956); 2) conversion by ammonia oxidizers to nitrite and carbon dioxide; or 3) conversion by nitrite oxidizers to ammonium and carbon dioxide potentially including uptake of cyanate C (Palatinszky et al. 2015; Chapter IV; Chapter V). In oxygen deficient zones (ODZs) cyanate production may occur by one of two pathways: organic matter degradation, probably mediated by denitrifiers, or slow abiotic degradation of urea generated by diurnally migrating zooplankton (Bianchi et al. 2014). Cyanate N would then be oxidized to N_2 directly or indirectly by anammox bacteria (Babbin et al. submitted), thereby contributing to marine N loss.

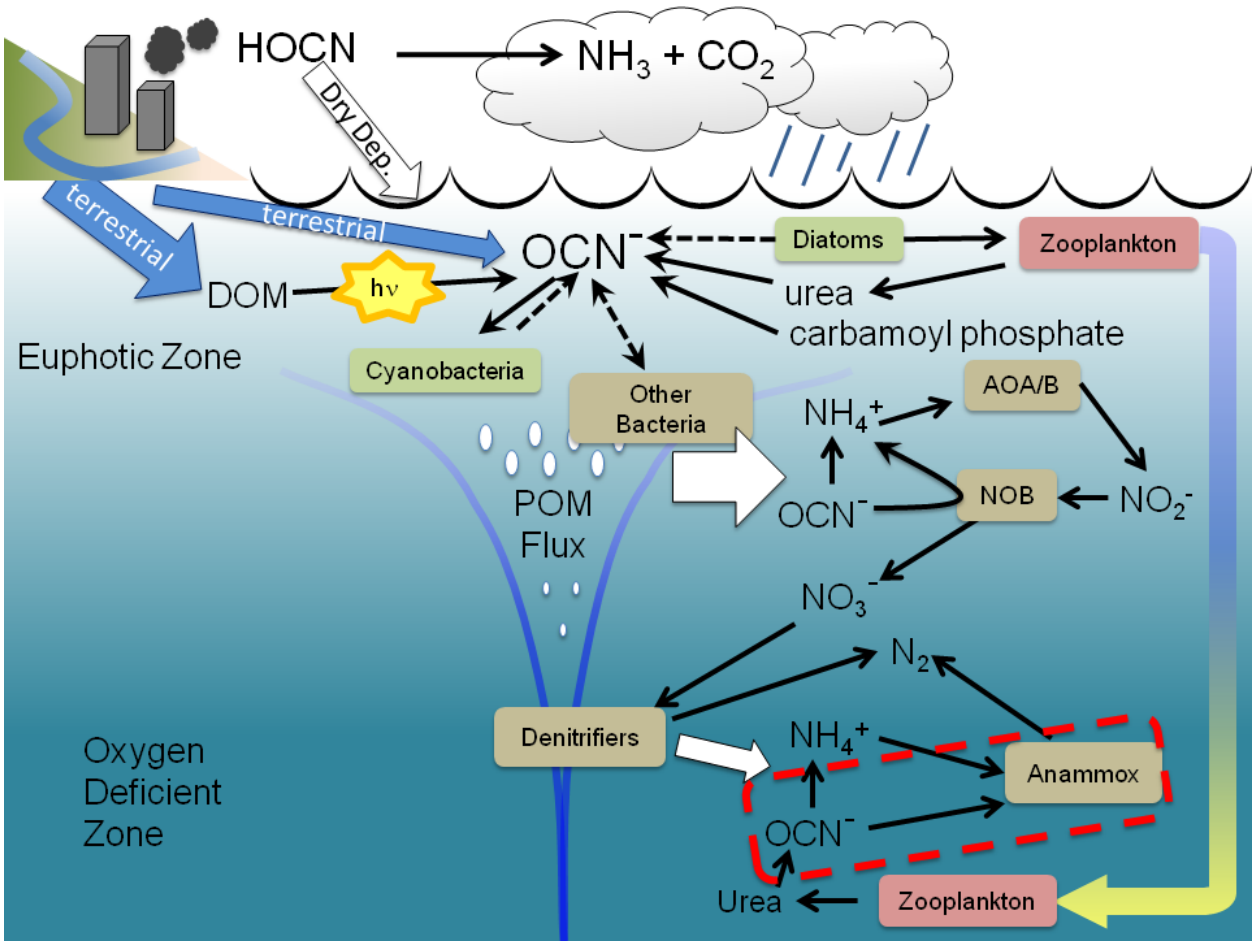

Figure 31. A conceptual model of the marine cyanate cycle. Sources of cyanate are atmospheric, terrestrial, and autochthonous. Sinks are phytoplankton and bacterial uptake, oxidation by nitrifiers to nitrite, and oxidation by anammox bacteria to dinitrogen gas. Abbreviations are: isocyanic acid (HOCN), cyanate (OCN^-), ammonia (NH_3), carbon dioxide (CO_2), dissolved organic matter (DOM), photochemistry (hν), particulate organic matter (POM), ammonium (NH_4^+), ammonia oxidizing archaea and bacteria (AOA/B), nitrite oxidizing bacteria (NOB), nitrite (NO_2^-), nitrate (NO_3^-), and dinitrogen gas (N_2). The "cyanammox" process is indicated by the red dashed box.

REFERENCES

Acker, J. G. and G. Leptoukh 2007. Online analysis enhances use of NASA earth science data. Eos, Transactions American Geophysical Union. 88: 14-17

Adornato, L. R., E. A. Kaltenbacher, T. A. Villareal and R. H. Byrne 2005. Continuous in situ determinations of nitrite at nanomolar concentrations. Deep Sea Res., Part I. 52: 543-551

Allen, C. M. and M. E. Jones 1964. Decomposition of carbamyl phosphate in aqueous solutions. Biochemistry. 3: 1238-1247

Alonso-Sáez, L., A. S. Waller, D. R. Mende, K. Bakker, H. Farnelid, P. L. Yager, C. Lovejoy, J.-É. Tremblay, and others. 2012. Role for urea in nitrification by polar marine Archaea. Proc. Natl. Acad. Sci. U.S.A. 109: 17989-17994

Amell, A. R. 1956. Kinetics of the hydrolysis of cyanic acid. J. Am. Chem. Soc. 78: 6234-6238

Anderson, P. M., Y. Sung and J. A. Fuchs 1990. The cyanase operon and cyanate metabolism. FEMS Microbiol. Rev. 87: 247-252

Babbin, A. R., B. D. Peters, C. W. Mordy, B. Widner, K. L. Casciotti and B. B. Ward submitted. Novel metabolisms support the anaerobic nitrite budget in the Eastern Tropical South Pacific. Nature Geoscience.

Badger, M. R., T. J. Andrews, S. M. Whitney, M. Ludwig, D. C. Yellowlees, W. Leggat and G. D. Price 1998. The diversity and coevolution of Rubisco, plastids, pyrenoids, and chloroplast-based CO2-concentrating mechanisms in algae. Canadian Journal of Botany. 76: 1052-1071

Baker, A., S. Kelly, K. Biswas, M. Witt and T. Jickells 2003. Atmospheric deposition of nutrients to the Atlantic Ocean. Geophysical Research Letters. 30:

Baker, A. R., K. Weston, S. D. Kelly, M. Voss, P. Streu and J. N. Cape 2007. Dry and wet deposition of nutrients from the tropical Atlantic atmosphere: Links to primary productivity and nitrogen fixation. Deep-Sea Research I. 54: 1704-1720

Barth, M., A. Cochran, M. Fiddler, J. Roberts and S. Bililign 2013. Numerical modeling of cloud chemistry effects on isocyanic acid (HNCO). Journal of Geophysical Research: Atmospheres. 118: 8688-8701

Berg, G. M., J. Shrager, G. Glöckner, K. R. Arrigo and A. R. Grossman 2008. Understanding nitrogen limitation in *Aureococcus anophagefferens* (pelagophyceae) through cDNA and qRT-PCR analysis. J. Phycol. 44: 1235-1249

Berges, J. A. and M. R. Mulholland 2008. Enzymes and Nitrogen Cycling, p. In D. G. Capone, D. A. Bronk, M. R. Mulholland and E. J. Carpenter [eds.], Nitrogen in the Marine Environment. Academic Press.

Berube, P. M., S. J. Biller, A. G. Kent, J. W. Berta-Thompson, S. E. Roggensack, K. H. Roache-Johnson, M. Ackerman, L. R. Moore, and others. 2015. Physiology and evolution of nitrate acquisition in Prochlorococcus. ISME J. 9: 1195-1207

Bianchi, D., A. R. Babbin and E. D. Galbraith 2014. Enhancement of anammox by the excretion of diel vertical migrators. Proc. Natl. Acad. Sci. U.S.A. 111: 15653-15658

Black, S. B. and R. S. Schulz 1999. Ion chromatographic determination of cyanate in saline gold processing samples. J. Chromatogr. A. 855: 267-272

Boening, D. W. and C. M. Chew 1999. A critical review: general toxicity and environmental fate of three aqueous cyanide ions and associated ligands. Water, Air, Soil Pollut. 109: 67-79

Boneillo, G. and M. R. Mulholland 2014. Interannual variability influences brown tide (*Aureococcus anophagefferens*) blooms in coastal embayments. Estuaries & Coasts. 37: 147-163

Bronk, D. A., P. M. Glibert, T. C. Malone, S. Banahan and E. Sahlsten 1998. Inorganic and organic nitrogen cycling in Chesapeake Bay: autotrophic versus heterotrophic processes and relationships to carbon flux. Aquat. Microb. Ecol. 15: 177-189

Bronk, D. A. and D. K. Steinberg 2008. Nitrogen Regeneration, p. 385-467. In D. G. Capone, D. A. Bronk, M. R. Mulholland and E. J. Carpenter [eds.], Nitrogen in the Marine Environment. Elsevier.

Bryant, D. A. 2003. The beauty in small things revealed. Proc. Natl. Acad. Sci. U.S.A. 100: 9647-9649

Bushaw-Newton, K. L. and M. A. Moran 1999. Photochemical formation of biologically available nitrogen from dissolved humic substances in coastal marine systems. Aquat. Microb. Ecol. 18: 285-292

Carepo, M. S. P., J. S. N. de Azevedo, J. I. R. Porto, A. R. Bentes-Sousa, J. d. S. Batista, A. L. C. Silva and M. P. C. Schneider 2004. Identification of *Chromobacterium violaceum* genes with potential biotechnological application in environmental deteoxification. Genet. Mol. Res. 3: 181-194

Cho, B. C. and F. Azam 1995. Urea decomposition by bacteria in the Southern California Bight and its implications for the mesopelagic nitrogen cycle. Mar. Ecol.: Prog. Ser. 122: 21-26

Church, M. J., B. Wai, D. M. Karl and E. F. DeLong 2010. Abundances of crenarchaeal amoA genes and transcripts in the Pacific Ocean. Environ. Microbiol. 12: 679-688

Codispoti, L. A. 2007. An oceanic fixed nitrogen sink exceeding 400 Tg N a? 1 vs the concept of homeostasis in the fixed-nitrogen inventory. Biogeosciences. 4: 233-253

Codispoti, L. A., J. A. Brandes, J. P. Christensen, A. H. Devol, S. W. A. Naqvi, H. W. Paerl and T. Yoshinari 2001. The oceanic fixed nitrogen and nitrous oxide budgets: Moving targets as we enter the anthropocene? Scientia Marina. 65: 85-105

Cole, C. A., Z. Wang, T. P. Snow and V. M. Bierbaum 2015. Gas-phase chemistry of the cyanate ion, OCN. The Astrophysical Journal. 812: 77

Commeyras, A., L. Boiteau, O. Vandenabeele-Trambouze, and F. Selsis. 2005. Peptide emergence, evolution and selection on the primitive earth. p. 517-545. In M. Gargaud, B. Barbier, H. Martin, and R. Jacques [eds.]. Lectures in astrobiology. Springer.

Dalsgaard, T., D. E. Canfield, J. Petersen, B. Thamdrup and J. Acuna-Gonzalez 2003. N2 production by the anammox reaction in the anoxic water column of Golfo Dulce, Costa Rica. Nature. 422: 606-608

Danger, G., L. Boiteau, H. Cottet and R. Pascal 2006. The peptide formation mediated by cyanate revisited. N-carboxyanhydrides as accessible intermediates in the decomposition of N-carbamoylamino acids. J. Am. Chem. Soc. 128: 7412-7413

Danger, G., S. Charlot, L. Boiteau and R. Pascal 2012. Activation of carboxyl group with cyanate: peptide bond formation from dicarboxylic acids. Amino Acids. 42: 2331-2341

Devol, A. H. 2008. Denitrification Including Anammox, p. 263-301. In D. G. Capone, D. A. Bronk, M. R. Mulholland and E. J. Carpenter [eds.], Nitrogen in the Marine Environment. Elsevier.

Dirnhuber, P. and F. Schutz 1948. The isomeric transformation of urea into ammonium cyanate in aqueous solutions. Biochem. J. 42: 628-632

Dore, J. E. and D. M. Karl 1996. Nitrite distributions and dynamics at Station ALOHA. Deep Sea Res., Part II. 43: 385-402

Dorr, P. K. and C. J. Knowles 1989. Cyanide oxygenase and cyanase activities of *Pseudomonas fluorescens* NCIMB- 11764. FEMS Microbiol. Lett. 60: 289-294

Egerton, T. A., R. E. Morse, H. G. Marshall and M. R. Mulholland 2014. Emergence of Algal Blooms: The Effects of Short-Term Variability in Water Quality on Phytoplankton Abundance, Diversity, and Community Composition in a Tidal Estuary. Microorganisms. 2: 33-57

Eiger, S. and S. D. Black 1985. Analysis of plasma cyanate as 2-nitro-5-thiocarbamylbenzoic acid by high-performance liquid-chromatography. Anal. Biochem. 146: 321-326

Emerson, S. R. and J. I. Hedges. 2008. Chemical Oceanography and the Marine Carbon Cycle. Cambridge University Press.

Espie, G. S., F. Jalali, T. Tong, N. J. Zacal and A. K. C. So 2007. Involvement of the cynABDS operon and the CO2-concentrating mechanism in the light-dependent transport and metabolism of cyanate by cyanobacteria. J. Bacteriol. 189: 1013-1024

Falkowski, P. G. 1997. Evolution of the nitrogen cycle and its influence on the biological sequestration of CO_2 in the ocean. Nature. 387: 272-275

Ferris, J. P., R. A. Sanchez and L. E. Orgel 1968. Studies in prebiotic synthesis III. Synthesis of pyrimidine from cyanoacetylene and cyanate. J. Mol. Biol. 33: 693-704

Field, C. B., M. J. Behrenfeld, J. T. Randerson and P. Falkowski 1998. Primary production of the biosphere: integrating terrestrial and oceanic components. Science. 281: 237-240

Filippino, K. C., M. R. Mulholland and P. W. Bernhardt 2011. Nitrogen uptake and primary productivity rates in the Mid-Atlantic Bight (MAB). Estuarine, Coastal Shelf Sci. 91: 13-23

Garcia-Fernandez, J. M., N. T. de Marsac and J. Diez 2004. Streamlined regulation and gene loss as adaptive mechanisms in *Prochlorococcus* for optimized nitrogen utilization in oligotrophic environments. Microbiol. Mol. Biol. Rev. 68: 630-638

Glibert, P. M., J. Harrison, C. Heil and S. Seitzinger 2006. Escalating worldwide use of urea - a global change contributing to coastal eutrophication. Biogeochemistry. 77: 441-463

Goericke, R., R. J. Olson and A. Shalapyonok 2000. A novel niche for *Prochlorococcus* sp. in low-light suboxic environments in the Arabian Sea and the Eastern Tropical North Pacific. Deep-Sea Research I. 47: 1183-1205

Gruber, N. 2008. The marine nitrogen cycle: Overview and Challenges, p. 1-50. In D. G. Capone, D. A. Bronk, M. R. Mulholland and E. J. Carpenter [eds.], Nitrogen in the marine environment. Elsevier.

Guillard, R. R. L. 1975. Culture of phytoplankton for feeding marine invertebrates, p. 29-60. In W. L. Smith and M. H. Chanley [eds.], Culture of marine invertebrate animals. Plenum Press.

Guilloton, M., G. S. Espie and P. M. Anderson 2002. What is the role of cyanase in plants?, p. 57-79. In A. Goyal, S. L. Mehta and M. L. Lodha [eds.], Reviews in Plant Biochemistry and Biotechnology. Society for Plant Biochemistry and Biotechnology.

Guilloton, M. and F. Karst 1985. A spectrophotometric determination of cyanate using reaction with 2-aminobenzoic acid. Anal. Biochem. 149: 291-295

Guilloton, M. and F. Karst 1987. Isolation and characterization of Escherichia coli mutants lacking inducible cyanase. J. Gen. Microbiol. 133: 645-653

Guilloton, M. B., A. F. Lamblin, E. I. Kozliak, M. Geraminejad, C. Tu, D. Silverman, P. M. Anderson and J. A. Fuchs 1993. A physiological role for cyanate-induced carbonic-anhydrase in *Esherichia coli*. J. Bacteriol. 175: 1443-1451

Hagan, W. J., A. Parker, A. Steuerwald and M. Hathaway 2007. Phosphate solubility and the cyanate-mediated synthesis of pyrophosphate. Origins Life Evol. Biosphere. 37: 113-112

Hagel, P., J. J. T. Gerding, W. Fieggen and Bloemend.H 1971. Cyanate formation in solutions of urea. 1. Calculations of cyanate concentrations at different temperature and pH. Biochim. Biophys. Acta. 243: 366-373

Harano, Y., I. Suzuki, S. I. Maeda, T. Kaneko, S. Tabata and T. Omata 1997. Identification and nitrogen regulation of the cyanase gene from the cyanobacteria *Synechocystis sp.* strain PCC 6803 and *Synechococcus sp.* strain PCC 7942. J. Bacteriol. 179: 5744-5750

Harrison, P. J., R. E. Waters and F. J. R. Taylor 1980. A broad spectrum artificial seawater medium for coastal and open ocean phytoplankton. J. Phycol. 16: 28-35

Helms, J. R., A. Stubbins, J. D. Ritchie, E. C. Minor, D. J. Kieber and K. Mopper 2008. Absorption spectral slopes and slope ratios as indicators of molecular weight, source, and photobleaching of chromophoric dissolved organic matter. Limnol. Oceanogr. 53: 955-969

Hewson, I. and J. A. Fuhrman 2008. Viruses, bacteria, and the microbial loop, p. 1097-1134. In D. G. Capone, D. A. Bronk, M. R. Mulholland and E. J. Carpenter [eds.], Nitrogen in the marine environment. Elsevier.

Holmes, R. M., A. Aminot, R. Kerouel, B. A. Hooker and B. J. Peterson 1999. A simple and precise method for measuring ammonium in marine and freshwater ecosystems. Canadian Journal of Fisheries and Aquatic Sciences. 56: 1801-1808

Hooper, A. B. and K. R. Terry 1974. Photoinactivation of ammonia oxidation in Nitrosomonas. J. Bacteriol. 119: 899-906

Howarth, R. W. and R. Marino 2006. Nitrogen as the limiting nutrient for eutrophication in coastal marine ecosystems: evolving views over three decades. Limnol. Oceanogr. 51: 364-376

Hu, Z., M. R. Mulholland, S. Duan and N. Xu 2012. Effects of nitrogen supply and its composition on the growth of *Prorocentrum donghaiense*. Harmful Algae. 13: 72-82

Johnson, C. A. 2015. The fate of cyanide in leach wastes at gold mines: An environmental perspective. Appl. Geochem. 57: 194-205

Jones, M. E. 1963. Carbamyl Phosphate. Science. 140: 1373-1379

Jones, M. E. and F. Lipmann 1960. Chemical and enzymatic synthesis of carbamyl phosphate. Proc. Natl. Acad. Sci. U.S.A. 46: 1194-1205

Kamennaya, N. A., M. Chernihovsky and A. F. Post 2008. The cyanate utilization capacity of marine unicellular cyanobacteria. Limnol. Oceanogr. 53: 2485-2494

Kamennaya, N. A. and A. F. Post 2011. Characterization of Cyanate Metabolism in Marine Synechococcus and Prochlorococcus spp. Appl. Environ. Microbiol. 77: 291-301

Kamennaya, N. A. and A. F. Post 2013. Distribution and expression of the cyanate aquisition potential among cyanobacterial populations in oligotrophic marine waters. Limnol. Oceanogr. 58: 1959-1971

Kamyshny, A., H. Oduro, Z. F. Mansaray and J. Farquhar 2013. Hydrogen cyanide accumulation and transformation in non-polluted salt marsh sediments. Aquat. Geochem. 19: 97-113

Kantor, R. S., A. W. Zyl, R. P. Hille, B. C. Thomas, S. T. Harrison and J. F. Banfield 2015. Bioreactor microbial ecosystems for thiocyanate and cyanide degradation unravelled with genome-resolved metagenomics. Environ. Microbiol. 17: 4929-4941

Kieber, D. J., J. McDaniel and K. Mopper 1989. Photochemical source of biological substrates in sea-water - implications for carbon cycling. Nature. 341: 637-639

Kiefer, D. A., R. J. Olson and O. Holm-Hansen 1976. Another look at the nitrite and chlorophyll maxima in the central North Pacific. Deep-Sea Res. Oceanogr. Abstr. 23: 1199-1208

Kiko, R., H. Hauss, F. Buchholz and F. Melzner 2015. Ammonium excretion and oxygen respiration of tropical copepods and euphausiids exposed to oxygen minimum zone conditions. Biogeosciences Discuss. 12: 17329-17366

Klotz, M. G., D. J. Arp, P. S. Chain, G., A. F. El-Sheikh, L. J. Hauser, N. G. Hommes, F. W. Larimer, S. A. Malfatti, and others. 2006. Complete genome sequence of the marine chemolithoautotrophic, ammonia-oxidizing bacterium *Nitrosococcus oceani* ATCC 19707. Appl. Environ. Microbiol. 72: 6299-6315

Koops, H.-P. and A. Pommerening-Röser 2001. Distribution and ecophysiology of the nitrifying bacteria emphasizing cultured species. FEMS Microbiol. Ecol. 37: 1-9

Koshiishi, I., Y. Mamura and T. Imanari 1997. Cyanate causes depletion of ascorbate in organisms. Biochim. Biophys. Acta. 1336: 566-574

Lalli, C. M. and T. R. Parsons. 1997. Biological Oceanography an Introduction. 2. Elsevier Butterworth- Heinemann.

Lange, N. A. and F. E. Sheibley 1963. Benzoylene Urea. Organic Syntheses. 2: 79-80

Lavin, P., B. González, J. Santibánez, D. J. Scanlan and O. Ulloa 2010. Novel lineages of *Prochlorococcus* thrive within the oxygen minimum zone of the eastern tropical South Pacific. Environmental microbiology reports. 2: 728-738

Lin, H. K., D. E. Walsh, J. L. Oleson and X. Chen 2008. Reduction of cyanate to cyanide in cyanidation tailings under reducing environments. Minerals & Metallurgical Processing. 25: 41-45

Lin, M. F., C. Williams, M. V. Murray, G. Conn and P. A. Ropp 2004. Ion chromatographic quantification of cyanate in urea solutions: estimation of the efficiency of cyanate scavengers for use in recombinant protein manufacturing. Journal of Chromatography B-Analytical Technologies in the Biomedical and Life Sciences. 803: 353-362

Lomas, M. W. and F. Lipschultz 2006. Forming the primary nitrite maximum: Nitrifiers or phytoplankton? Limnol. Oceanogr. 51: 2453-2467

Lundquist, P., B. Backmangullers, B. Kagedal, L. Nilsson and H. Rosling 1993. Fluorometric determination of cyanate in plasma by conversion to 2,4(1H,3H)-quinazolinedione and separation by high-performance liquid-chromatography. Anal. Biochem. 211: 23-27

Luque-Almagro, V. M., R. Blasco, J. M. Fernandez-Romero and M. D. Luque de Castro 2003. Flow-injection spectrophotometric determination of cyanate in bioremediation processes

by use of immobilised inducible cyanase. Analytical Bioanalytical Chemistry. 377: 1071-1078

Mackey, K. R. M., L. Bristow, D. R. Parks, M. A. Altabet, A. F. Post and A. Paytan 2011. The influence of light on nitrogen cycling and the primary nitrite maximum in a seasonally stratified sea. Prog. Oceanogr. 91: 545-560

Manly, B. F. J. 1997. Randomization, Bootstrap and Monte Carlo Methods in Biology. 2. Chapman & Hall.

Marier, J. R. and D. Rose 1964. Determination of cyanate + study of its accumulation in aqueous solutions of urea. Anal. Biochem. 7: 304-314

Martin, J. H., G. A. Knauer, D. M. Karl and W. W. Broenkow 1987. VERTEX: carbon cycling in the northeast Pacific. Deep Sea Research Part A. Oceanographic Research Papers. 34: 267-285

McCarthy, M. D. and D. A. Bronk 2008. Analytical Methods for the Study of Nitrogen, p. 1219-1276. In D. G. Capone, D. A. Bronk, M. R. Mulholland and E. J. Carpenter [eds.], Nitrogen in the Marine Environment. Academic Press.

McElroy, M. 1983. Marine biological controls on atmospheric CO2 and climate. Nature. 302: 328-329

Meeder, E., K. R. M. Mackey, A. Paytan, Y. Shaked, D. Iluz, N. Stambler, T. Rivlin, A. F. Post, and others. 2012. Nitrite dynamics in the open ocean - clues from seasonal and diurnal variations. Mar. Ecol.: Prog. Ser. 453: 11-26

Miller, A. G. and G. S. Espie 1994. Photosynthetic metabolism of cyanate by the cyanobacterium *Synechococcus* UTEX-625. Arch. Microbiol. 162: 151-157

Miller, S. L. and M. Parris 1964. Synthesis of pyrophosphate under primitive earth conditions. Nature. 204: 1248-1250

Minor, E. C., J. Pothen, B. J. Dalzell, H. Abdulla and K. Mopper 2006. Effects of salinity changes on the photodegradation and ultraviolet-visible absorbance of terrestrial dissolved organic matter. Limnol. Oceanogr. 51: 2181-2186

Montoya, J. P., M. Voss, P. Kaehler and D. G. Capone 1996. A simple, high precision tracer assay for dinitrogen fixation. Applied Environmental Microbiololgy. 62: 986-993

Montoya, J. P., M. Voss, P. Kahler and D. G. Capone 1996. A simple, high-precision, high-sensitivity tracer assay for N-2 fixation. Appl. Environ. Microbiol. 62: 986-993

Mopper, K., D. J. Kieber and A. Stubbins 2015. Marine Photochemistry of Organic Matter: Processes and Impacts, p. 389-450. In D. A. Carlson and H. C. A. [eds.], Biogeochemistry of Marine Dissolved Organic Matter. Academic Press.

Mulholland, M. R., P. W. Bernhardt, C. A. Heil, D. A. Bronk and J. M. O'Neil 2006. Nitrogen fixation and release of fixed nitrogen by *Trichodesmium* spp. in the Gulf of Mexico. Limnol. Oceanogr. 51: 1762-1776

Mulholland, M. R., G. E. Boneillo, P. W. Bernhardt and E. C. Minor 2009. Comparison of Nutrient and Microbial Dynamics over a Seasonal Cycle in a Mid-Atlantic Coastal Lagoon Prone to Aureococcus anophagefferens (Brown Tide) Blooms. Estuaries Coasts. 32: 1176-1194

Mulholland, M. R. and M. W. Lomas 2008. Nitrogen Uptake and Assimilation, p. 303-384. In D. G. Capone, D. A. Bronk, M. R. Mulholland and E. J. Carpenter [eds.], Nitrogen in the marine environment. Elsevier.

Nelson, D. L. and Cox, M. M. 2008. Lehninger Principles of Biochemistry, 5th Ed. W.H. Freeman and Company.

Nicholls, P. M. and P. F. Nelson 2000. Detection of HNCO during the low-temperature combustion of coal chars. Energy & fuels. 14: 943-944

Nonomura, M. and T. Hobo 1989. Ion chromatographic determination of cyanide compounds by chloramine-T and conductivity measurement. J. Chromatogr. 465: 395-401

Orcutt, K. M., F. Lipschultz, K. Gundersen, R. Arimoto, A. F. Michaels, A. H. Knap and J. R. Gallon 2001. A seasonal study of the significance of N_2 fixation by Trichodesmiuim spp. at the Bermuda Atlantic Time-series Study (BATS) site. Deep Sea Res., Part II. 48: 1583-1608

Orcutt, K. M., F. Lipschultz, K. Gundersen, R. Arimoto, A. F. Michaels, A. H. Knap and J. R. Gallon 2001. A seasonal study of the significance of N-2 fixation by Trichodesmium spp. at the Bermuda Atlantic Time-series Study (BATS) site. Deep-Sea Res. Part II-Top. Stud. Oceanogr. 48: 1583-1608

Palatinszky, M., C. Herbold, N. Jehmlich, M. Pogoda, P. Han, M. von Bergen, I. Lagkouvardos, S. M. Karst, and others. 2015. Cyanate as an energy source for nitrifiers. Nature. 524: 105-108

Palenik, B., B. Brahamsha, F. W. Larimer, M. Land, L. Hauser, P. Chain, J. Lamerdin, W. Regala, and others. 2003. The genome of a motile marine *Synechococcus*. Nature. 424: 1037-1042

Pan, X., A. Mannino, H. G. Marshall, K. C. Filippino and M. R. Mulholland 2011. Remote sensing of phytoplankton community composition along the northeast coast of the United States. Remote Sensing of Environment. 115: 3731-3747

Pao, S. S., I. T. Paulsen and M. H. Saier 1998. Major Facilitator Superfamily. Microbiol. Mol. Biol. Rev. 62: 1-34

Parsons, T. R., Y. Maita and C. M. Lalli. 1984. A Manual of Chemical and Biological Methods for Seawater Analysis. 1. Pergamon Press Inc.

Partensky, F., W. R. Hess and D. Vaulot 1999. *Prochlorococcus,* a marine photosynthetic prokaryote of global significance. Microbiol. Mol. Biol. Rev. 63: 106-127

Paulmier, A. and D. Ruiz-Pino 2009. Oxygen minimum zones (OMZs) in the modern ocean. Prog. Oceanogr. 80: 113-128

Pedneault, E., P. E. Galand, M. Potvin, J.-É. Tremblay and C. Lovejoy 2014. Archaeal amoA and ureC genes and their transcriptional activity in the Arctic Ocean. Scientific reports. 4:

Pennington, J. T., K. L. Mahoney, V. S. Kuwahara, D. D. Kolber, R. Calienes and F. P. Chavez 2006. Primary production in the eastern tropical Pacific: A review. Prog. Oceanogr. 69: 285-317

Price, N. M. and P. J. Harrison 1987. Comparison of methods for the analysis of dissolved urea in seawater. Mar. Biol. 94: 307-317

Qin, W., S. A. Amin, W. Martens-Habbena, C. B. Walker, H. Urakawa, A. H. Devol, A. E. Ingalls, J. W. Moffett, and others. 2014. Marine ammonia-oxidizing archaeal isolates display obligate mixotrophy and wide ecotypic variation. Proc. Natl. Acad. Sci. U.S.A. 111: 12504-12509

Raymond, P. A. and R. G. M. Spencer 2015. Riverine DOM, p. 509-535. In D. A. Hansell and C. A. Carlson [eds.], Biogeochemistry of Marine Dissolved Organic Matter. Elsevier.

Revsbech, N. P., L. H. Larsen, J. Gundersen, T. Dalsgaard, O. Ulloa and B. Thamdrup 2009. Determination of ultra-low oxygen concentrations in oxygen minimum zones by the STOX sensor. Limnology and Oceanography: Methods. 7: 371-381

Roberts, J. M., P. R. Veres, A. K. Cochran, C. Warneke, I. R. Burling, R. J. Yokelson, B. Lerner, J. B. Gilman, and others. 2011. Isocyanic acid in the atmosphere and its possible link to smoke-related health effects. Proc. Natl. Acad. Sci. U.S.A. 108: 8966-8971

Rocap, G., F. W. Larimer, J. Lamerdin, S. Malfatti, P. Chain, N. A. Ahlgren, A. Arellano, M. Coleman, and others. 2003. Genome divergence in two *Prochlorococcus* ecotypes reflects oceanic niche differentiation. Nature. 424: 1042-1047

Santoro, A. E., K. L. Casciotti and C. A. Francis 2010. Activity, abundance and diversity of nitrifying archaea and bacteria in the central California Current. Environ. Microbiol. 12: 1989-2006

Santoro, A. E., C. L. Dupont, R. A. Richter, M. T. Craig, P. Carini, M. R. McIlvin, Y. Yang, W. D. Orsi, and others. 2015. Genomic and proteomic characterization of "Candidatus Nitrosopelagicus brevis": An ammonia-oxidizing archaeon from the open ocean. Proc. Natl. Acad. Sci. U.S.A. 112: 1173-1178

Scanlan, D. J., M. Ostrowski, S. Mazard, A. Dufresne, L. Garczarek, W. R. Hess, A. F. Post, M. Hagemann, and others. 2009. Ecological Genomics of Marine Picocyanobacteria. Microbiol. Mol. Biol. Rev. 73: 249-299

Scanlan, D. J. and A. F. Post 2008. Aspects of the marine cyanobacterial nitrogen physiology and connection to the nitrogen cycle, p. 1073-1096. In D. G. Capone, D. A. Bronk, M. R. Mulholland and E. J. Carpenter [eds.], Nitrogen in the marine environment. Elsevier, Inc.

Sedwick, P. N., E. R. Sholkovitz and T. M. Church 2007. Impact of anthropogenic combustion emissions on the fractional solubility of aerosol iron: Evidence from the Sargasso Sea. Geochem. Geophys. Geosyst. 8, Q10Q06, doi:10.1029/2007GC001586:

Seitzinger, S. P. and J. A. Harrison 2008. Land-based nitrogen sources and their delivery to coastal systems, p. 469-510. In D. G. Capone, D. A. Bronk, M. R. Mulholland and E. J. Carpenter [eds.], Nitrogen in the Marine Environment. Elsevier.

Sipler, R. E. and D. A. Bronk 2015. Dynamics of Dissolved Organic Nitrogen, p. In D. A. Hansell and C. A. Carlson [eds.], Biogeochemistry of Marine Dissolved Organic Matter. Academic Press.

Smith, J. M., F. P. Chavez and C. A. Francis 2014. Ammonium uptake by phytoplankton regulates nitrification in the sunlit ocean. PloS one. 9: e108173

Solomon, C. M., J. L. Collier, G. M. Berg and P. M. Glibert 2010. Role of urea in microbial metabolism in aquatic ecosystems: a biochemical and molecular review. Aquat. Microb. Ecol. 59: 67-88

Solorzano, L. 1969. Determination of ammonia in natural waters by phenolhypochlorite method. Limnol. Oceanogr. 14: 799-801

Sorokin, D. Y., T. P. Tourova, A. M. Lysenko and J. G. Kuenen 2001. Microbial thiocyanate utilization under highly alkaline conditions. Appl. Environ. Microbiol. 67: 528-538

Spang, A., A. Poehlein, P. Offre, S. Zumbrägel, S. Haider, N. Rychlik, B. Nowka, C. Schmeisser, and others. 2012. The genome of the ammonia-oxidizing CandidatusNitrososphaera gargensis: insights into metabolic versatility and environmental adaptations. Environ. Microbiol. 14: 3122-3145

Taussig, A. 1960. The synthesis of the induced enzyme, cyanase, in *E. coli*. Biochim. Biophys. Acta. 44: 510-519

Taylor, B. W., C. F. Keep, R. O. Hall, Jr., B. J. Koch and L. M. Tronstad 2007. Improving the fluorometric ammonium method: matrix effects, background fluorescence, and standard additions. Journal of North American Benthological Society. 26: 167-177

Tiano, L., E. Garcia-Robledo, T. Dalsgaard, A. H. Devol, B. B. Ward, O. Ulloa, D. E. Canfield and N. P. Revsbech 2014. Oxygen distribution and aerobic respiration in the north and south eastern tropical Pacific oxygen minimum zones. Deep Sea Res., Part I. 94: 173-183

Townsend, D. W. 1998. Sources and cycling of nitrogen in the Gulf of Maine. Journal of Marine Systems. 16: 283-295

Townsend, D. W., J. P. Christensen, D. K. Stevenson, J. J. Graham and S. B. Chenoweth 1987. The importance of a plume of tidally-mixed water to the biological oceanography of the Gulf of Maine. J. Mar. Res. 45: 699-728

Townsend, D. W., A. C. Thomas, L. M. Mayer, M. A. Thomas and J. A. Quinlan 2004. Oceanography of the Northwest Atlantic Continental Shelf, p. In A. R. Robinson and K. H. Brink [eds.], The Sea: The Global Coastal Ocean: Interdisciplinary Regional Studies and Syntheses. Harvard University Press.

Townsend, D. W., A. C. Thomas, L. M. Mayer, M. A. Thomas and J. A. Quinlan 2006. Oceanography of the Northwest Atlantic continental shelf (1, W), p. 119-168. In A. R. Robinson and K. H. Brink [eds.], The Sea. Harvard University Press.

Vajrala, N., W. Martens-Habbena, L. A. Sayavedra-Soto, A. Schauer, P. J. Bottomley, D. A. Stahl and D. J. Arp 2013. Hydroxylamine as an intermediate in ammonia oxidation by globally abundant marine archaea. Proc. Natl. Acad. Sci. U.S.A. 110: 1006-1011

van Niftrik, L., J. Fuerst, J. S. Sinningh Damste, G. Kuenen, M. S. M. Jetten and M. Strous 2004. The anammoxasome: an intracytoplasmic compartment in anammox bacteria. FEMS Microbiol. Lett. 233: 7-13

Walker, C., J. De La Torre, M. Klotz, H. Urakawa, N. Pinel, D. Arp, C. Brochier-Armanet, P. Chain, and others. 2010. Nitrosopumilus maritimus genome reveals unique mechanisms for nitrification and autotrophy in globally distributed marine crenarchaea. Proc. Natl. Acad. Sci. U.S.A. 107: 8818-8823

Walsh, M. A., Z. Otwinowski, A. Perrakis, P. M. Anderson, and A. Joachimiak. 2000. Structure of cyanate reveals that a novel dimeric and decameric arrangement of subunits is required for formation of the enzyme active site. Structure. 8(5): 505-514

Wang, Q., J. Xia, V. Guallar, G. Krilov, and E. R. Kantrowitz. 2008. Mechanism of thermal decomposition of carbamoyl phosphate and its stabilization by aspartate and ornithine transcarbamoylases. Proceedings of the National Academy of Sciences. 105(44): 16918-16923

Ward, B. B., A. Devol, J. Rich, B. Chang, S. Bulow, H. Naik, A. Pratihary and A. Jayakumar 2009. Denitrification as the dominant nitrogen loss process in the Arabian Sea. Nature. 461: 78-81

Ward, B. B. 2008. Nitrification in Marine Systems, p. 199-262. In D. G. Capone, D. A. Bronk, M. R. Mulholland and E. J. Carpenter [eds.], Nitrogen in the Marine Environment. Elsevier.

Welschmeyer, N. A. 1994. Fluorometric analysis of chlorophyll-a in the presence of chlorophyll-b and pheopigments. Limnol. Oceanogr. 39: 1985-1992

Werner, E. A. 1923. The constitution of carbamides Part XV A delicate and trustworthy test for the recognition of cyanic acid. J. Chem. Soc. 123: 2577-2579

Widner, B. and M. R. Mulholland submitted. Cyanate distribution and uptake in North Atlantic coastal waters.

Widner, B., M. R. Mulholland and K. Mopper 2013. Chromatographic Determination of Nanomolar Cyanate Concentrations in Sea and Estuarine Waters by Precolumn Fluorescence Derivatization. Anal. Chem. 85: 6661-6666

Widner, B., M. R. Mulholland and K. Mopper submitted. New Insights into the Marine Nitrogen Cycle: The Role of Cyanate.

Wood, A. P., D. P. Kelly, I. R. McDonald, S. L. Jordan, T. D. Morgan, S. Khan, J. C. Murrell and E. Borodina 1998. A novel pink-pigmented facultative methylotroph, *Methylobacterium thiocyanatum sp. nov*., capable of growth on thiocyanate or cyanate as sole nitrogen sources. Arch. Microbiol. 169: 148-158

Wurch, L. L., S. T. Haley, E. D. Orchard, C. J. Gobler and S. T. Dyhrman 2011. Nutrient-regulated transcriptional responses in the brown tide forming alga *Aureococcus anophagefferens*. Environ. Microbiol. 13: 468-481

Yamagata, Y. 1999. Prebiotic formation of ADP and ATP from AMP, calcium phosphates and cyanate in aqueous solution. Origins Life Evol. Biosphere. 29: 511-520

Yamagata, Y. and T. Mohri 1982. Formation of cyanate and carbamyl phosphate by electric discharges of model primitive gas. Origins of Life. 12: 41-44

Zhang, J.-Z. 2000. Shipboard automated determination of trace concentrations of nitrite and nitrate in oligotrophic water by gas-segmented continuous flow analysis with a liquid waveguide capillary flow cell. Deep Sea Res., Part I. 47: 1157-1171

Zhuang, Y., H. Zhang, L. Hannick and S. Lin 2015. Metatranscriptome profiling reveals versatile N-nutrient utilization, CO2 limitation, oxidative stress, and active toxin production in an Alexandrium fundyense bloom. Harmful Algae. 42: 60-70

Zvinowanda, C. M., J. O. Okonkwo and R. C. Gurira 2008. Improved derivatisation methods for the determination of free cyanide and cyanate in mine effluent. J. Hazard. Mater. 158: 196-201

APPENDIX A

CYANASE STRUCTURE

Figure 1. Molecular structure of cyanate hydratase (CynS) showing alpha helices (magenta), beta sheets (yellow), and other residues (white). The five active sites of CynS are dimers which bind bicarbonate and cyanate, and CynS requires no cofactors. Redrawn from Walsh et al. (2000) using RCSB Protein Data Bank and Rasmol 2.7.5.2.

APPENDIX B

UREA AND CYANATE CYCLES

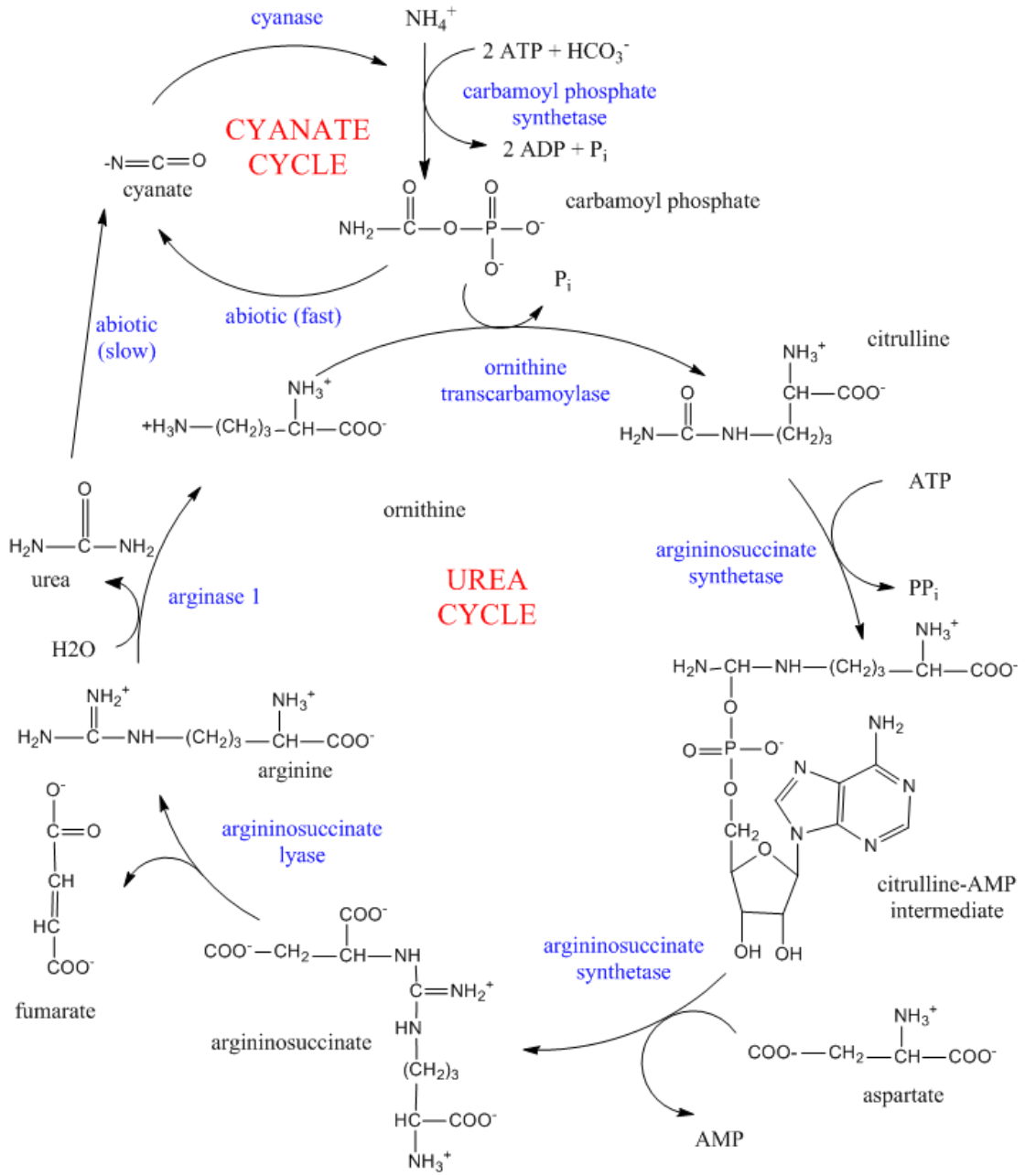

Figure 1. Urea cycle and proposed cyanate cycle where enzymes are shown in blue. The urea cycle is redrawn from Nelson and Cox (2008) and the cyanate cycle is redrawn from Guilloton et al. (2002).

APPENDIX C

CARBAMOYL PHOSPHATE DECOMPOSITION

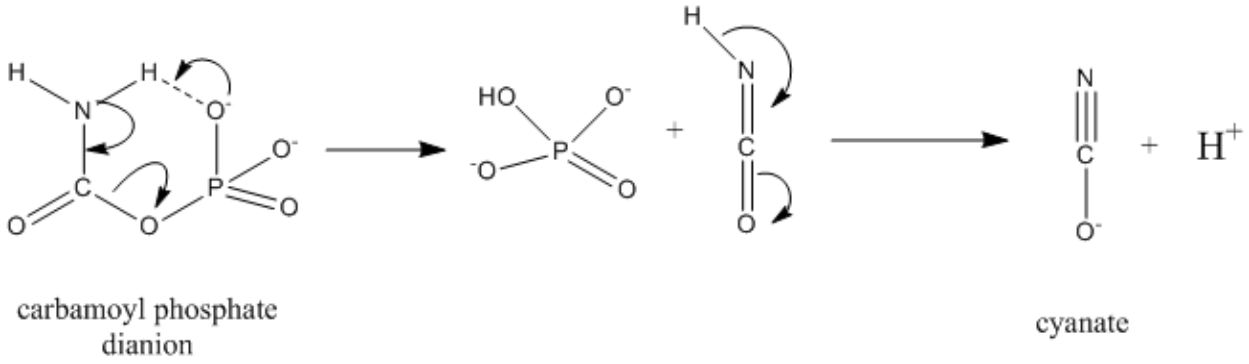

Scheme 1. Abiotic decomposition of carbamoyl phosphate to cyanate. In the absence of stabilizing enzymes, the half life of carbamoyl phosphate is < 2 s (Wang et al. 2008). Redrawn from Wang et al. (2008).

APPENDIX D

COPYRIGHT PERMISSIONS

Permission for Chapter II, which is published in Analytical Chemistry.

Dear Brittany Widner,

You have my permission to use this article "Chomatographic determination of nanomolar cyanate concentrations in estuarine and sea waters by precolumn fluorescence derivatization. " in your thesis as long as the correct citations are made as directed in the ACS Thesis/Dissertation Policy and the ACS Journal Publishing Agreement.

Sincerely,

Prof. Jonathan V. Sweedler
Editor-in-Chief
Analytical Chemistry
Phone: 217-244-7359
Fax: 202-513-8699
Email: eic@anchem.acs.org

The following wording is from the ACS Thesis/Dissertation Policy and the ACS Journal Publishing Agreement:

Reuse/Republication of the Entire Work in Theses or Collections: Authors may reuse all or part of the Submitted, Accepted or Published Work in a thesis or dissertation that the author writes and is required to submit to satisfy the criteria of degree-granting institutions. Such reuse is permitted subject to the ACS' "Ethical Guidelines to Publication of Chemical Research"; the author should secure written confirmation (via letter or email) from the respective ACS journal editor(s) to avoid potential conflicts with journal prior publication*/embargo policies. Appropriate citation of the Published Work must be made**. If the thesis or dissertation to be published is in electronic format, a direct link to the Published Work must also be included using the ACS Articles on Request author-directed link.

* Prior publication policies of ACS journals are posted on the ACS website.

** "Reprinted with permission from [COMPLETE REFERENCE CITATION]. Copyright [YEAR] American Chemical Society." Insert the appropriate wording in place of the capitalized words. This credit line wording should appear **on the first page of your ACS journal article**.

The manuscript can be found online at http://pubs.acs.org/doi/abs/10.1021/ac400351c.

APPENDIX E

CONCENTRATIONS FOR THE GULF OF MAINE TRANSECT

Concentrations are given ± 1 standard deviation in parentheses for nitrate, ammonium, nitrite, and cyanate. Concentrations that were below the detection limit are listed as b.d.l. The method detection limits were 70, 40, 70, and 0.4 nM for nitrite, ammonium, nitrate, and cyanate, respectively.

Station ID	Latitude	Longitude	Depth	Nitrate (µM)	Ammonium (µM)	Nitrite (µM)	Cyanate (nM)
1	40.24224	67.69576	512.2	15.3(.11)	0.08(.06)	b.d.l.	2.0(0.2)
1	40.24224	67.69576	249.1	14.6(.03)	0.07(.02)	b.d.l.	2.0(0.2)
1	40.24224	67.69576	100.1	7.4(.02)	b.d.l.	b.d.l.	2.1(0.0)
1	40.24224	67.69576	79.9	3.7(.11)	0.05(.01)	b.d.l.	3.4(0.3)
1	40.24224	67.69576	60.1	2.8(.06)	b.d.l.	b.d.l.	3.8(0.2)
1	40.24224	67.69576	49.6	3.3(.03)	0.06(.02)	b.d.l.	3.4(0.2)
1	40.24224	67.69576	40.8	2.5(.04)	0.06(.03)	b.d.l.	3.6(1.1)
1	40.24224	67.69576	35.4	b.d.l.	0.05(.02)	b.d.l.	4.2(0.3)
1	40.24224	67.69576	20.4	0.3(.04)	b.d.l.	b.d.l.	3.1(0.1)
1	40.24224	67.69576	10.6	b.d.l.	0.06(.01)	b.d.l.	2.3(0.4)
1	40.24224	67.69576	3.8	b.d.l.	0.07(.03)	b.d.l.	3.0(0.2)
2	40.38454	67.67678	420.3	14.5(.35)	0.05(.00)	b.d.l.	1.8(0.2)
2	40.38454	67.67678	344.4	11.0(.12)	b.d.l.	b.d.l.	1.0(0.2)
2	40.38454	67.67678	196.9	14.9(.06)	b.d.l.	b.d.l.	2.7(0.3)
2	40.38454	67.67678	87.5	5.4(.04)	b.d.l.	b.d.l.	5.0(0.2)
2	40.38454	67.67678	64.9	4.6(.03)	b.d.l.	0.28	4.5(0.8)
2	40.38454	67.67678	50.6	0.3(.01)	b.d.l.	0.20	2.9(0.7)
2	40.38454	67.67678	39.9	0.4(.03)	b.d.l.	b.d.l.	3.0(0.4)
2	40.38454	67.67678	34.5	0.2(.01)	b.d.l.	b.d.l.	1.5(0.2)
2	40.38454	67.67678	27.3	0.1(.02)	b.d.l.	b.d.l.	1.3(0.1)
2	40.38454	67.67678	20.1	b.d.l.	b.d.l.	b.d.l.	1.3(0.1)
2	40.38454	67.67678	10.6	b.d.l.	b.d.l.	b.d.l.	1.2(0.1)
2	40.38454	67.67678	4.4	b.d.l.	b.d.l.	b.d.l.	1.4(0.2)
3	40.86695	67.65907	3.7	0.2(.02)	0.18(.03)	b.d.l.	2.5(0.0)
3	40.86695	67.65907	19.8	0.5(.12)	0.18(.01)	b.d.l.	1.6(0.4)
4	40.92918	67.70489	61.2	7.5(.19)	0.72(.01)	0.04	5.1(0.6)
4	40.92918	67.70489	44.6	6.4(.03)	0.74(.00)	0.02	5.9(0.3)
4	40.92918	67.70489	34.4	7.3(.01)	0.92(.02)	0.02	5.2(0.4)
4	40.92918	67.70489	26.1	5.9(.04)	0.59(.00)	0.02	6.3(0.4)

APPENDIX E Continued.

Station ID	Latitude	Longitude	Depth	Nitrate (µM)	Ammonium (µM)	Nitrite (µM)	Cyanate (nM)
4	40.92918	67.70489	20.1	3.7(.02)	b.d.l.	0.01	2.8(0.1)
4	40.92918	67.70489	10.9	b.d.l.	b.d.l.	0.04	1.7(0.5)
4	40.92918	67.70489	4.5	3.7(.03)	b.d.l.	0.03	1.9(0.2)
5	41.46176	67.68459	34.7	b.d.l.	b.d.l.	b.d.l.	7.0(0.3)
5	41.46176	67.68459	30.3	b.d.l.	b.d.l.	b.d.l.	7.3(0.5)
5	41.46176	67.68459	25.6	b.d.l.	b.d.l.	b.d.l.	7.2(0.4)
5	41.46176	67.68459	20.8	b.d.l.	b.d.l.	b.d.l.	8.1(0.6)
5	41.46176	67.68459	15.3	b.d.l.	b.d.l.	b.d.l.	7.7(0.7)
5	41.46176	67.68459	10.4	.4(.04)	b.d.l.	b.d.l.	7.1(0.6)
5	41.46176	67.68459	4.5	b.d.l.	b.d.l.	b.d.l.	7.2(0.5)
6	42.01527	67.67633	60.2	6.1(.11)	0.56(.01)	0.03	7.2(0.4)
6	42.01527	67.67633	49.8	5.5(.06)	0.42(.01)	0.01	7.2(0.2)
6	42.01527	67.67633	40.8	.3(.06)	0.07(.00)	0.01	6.5(0.5)
6	42.01527	67.67633	24.2	.2(.00)	b.d.l.	b.d.l.	7.4(0.7)
6	42.01527	67.67633	15.4	.1(.00)	b.d.l.	b.d.l.	5.5(0.2)
6	42.01527	67.67633	4.1	b.d.l.	b.d.l.	b.d.l.	3.9(0.4)
7	43.02865	67.7107	178.7	15.3(.05)	b.d.l.	b.d.l.	5.8(1.7)
7	43.02865	67.7107	86.2	15.1(.01)	b.d.l.	b.d.l.	5.2(0.3)
7	43.02865	67.7107	40.7	9.3(.04)	b.d.l.	b.d.l.	7.3(0.7)
7	43.02865	67.7107	22.9	2.4(.03)	b.d.l.	b.d.l.	6.8(1.3)
7	43.02865	67.7107	16.7	0.9(.01)	0.12(.10)	b.d.l.	4.2(0.8)
7	43.02865	67.7107	4.4	0.2(.18)	0.14(.01)	b.d.l.	4.8(0.4)
8	43.39768	67.69833	240.4	13.6(.01)	b.d.l.	0.01	6.2(0.7)
8	43.39768	67.69833	147.1	13.6(.15)	b.d.l.	b.d.l.	6.1(0.2)
8	43.39768	67.69833	122.5	13.9(.16)	b.d.l.	b.d.l.	5.6(0.5)
8	43.39768	67.69833	98.9	15.3(.12)	0.15(.03)	b.d.l.	6.0(0.3)
8	43.39768	67.69833	80.3	8.3(.16)	b.d.l.	b.d.l.	7.6(0.1)
8	43.39768	67.69833	60.7	7.6(.06)	b.d.l.	b.d.l.	7.8(0.7)
8	43.39768	67.69833	50.4	9.7(.00)	b.d.l.	b.d.l.	7.4(0.8)
8	43.39768	67.69833	37.6	7.3(.03)	b.d.l.	b.d.l.	6.2(0.9)
8	43.39768	67.69833	21.7	2.3(.08)	0.11(.05)	0.00	6.7(0.2)
8	43.39768	67.69833	15.9	0.2(.02)	0.10(.00)	b.d.l.	5.0(0.3)
8	43.39768	67.69833	10.1	0.2(.01)	0.09(.01)	b.d.l.	4.6(0.7)
8	43.39768	67.69833	3.8	0.4(.00)	0.08(.00)	b.d.l.	4.2(0.4)
9	44.19895	67.70635	160.3	13.8(.15)	b.d.l.	0.01	6.0(0.8)
9	44.19895	67.70635	140	9.5(.06)	b.d.l.	b.d.l.	4.4(0.9)
9	44.19895	67.70635	119.7	10.9(.03)	b.d.l.	b.d.l.	6.4(0.5)
9	44.19895	67.70635	100.4	8.2(.06)	b.d.l.	0.00	6.4(0.5)
9	44.19895	67.70635	81.6	7.6(.08)	b.d.l.	0.01	6.2(0.7)

APPENDIX E Continued.

Station ID	Latitude	Longitude	Depth	Nitrate (µM)	Ammonium (µM)	Nitrite (µM)	Cyanate (nM)
9	44.19895	67.70635	60.9	5.7(.01)	b.d.l.	0.03	5.7(1.1)
9	44.19895	67.70635	50.7	7.1(.08)	0.13(.02)	0.02	7.1(1.3)
9	44.19895	67.70635	40.8	6.1(.07)	0.21(.01)	0.00	6.5(0.4)
9	44.19895	67.70635	30.7	2.3(.04)	0.15(.01)	0.01	5.7(1.0)
9	44.19895	67.70635	20.5	1.8(.01)	b.d.l.	0.02	6.9(1.7)
9	44.19895	67.70635	10.5	1.9(.02)	b.d.l.	0.00	6.7(0.9)
9	44.19895	67.70635	4.1	1.7(.03)	b.d.l.	0.02	5.8(1.3)

APPENDIX F

NO_2^-, NO_3^-, NH_4^+, AND OCN^- CONCENTRATIONS FOR CHAPTER IV

All concentrations from Chapter IV are presented as ± 1 standard deviation in parentheses for ammonium (NH_4^+, n=2) and cyanate (OCN^-, n=3). Samples for nitrate (NO_3^-) and nitrite (NO_2^-) were not replicated. Concentrations that were below the methodological detection limits are listed as b.d.l. The method detection limits are the same as those listed in Appendix E.

Latitude (°N)	Longitude (°W)	Depth (m)	Nitrite (μM)	Nitrate (μM)	Ammonium (μM)	Cyanate (nM)
41.0993	70.6402	38.9	0.28	2.05	1.57(0.10)	5.2(0.4)
41.0993	70.6402	25.5	0.18	1.20	1.59(0.05)	5.8(0.9)
41.0993	70.6402	15.4	b.d.l.	0.30	0.14(0.02)	3.7(0.2)
41.0993	70.6402	10.2	b.d.l.	0.36	b.d.l.	1.4(0.2)
41.0993	70.6402	3.2	b.d.l.	b.d.l.	b.d.l.	3.3(0.4)
40.3713	71.6712	2.7	b.d.l.	b.d.l.	0.38(0.19)	3.8(0.9)
40.3713	71.6712	15	b.d.l.	b.d.l.	0.30(0.10)	1.5(0.4)
39.0132	72.5875	496.3	b.d.l.	15.45	0.05(0.09)	2.2(0.9)
39.0132	72.5875	150.1	b.d.l.	4.90	0.17(0.07)	4.1(1.1)
39.0132	72.5875	55	b.d.l.	4.32	0.09(0.06)	7.0(0.1)
39.0132	72.5875	40.6	b.d.l.	b.d.l.	b.d.l.	4.2(0.9)
39.0132	72.5875	30.7	b.d.l.	b.d.l.	b.d.l.	1.4(0.0)
39.0132	72.5875	16.3	b.d.l.	b.d.l.	0.13(0.62)	1.7(0.0)
39.0132	72.5875	3	b.d.l.	b.d.l.	0.18(0.01)	1.5(0.3)
39.3579	73.3867	3	b.d.l.	b.d.l.	0.16(0.01)	4.6(0.4)
39.3579	73.3867	14	0.21	b.d.l.	0.18(0.01)	1.3(0.2)
37.7048	74.2531	109.1	b.d.l.	7.60	0.23(0.09)	3.4(0.4)
37.7048	74.2531	80.3	b.d.l.	5.13	1.07(0.13)	5.9(0.7)
37.7048	74.2531	70.3	b.d.l.	5.79	0.24(0.07)	6.3(0.4)
37.7048	74.2531	59.2	b.d.l.	4.91	0.55(0.10)	6.5(0.6)
37.7048	74.2531	49.4	b.d.l.	2.28	0.19(0.01)	5.8(0.5)
37.7048	74.2531	38.8	0.19	0.77	0.61(0.05)	2.9(1.9)
37.7048	74.2531	34.6	0.17	0.41	0.17(0.11)	1.9(0.5)
37.7048	74.2531	25	0.12	0.69	0.25(0.13)	0.8(0.2)
37.7048	74.2531	15.6	b.d.l.	0.17	b.d.l.	1.2(0.8)
37.7048	74.2531	11.1	b.d.l.	0.10	0.40(0.02)	N/A
37.7048	74.2531	4.3	b.d.l.	0.10	0.15(0.00)	N/A
37.8442	74.5792	50.6	0.19	4.18	0.08(0.00)	5.6(0.2)
37.8442	74.5792	25.4	0.46	b.d.l.	0.30(0.02)	2.6(0.5)

APPENDIX F Continued.

37.8442	74.5792	15.8	0.20	b.d.l.	N/A	0.9(0.2)
37.8442	74.5792	4.9	0.10	0.28	N/A	1.4(0.4)
37.4563	75.1006	4	0.31	b.d.l.	N/A	1.8(0.2)
37.4563	75.1006	26.4	0.43	b.d.l.	N/A	4.1(0.7)
36.0075	74.6684	496.4	0.07	13.19	0.05(0.01)	b.d.l.
36.0075	74.6684	298.2	b.d.l.	12.63	0.05(0.00)	b.d.l.
36.0075	74.6684	122	b.d.l.	13.24	0.05(0.01)	1.4(0.3)
36.0075	74.6684	49.5	b.d.l.	6.09	b.d.l.	16.9(0.4)
36.0075	74.6684	43.2	0.07	3.78	0.07(0.01)	11.1(2.3)
36.0075	74.6684	39.1	0.15	5.55	0.18(0.11)	4.4(0.8)
36.0075	74.6684	32.4	0.16	3.94	0.14(0.00)	4.1(2.0)
36.0075	74.6684	29.1	0.06	3.23	0.11(0.01)	b.d.l.
36.0075	74.6684	23.7	b.d.l.	b.d.l.	0.13(0.04)	b.d.l.
36.0075	74.6684	16.8	b.d.l.	0.43	0.09(0.01)	b.d.l.
36.0075	74.6684	9.1	b.d.l.	b.d.l.	0.10(0.04)	b.d.l.
36.0075	74.6684	7.1	b.d.l.	b.d.l.	0.09(0.07)	b.d.l.
36.0014	75.1636	24.1	0.20	3.73	0.12(0.01)	2.8(0.2)
36.0014	75.1636	20.1	0.12	0.10	0.09(0.02)	b.d.l.
36.0014	75.1636	14.2	0.10	0.13	0.08(0.03)	b.d.l.
36.0014	75.1636	9.2	b.d.l.	b.d.l.	0.06(0.00)	b.d.l.
36.0014	75.1636	4.9	b.d.l.	b.d.l.	0.07(0.07)	b.d.l.
35.9853	75.5209	17	0.43	3.87	1.23(0.02)	12.8(5.1)
35.9853	75.5209	10	0.34	b.d.l.	0.21(0.21)	8.2(2.0)
35.9853	75.5209	3	0.27	b.d.l.	0.12(0.15)	9.4(1.0)
38.8213	74.7399	3.1		0.30	0.14(0.03)	5.6(0.0)
38.8213	74.7399	8.4		b.d.l.	0.18(0.01)	3.8(1.0)
40.8743	72.1543	17.8	0.19	b.d.l.	0.18(0.02)	9.0(1.1)
40.8743	72.1543	5	0.18	b.d.l.	N/A	5.6(0.0)
39.8280	70.6209	500	0.12	13.56	0.09(0.01)	N/A
39.8280	70.6209	297.5	0.11	16.91	b.d.l.	N/A
39.8280	70.6209	120.9	0.08	8.78	b.d.l.	N/A
39.8280	70.6209	97.1	b.d.l.	6.09	b.d.l.	N/A
39.8280	70.6209	76.1	b.d.l.	5.37	0.05(0.00)	N/A
39.8280	70.6209	61.2	b.d.l.	5.22	0.05(0.00)	N/A
39.8280	70.6209	51	b.d.l.	2.61	0.05(0.00)	N/A
39.8280	70.6209	39.1	b.d.l.	1.21	0.07(0.01)	N/A
39.8280	70.6209	20.8	b.d.l.	0.03	0.07(0.00)	N/A
39.8280	70.6209	18.2	b.d.l.	0.03	0.08(0.02)	N/A
39.8280	70.6209	10.6	b.d.l.	0.03	0.11(0.02)	N/A
39.8280	70.6209	4.3	b.d.l.	0.03	0.07(0.00)	N/A
40.0477	70.6027	144.8	b.d.l.	7.86	0.12(0.04)	N/A

APPENDIX F Continued.

40.0477	70.6027	35.1	0.16	4.97	N/A	N/A
40.0477	70.6027	23.4	0.20	0.38	N/A	N/A
40.0477	70.6027	4.1	0.31	0.04	N/A	N/A
39.9334	69.5074	2.7	0.16	1.11	N/A	2.6(0.3)
39.9334	69.5074	30.5	0.26	1.42	N/A	6.0(0.1)
40.6814	68.7702	4.1	0.30	b.d.l.	N/A	3.5(0.5)
40.6814	68.7702	20.3	0.27	0.12	N/A	5.1(0.1)
40.2422	67.6958	512.2	0.07	15.33	0.08(0.06)	2.0(0.2)
40.2422	67.6958	249.1	0.07	14.57	0.07(0.02)	2.0(0.2)
40.2422	67.6958	100.1	0.07	7.38	b.d.l.	2.0(0.0)
40.2422	67.6958	79.9	0.07	3.74	0.05(0.01)	3.4(0.3)
40.2422	67.6958	60.1	0.07	2.78	b.d.l.	3.8(0.2)
40.2422	67.6958	49.6	0.07	3.30	0.06(0.02)	3.4(0.2)
40.2422	67.6958	40.8	0.07	2.54	0.06(0.03)	3.6(1.1)
40.2422	67.6958	35.4	0.07	b.d.l.	0.05(0.02)	4.2(0.3)
40.2422	67.6958	20.4	0.07	0.33	b.d.l.	3.1(0.1)
40.2422	67.6958	10.6	b.d.l.	b.d.l.	0.06(0.01)	2.3(0.4)
40.2422	67.6958	3.8	b.d.l.	b.d.l.	0.07(0.03)	3.0(0.2)
40.3845	67.6768	420.3	b.d.l.	14.54	0.05(0.00)	1.8(0.2)
40.3845	67.6768	344.4	b.d.l.	10.97	b.d.l.	1.0(0.2)
40.3845	67.6768	196.9	b.d.l.	14.90	b.d.l.	2.7(0.3)
40.3845	67.6768	87.5	b.d.l.	5.41	b.d.l.	5.0(0.2)
40.3845	67.6768	64.9	0.28	4.58	b.d.l.	4.5(0.8)
40.3845	67.6768	50.6	0.20	0.33	b.d.l.	2.9(0.7)
40.3845	67.6768	39.9	b.d.l.	0.37	b.d.l.	3.0(0.4)
40.3845	67.6768	34.5	b.d.l.	0.20	b.d.l.	1.5(0.2)
40.3845	67.6768	27.3	b.d.l.	0.14	b.d.l.	1.3(0.1)
40.3845	67.6768	20.1	b.d.l.	b.d.l.	b.d.l.	1.2(0.1)
40.3845	67.6768	10.6	b.d.l.	b.d.l.	b.d.l.	1.2(0.1)
40.3845	67.6768	4.4	b.d.l.	b.d.l.	b.d.l.	1.4(0.2)
40.9292	67.7049	61.2	0.47	7.51	0.72(0.01)	5.1(0.6)
40.9292	67.7049	44.6	0.39	6.41	0.74(0.00)	4.9(0.3)
40.9292	67.7049	34.4	0.43	7.27	0.92(0.02)	5.2(0.4)
40.9292	67.7049	26.1	0.48	5.92	0.59(0.00)	6.3(0.4)
40.9292	67.7049	20.1	0.28	3.72	b.d.l.	2.8(0.1)
40.9292	67.7049	10.9	0.20	b.d.l.	b.d.l.	1.7(0.5)
40.9292	67.7049	4.5	0.15	3.72	b.d.l.	1.9(0.2)
40.8670	67.6591	3.7	b.d.l.	0.24	0.18(0.03)	2.5(0.0)
40.8670	67.6591	19.8	b.d.l.	0.51	0.18(0.01)	1.6(0.4)
41.7555	65.4406	499.8	b.d.l.	12.99	b.d.l.	1.1(0.4)
41.7555	65.4406	241	b.d.l.	17.21	b.d.l.	0.8(0.1)

APPENDIX F Continued.

41.7555	65.4406	61.2	b.d.l.	8.84	b.d.l.	4.6(0.2)
41.7555	65.4406	27.6	b.d.l.	0.15	b.d.l.	1.2(0.4)
41.7555	65.4406	3.4	b.d.l.	0.29	b.d.l.	1.2(0.3)
42.2261	65.7702	100.6	0.42	6.71	b.d.l.	6.0(0.5)
42.2261	65.7702	54.6	0.19	5.59	b.d.l.	3.7(0.1)
42.2261	65.7702	35.4	b.d.l.	b.d.l.	b.d.l.	b.d.l.
42.2261	65.7702	4.5	b.d.l.	b.d.l.	b.d.l.	N/A
42.0153	67.6763	60.2	0.41	6.07	0.56(0.01)	7.1(0.4)
42.0153	67.6763	49.8	0.29	5.53	0.42(0.01)	7.2(0.2)
42.0153	67.6763	40.8	0.10	0.26	0.07(0.00)	6.5(0.5)
42.0153	67.6763	24.2	b.d.l.	0.23	b.d.l.	7.4(0.7)
42.0153	67.6763	15.4	b.d.l.	0.13	b.d.l.	5.5(0.2)
42.0153	67.6763	4.1	b.d.l.	b.d.l.	b.d.l.	3.9(0.4)
41.4618	67.6846	34.7	b.d.l.	b.d.l.	b.d.l.	7.0(0.3)
41.4618	67.6846	30.3	b.d.l.	0.11	b.d.l.	7.3(0.5)
41.4618	67.6846	25.6	b.d.l.	b.d.l.	b.d.l.	7.2(0.4)
41.4618	67.6846	20.8	b.d.l.	0.13	b.d.l.	8.1(0.6)
41.4618	67.6846	15.3	b.d.l.	b.d.l.	b.d.l.	7.7(0.7)
41.4618	67.6846	10.4	b.d.l.	0.35	b.d.l.	7.1(0.6)
41.4618	67.6846	4.5	b.d.l.	b.d.l.	b.d.l.	7.2(0.5)
42.6871	68.2800	15.8		0.21	N/A	1.9(0.5)
42.6871	68.2800	3		0.37	N/A	2.4(0.3)
42.4158	67.0022	363.8	b.d.l.	17.87	b.d.l.	4.2(0.4)
42.4158	67.0022	251.2	b.d.l.	11.21	b.d.l.	2.6(0.3)
42.4158	67.0022	99.8	b.d.l.	11.46	b.d.l.	3.3(0.1)
42.4158	67.0022	80.7	b.d.l.	7.49	b.d.l.	4.1(1.4)
42.4158	67.0022	60.8	b.d.l.	8.71	b.d.l.	5.2(1.0)
42.4158	67.0022	50.8	b.d.l.	7.63	b.d.l.	3.7(0.4)
42.4158	67.0022	40.6	0.12	4.73	b.d.l.	5.3(0.9)
42.4158	67.0022	30.5	0.14	4.74	b.d.l.	3.9(0.6)
42.4158	67.0022	17.8	b.d.l.	b.d.l.	b.d.l.	1.0(0.9)
42.4158	67.0022	10.1	0.13	0.20	b.d.l.	1.5(0.7)
42.4158	67.0022	3.5	0.18	0.37	b.d.l.	0.9(0.2)
43.0283	66.3434	119.8	0.14	10.10	b.d.l.	3.1(1.3)
43.0283	66.3434	50.2	N/A	N/A	N/A	3.2(0.7)
43.0283	66.3434	20	N/A	N/A	N/A	3.5(0.2)
43.0283	66.3434	4.3	N/A	N/A	N/A	3.4(0.0)
43.3999	67.0767	3.7	N/A	N/A	N/A	2.3(0.1)
43.3999	67.0767	21.5	N/A	N/A	N/A	1.6(0.1)
44.4755	67.2268	107.4	0.23	5.93	0.07(0.00)	7.5(0.2)
44.4755	67.2268	79.5	0.33	4.66	0.06(0.02)	9.3(0.4)

APPENDIX F Continued.

44.4755	67.2268	59.6	0.34	6.72	0.05(0.01)	7.6(1.2)
44.4755	67.2268	40.3	0.23	7.24	0.07(0.01)	7.8(1.2)
44.4755	67.2268	20.5	0.25	5.75	b.d.l.	9.0(0.4)
44.4755	67.2268	11.3	0.33	6.91	b.d.l.	9.5(0.3)
44.4755	67.2268	4	0.31	6.28	b.d.l.	10.1(0.4)
44.1990	67.7063	160.3	0.10	13.82	b.d.l.	6.0(0.8)
44.1990	67.7063	140	b.d.l.	9.45	b.d.l.	4.4(0.9)
44.1990	67.7063	119.7		10.92	b.d.l.	6.4(0.5)
44.1990	67.7063	100.4	0.11	8.16	b.d.l.	6.4(0.5)
44.1990	67.7063	81.6	0.16	7.55	b.d.l.	6.1(0.7)
44.1990	67.7063	60.9	0.20	5.73	b.d.l.	5.7(1.1)
44.1990	67.7063	50.7	0.23	7.10	0.13(0.02)	7.1(1.3)
44.1990	67.7063	40.8	0.23	6.09	0.21(0.01)	6.5(0.4)
44.1990	67.7063	30.7	0.15	2.30	0.15(0.01)	5.7(1.0)
44.1990	67.7063	20.5	0.12	1.81	b.d.l.	6.9(1.7)
44.1990	67.7063	10.5	0.11	1.94	b.d.l.	6.7(0.9)
44.1990	67.7063	4.1	0.10	1.66	b.d.l.	5.8(1.3)
43.3977	67.6983	240.4	0.10	13.56	b.d.l.	6.2(0.7)
43.3977	67.6983	147.1	b.d.l.	13.57	b.d.l.	6.1(0.2)
43.3977	67.6983	122.5	b.d.l.	13.85	b.d.l.	5.6(0.5)
43.3977	67.6983	98.9	b.d.l.	15.26	0.15(0.03)	6.0(0.3)
43.3977	67.6983	80.3	b.d.l.	8.33	b.d.l.	7.6(0.1)
43.3977	67.6983	60.7	b.d.l.	7.55	b.d.l.	7.8(0.7)
43.3977	67.6983	50.4	b.d.l.	9.73	b.d.l.	7.4(0.8)
43.3977	67.6983	37.6	b.d.l.	7.29	b.d.l.	6.2(0.9)
43.3977	67.6983	21.7	b.d.l.	2.31	0.11(0.05)	6.7(0.2)
43.3977	67.6983	15.9	b.d.l.	0.19	0.10(0.00)	5.0(0.3)
43.3977	67.6983	10.1	b.d.l.	0.24	0.09(0.01)	4.6(0.7)
43.3977	67.6983	3.8	b.d.l.	0.37	0.08(0.00)	4.2(0.4)
43.0286	67.7107	178.7	b.d.l.	15.32	b.d.l.	5.7(1.7)
43.0286	67.7107	86.2	b.d.l.	15.13	b.d.l.	5.2(0.3)
43.0286	67.7107	40.7	b.d.l.	9.32	b.d.l.	7.3(0.7)
43.0286	67.7107	22.9	b.d.l.	2.40	b.d.l.	6.8(1.3)
43.0286	67.7107	16.7	b.d.l.	0.86	N/A	4.2(0.8)
43.0286	67.7107	4.4	b.d.l.	0.23	N/A	4.8(0.4)
43.0010	70.4190	99.1	b.d.l.	12.33	0.05(0.00)	9.8(0.1)
43.0010	70.4190	23.2	N/A	1.29	N/A	7.4(0.8)
43.0010	70.4190	17.1	N/A	0.25	N/A	2.9(0.6)
43.0010	70.4190	3.4	N/A	0.32	N/A	3.9(0.5)
42.3014	70.2794	31	N/A	N/A	N/A	6.3(0.7)
42.3014	70.2794	13.2	N/A	N/A	N/A	6.4(0.1)

APPENDIX F Continued.

42.3014	70.2794	4.6	N/A	N/A	N/A	4.6(0.4)
42.3542	70.4541	70.5	b.d.l.	9.28	b.d.l.	6.7(0.6)
42.3542	70.4541	59.8	b.d.l.	9.43	b.d.l.	5.2(0.3)
42.3542	70.4541	50.3	b.d.l.	6.59	b.d.l.	6.1(0.0)
42.3542	70.4541	40.4	0.07	6.23	b.d.l.	6.6(0.6)
42.3542	70.4541	30	0.12	5.72	0.06(0.00)	4.9(0.2)
42.3542	70.4541	26	0.11	2.84	0.07(0.01)	5.1(0.1)
42.3542	70.4541	21.2	0.08	2.67	0.06(0.00)	4.4(0.3)
42.3542	70.4541	14.8	0.10	0.61	0.09(0.04)	1.9(0.3)
42.3542	70.4541	10.4	b.d.l.	0.46	0.11(0.01)	2.0(0.3)
42.3542	70.4541	3.8	b.d.l.	0.13	0.10(0.00)	1.1(0.1)
42.4200	70.6182	80.7	0.12	6.81	0.09(0.01)	6.6(0.4)
42.4200	70.6182	70	0.11	8.09	0.09(0.01)	6.7(0.7)
42.4200	70.6182	59.9	b.d.l.	8.51	0.08(0.04)	6.8(0.3)
42.4200	70.6182	50.4	b.d.l.	8.10	0.05(0.01)	6.2(0.6)
42.4200	70.6182	41.1	b.d.l.	7.52	0.06(0.01)	7.1(0.8)
42.4200	70.6182	35.1	b.d.l.	5.46	0.06(0.00)	6.1(1.3)
42.4200	70.6182	25.2	b.d.l.	3.82	0.08(0.00)	5.3(0.1)
42.4200	70.6182	14.3	b.d.l.	1.69	0.09(0.01)	3.1(0.3)
42.4200	70.6182	10.8	b.d.l.	b.d.l.	0.10(0.00)	1.9(0.5)
42.4200	70.6182	3.8	b.d.l.	b.d.l.	0.10(0.00)	1.1(0.0)
42.4167	70.8542	13.2	N/A	N/A	N/A	3.7(0.2)
42.4167	70.8542	4.2	N/A	N/A	N/A	2.4(0.3)

APPENDIX G

CTD DATA FOR CHAPTER IV

Continuous profiles of chlorophyll *a* fluorescence, salinity, temperature, and photosynthetically active radiation (PAR) can be found on the NOAA website as given below. The cruise IDs are del1004 for May/June 2010, del1012 for November 2010, del1105 for June 2011, and hb1205 for August 2012.

ftp://ftp.nefsc.noaa.gov/pub/hydro/nodc_files/

ftp://ftp.nefsc.noaa.gov/pub/hydro/matlab_files/

VITA

Brittany Widner
Graduate Research Assistant - PhD Candidate
Department of Ocean, Earth and Atmospheric Sciences
Old Dominion University
4600 Elkhorn Avenue
Norfolk, VA 23529-0276

EDUCATION

PhD, Oceanography, Old Dominion University, 2016
M.S., Oceanography, Old Dominion University, 2011
B.S., Chemistry and Biology, The University of Akron, 2008

PUBLICATIONS

Widner B. and Mulholland, M.R. (*submitted*) Cyanate distribution and uptake in North Atlantic coastal waters. Limnology and Oceanography.

Widner B., Muholland, M.R., and Mopper, K. (*submitted*) New insights into the marine nitrogen cycle: The role of cyanate. ES&T Letters.

Babbin, A.R., Peters, B.D., Mordy, C.A., **Widner, B.**, Casciotti, K.L., Ward, B.B. (*submitted*) Novel metabolisms support the anaerobic nitrite budget in the Eastern Tropical South Pacific. Nature Geoscience.

Widner B., Mulholland, M.R., and Mopper, K. 2013. Chromatographic determination of nanomolar cyanate concentrations in sea and estuarine waters by precolumn fluorescence derivatization. Analytical Chemistry 85 (14):6661-6666.

Grote J., Bayindirli C., Bergauer K., Carpintero de Moraes P., Chen H., D'Ambrosio L., Edwards B., Fernández-Gómez B., Hamisi M., Logares R., Nguyen D., Rii Y., Saeck R., Schutte C., **Widner B.,** Church M., Steward G., Karl D., DeLong E.F., Eppley J., Schuster S.C., Kyrpides N., Rappe M. 2011. Draft genome sequence of strain HIMB100, a cultured representative of the SAR116 clade of marine Alphaproteobacteria. Standards in Genomic Sciences, doi:10.4056/sigs.1854551.

Pan, J.J., **Widner B.**, Ammerman D., and Drenovsky R.E. 2010. Plant community and tissue chemistry responses to fertilizer and litter nutrient manipulations in a temperate grassland. Plant Ecology 206(1):139-150

PUBLICATIONS IN PREPARATION

Widner B., Mulholland, M.R., Mopper, K. Allochthonous sources of cyanate to marine systems.

Widner B. and Mulholland, M.R. Uptake and distribution of cyanate and urea in and above the Eastern Tropical South Pacific Oxygen Deficient Zone.

Widner B., Fuchsman, C., and Mulholland, M.R. Uptake, distribution, and metagenomic studies of cyanate and urea metabolism in the Eastern Tropical North Pacific Oxygen Deficient Zone.